Supporting Information

Acetylene and terminal alkyne complexes of copper(I) supported by fluorinated pyrazolates: Syntheses, structures, and transformations

Devaborniny Parasar, Tharun T. Ponduru, Anurag Noonikara Poyil, Naleen B. Jayaratna, and H. V. Rasika Dias*

Affiliations:

Department of Chemistry and Biochemistry, The University of Texas at Arlington, Arlington, Texas 76019, United States

*Correspondence to: dias@uta.edu (H.V.R.D.)

Figure S1. ^{1}H NMR spectrum of $Cu_4(\mu\text{-}[3,5\text{-}(CF_3)_2Pz])_4(\mu\text{-}HC{\equiv}CH)_2$ **(4)** in $CDCl_3$ at room temperature (Top figure); and $Cu_2(\mu\text{-}[3,5\text{-}(CF_3)_2Pz])_2(\mu\text{-}HC{\equiv}CH)_2$ **(5)** with excess acetylene in CD_2Cl_2 at -70 °C (bottom figure). A signal corresponding to $\{\mu\text{-}[3,5\text{-}(CF_3)_2Pz]Cu\}_3$ (δ 7.01 ppm, br s, Pz-H) was also observed in the solutions of **4** at room temperature (top figure), which is a result of some acetylene loss from **4** leading to the formation of $\{\mu\text{-}[3,5\text{-}(CF_3)_2Pz]Cu\}_3$.

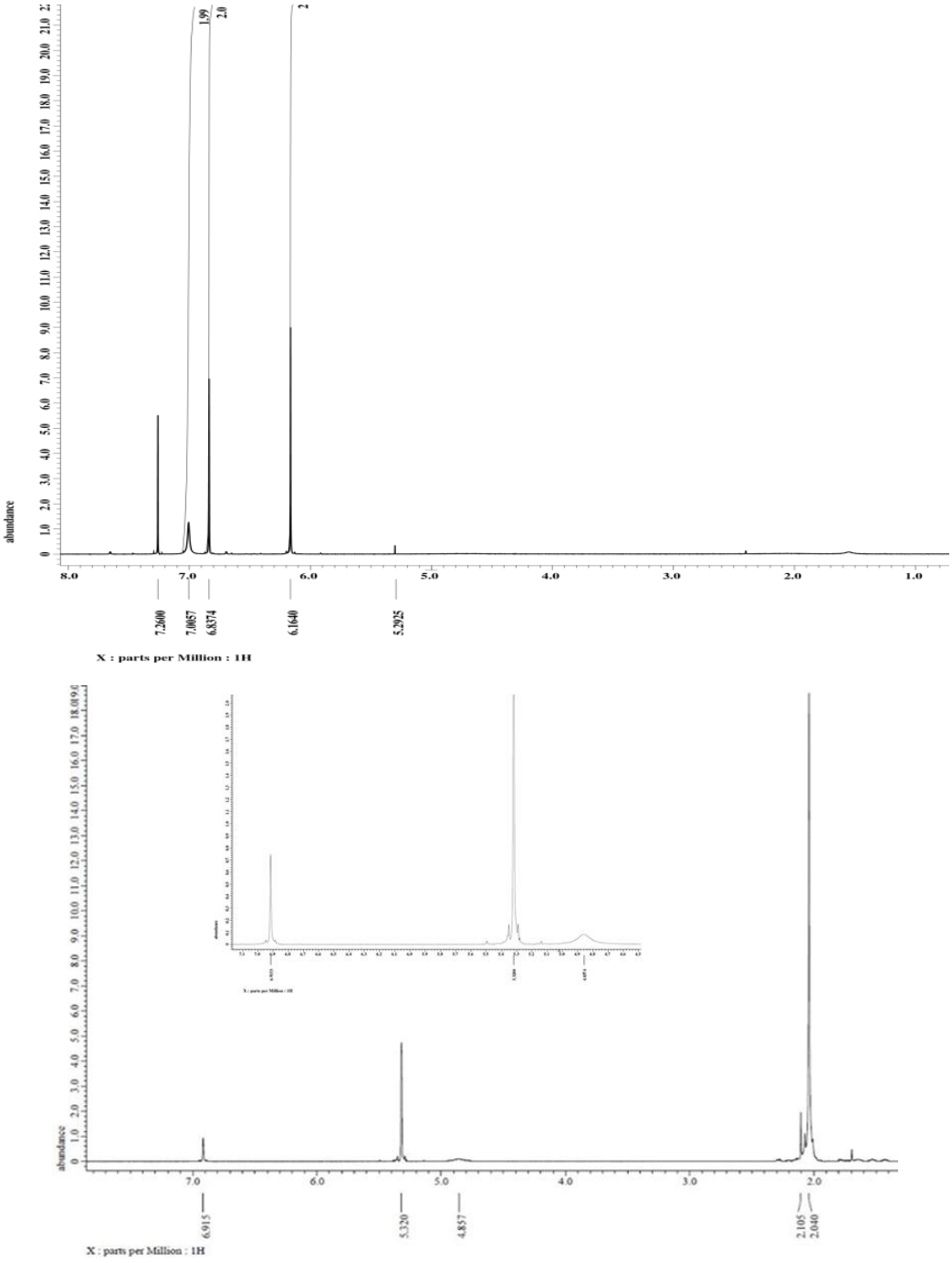

Figure S2. ^{19}F NMR spectrum of $Cu_4(\mu\text{-}[3,5\text{-}(CF_3)_2Pz])_4(\mu\text{-}HC{\equiv}CH)_2$ **(4)** in $CDCl_3$ at room temperature (top) and $Cu_2(\mu\text{-}[3,5\text{-}(CF_3)_2Pz])_2(\mu\text{-}HC{\equiv}CH)_2$ **(5)** with excess acetylene in CD_2Cl_2 at -70 °C (bottom). Broad signal at δ -61.0 (br s) ppm in the top figure is due to $\{\mu\text{-}[3,5\text{-}(CF_3)_2Pz]Cu\}_3$, which is a result of some acetylene loss from **4** leading to the formation of $\{\mu\text{-}[3,5\text{-}(CF_3)_2Pz]Cu\}_3$.

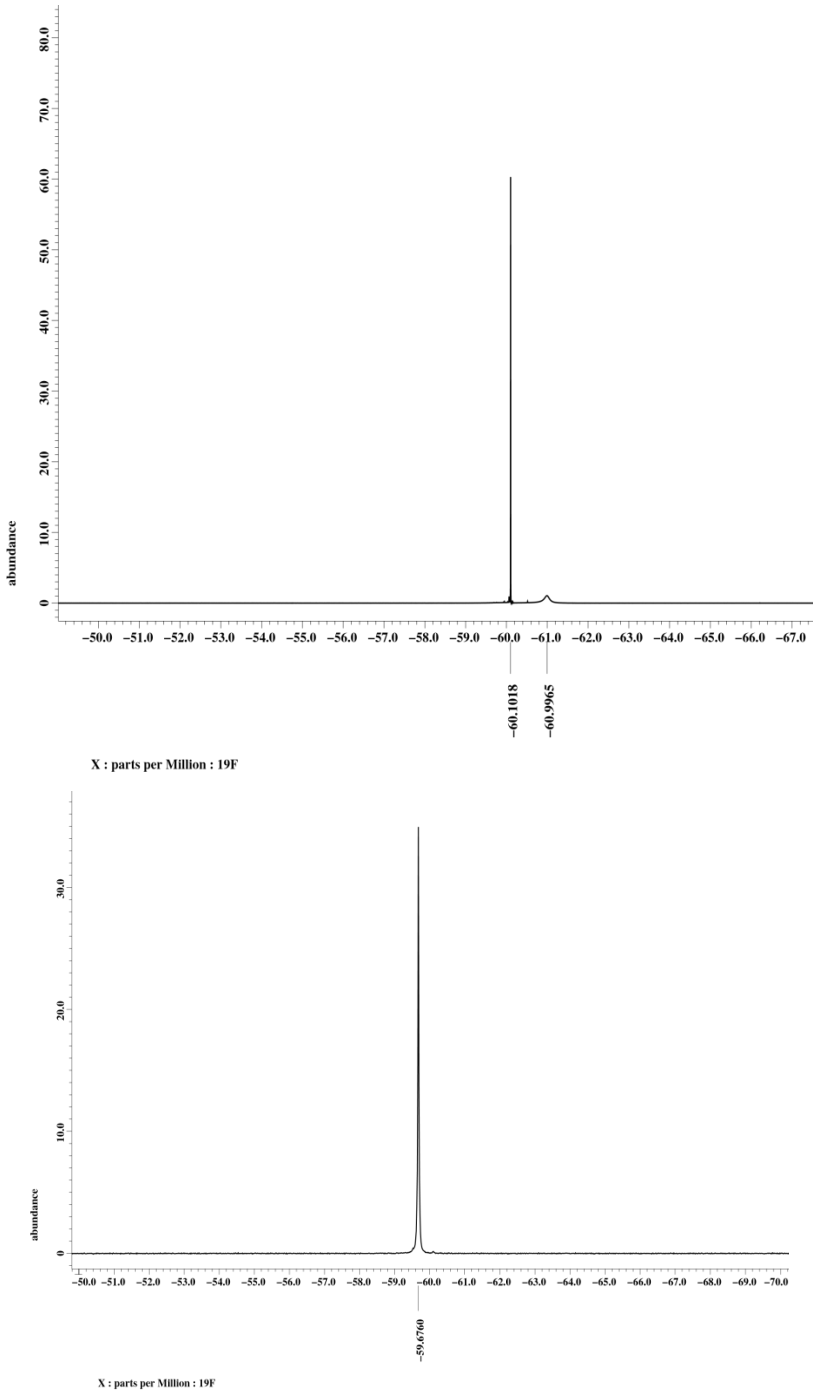

Figure S3. $^{13}C\{^{1}H\}$NMR spectrum of $Cu_4(\mu\text{-}[3,5\text{-}(CF_3)_2Pz])_4(\mu\text{-}HC{\equiv}CH)_2$ **(4)** in $CDCl_3$ at room temperature. Peaks due to $\{\mu\text{-}[3,5\text{-}(CF_3)_2Pz]Cu\}_3$ are also present.

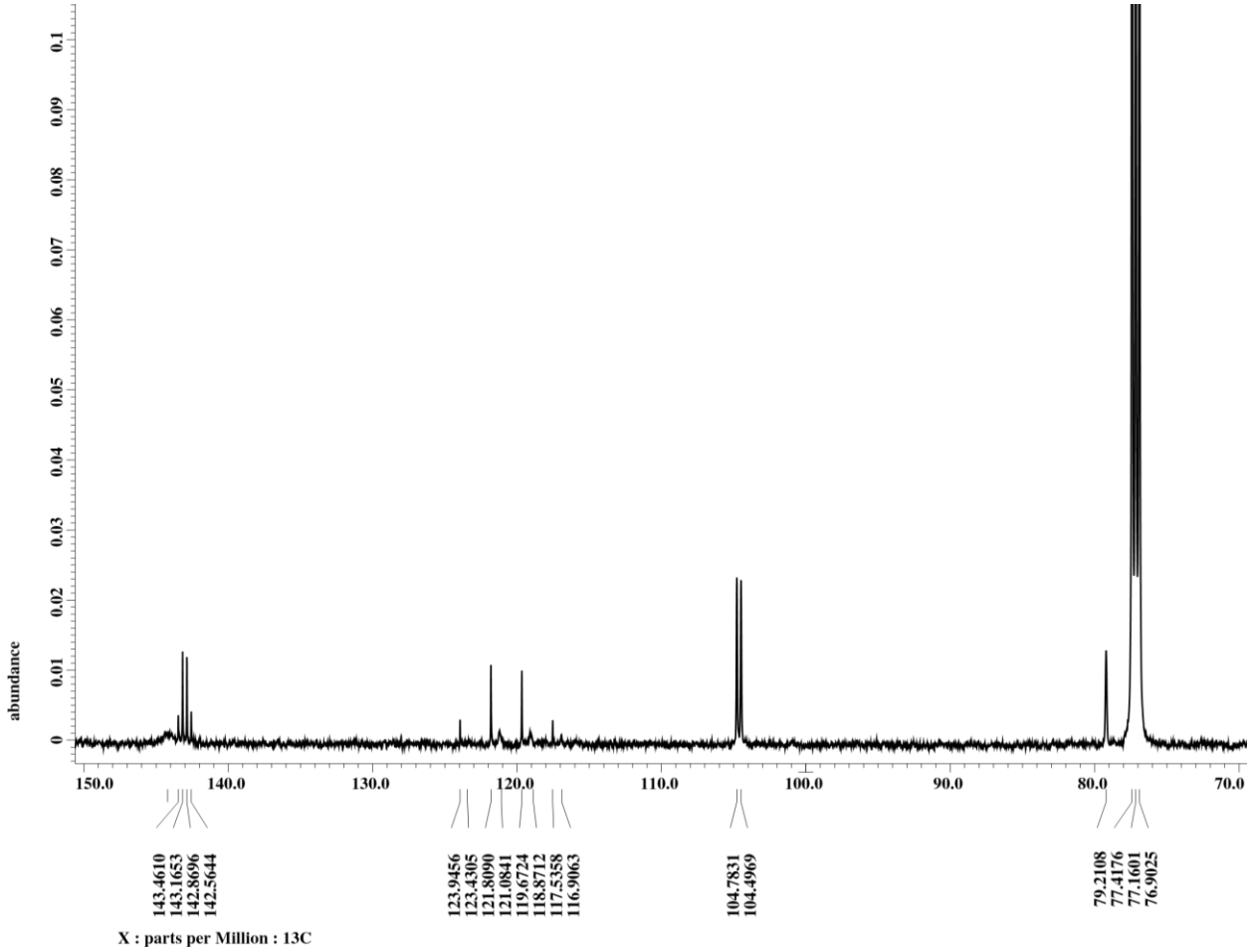

Figure S4. HMQC NMR spectrum of $Cu_4(\mu\text{-}[3,5\text{-}(CF_3)_2Pz])_4(\mu\text{-}HC{\equiv}CH)_2$ **(4)** in $CDCl_3$ at room temperature.

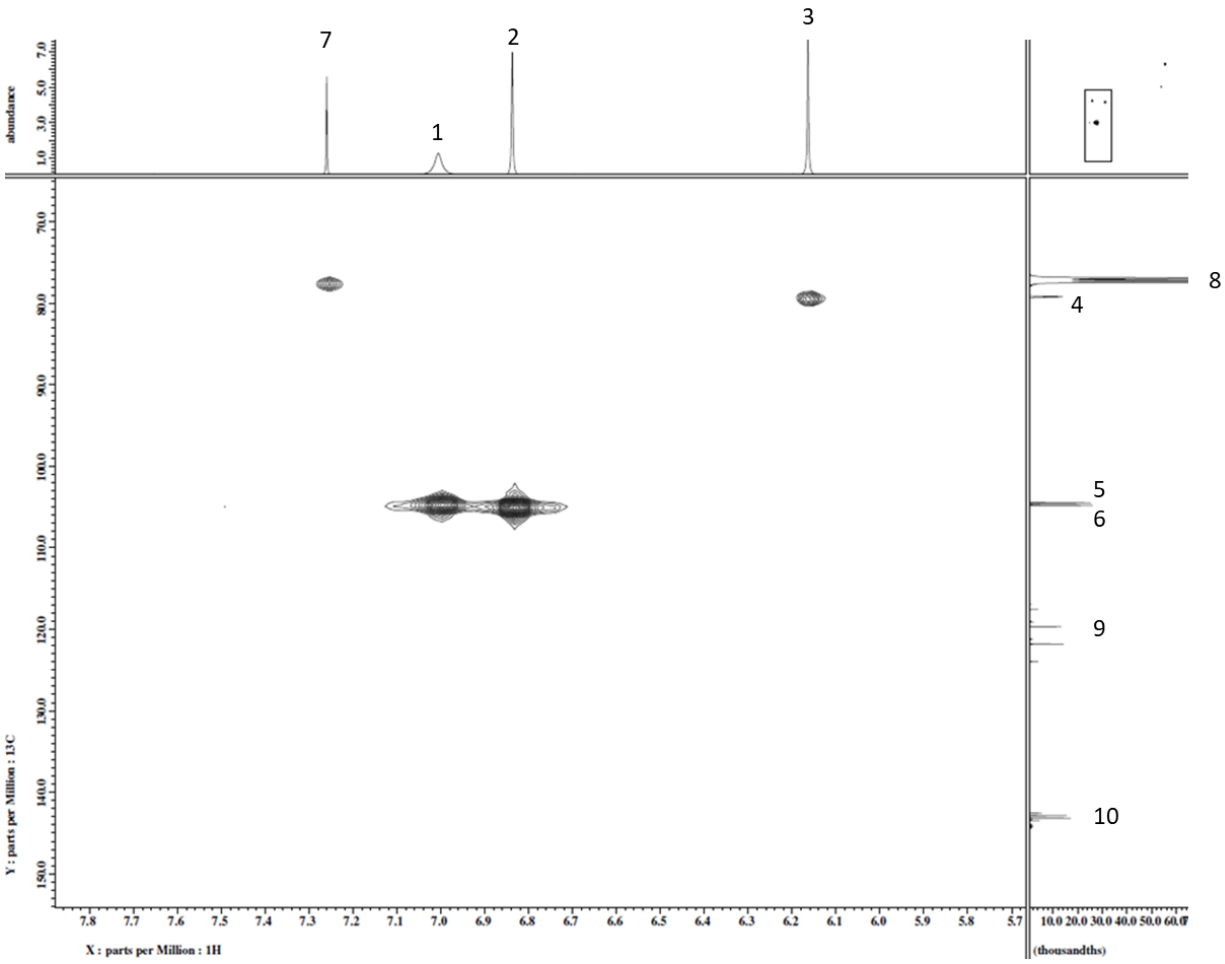

^{1}H NMR spectrum-

Peaks for $Cu_4(\mu\text{-}[3,5\text{-}(CF_3)_2Pz])_4(\mu\text{-}HC{\equiv}CH)_2$: δ (ppm) 6.16 (CH), 6.84 (Pz-H)
Peak for$\{\mu\text{-}[3,5\text{-}(CF_3)_2Pz]Cu\}_3$: 7.01 (Pz-H)

^{13}C NMR spectrum-

Peaks for $Cu_4(\mu\text{-}[3,5\text{-}(CF_3)_2Pz])_4(\mu\text{-}HC{\equiv}CH)_2$: δ (ppm) 79.2 (C≡C), 104.8 (C-4)
Peak for$\{\mu\text{-}[3,5\text{-}(CF_3)_2Pz]Cu\}_3$: 104.5 (Pz-H)

In the HMQC spectrum, ^{1}H signals # 3 and 2 (6.16 ppm (CH), 6.84 ppm (Pz-H) respectively, of $Cu_4(\mu\text{-}[3,5\text{-}(CF_3)_2Pz])_4(\mu\text{-}HC{\equiv}CH)_2$) corresponds to ^{13}C signals # 4 and 6 (79.2 (C≡C), 104.8 (C-4) respectively), while # 1 (7.01 ppm (Pz-H)) corresponds to # 5 (104.5 ppm (Pz-H) of $\{\mu\text{-}[3,5\text{-}(CF_3)_2Pz]Cu\}_3$). The # 7 is the solvent peak corresponding to # 8. There are no proton cross-peaks for # 9 and 10 as these peaks corresponds to CF_3 and C-3/C-5 carbons.

Figure S5. ^{1}H NMR spectra of $Cu_2(\mu\text{-}[3,5\text{-}(CF_3)_2Pz])_2(HC{\equiv}CH)_2$ **(5)** (in CD_2Cl_2) in the presence of excess acetylene at various temperatures. Peak at 4.86 ppm (-70 °C) is the signal corresponding to coordinated acetylene.

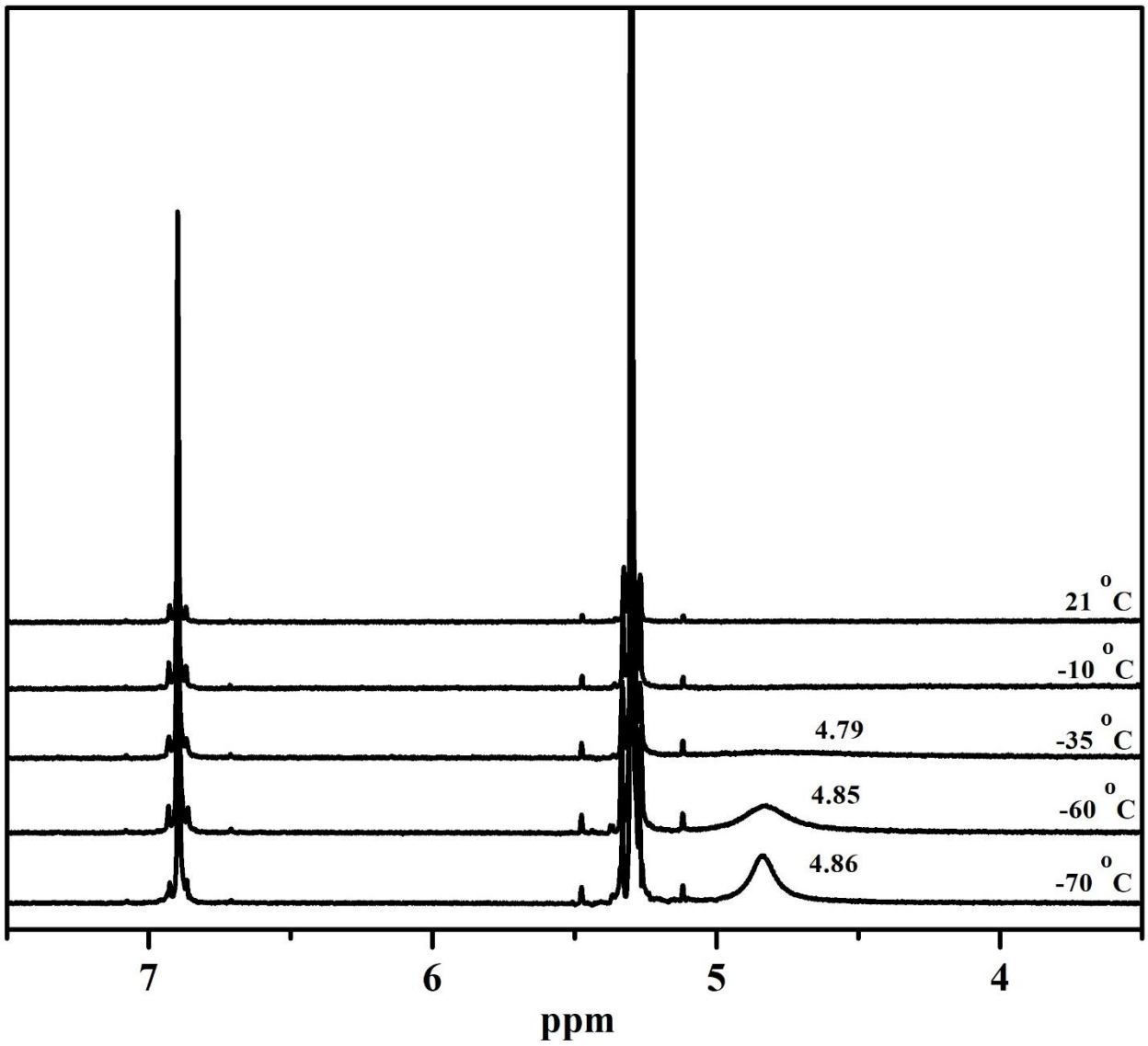

Figure S6. ^{19}F NMR spectra of $Cu_2(\mu\text{-}[3,5\text{-}(CF_3)_2Pz])_2(HC{\equiv}CH)_2$ **(5)** (in CD_2Cl_2) in presence of excess acetylene at various temperatures. Peak at -59.68 ppm (-70 °C) is the signal corresponding to **5**.

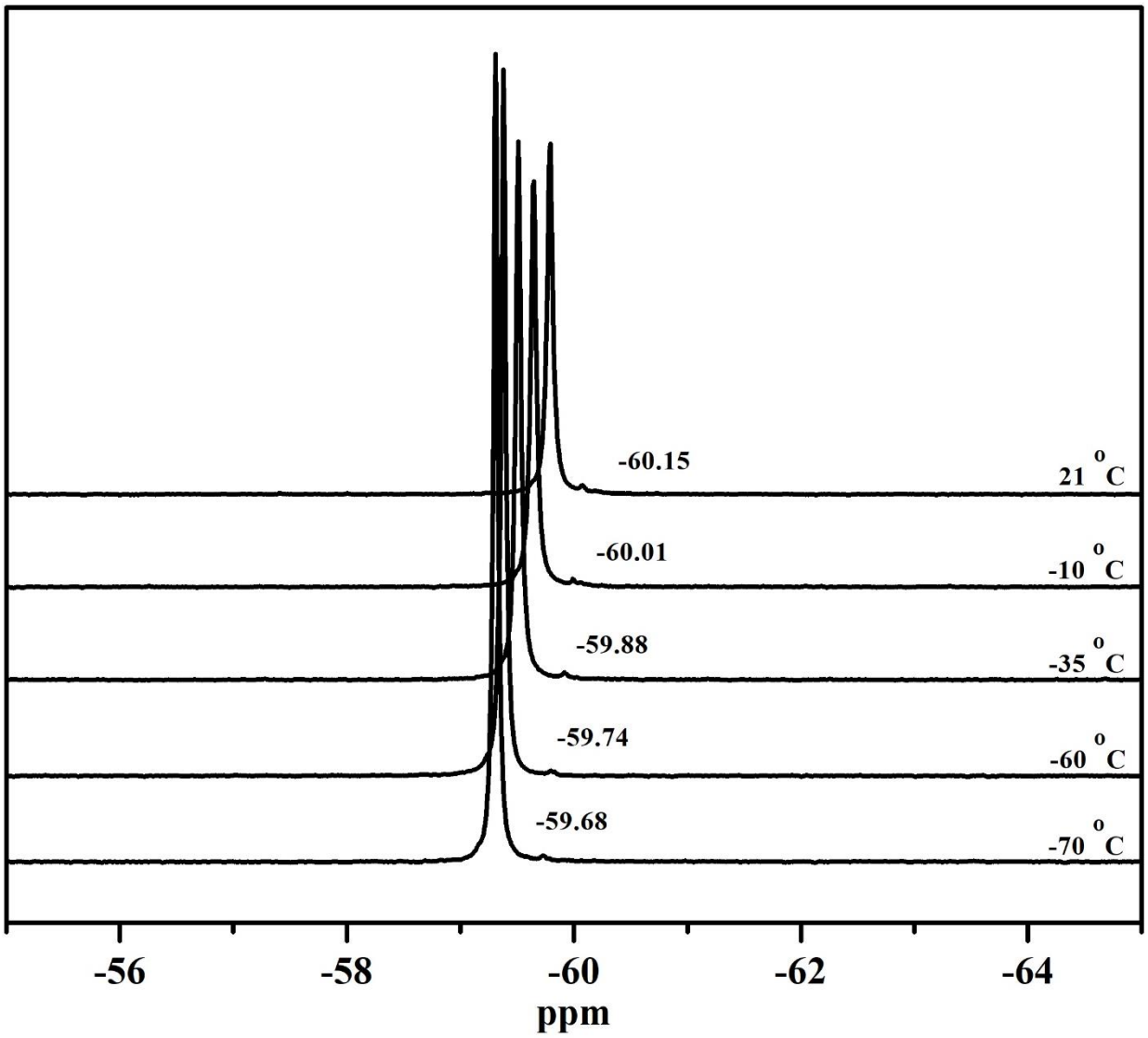

Figure S7. Raman spectrum of solid $Cu_4(\mu\text{-}[3,5\text{-}(CF_3)_2Pz])_4(\mu\text{-}HC{\equiv}CH)_2$ **(4)**

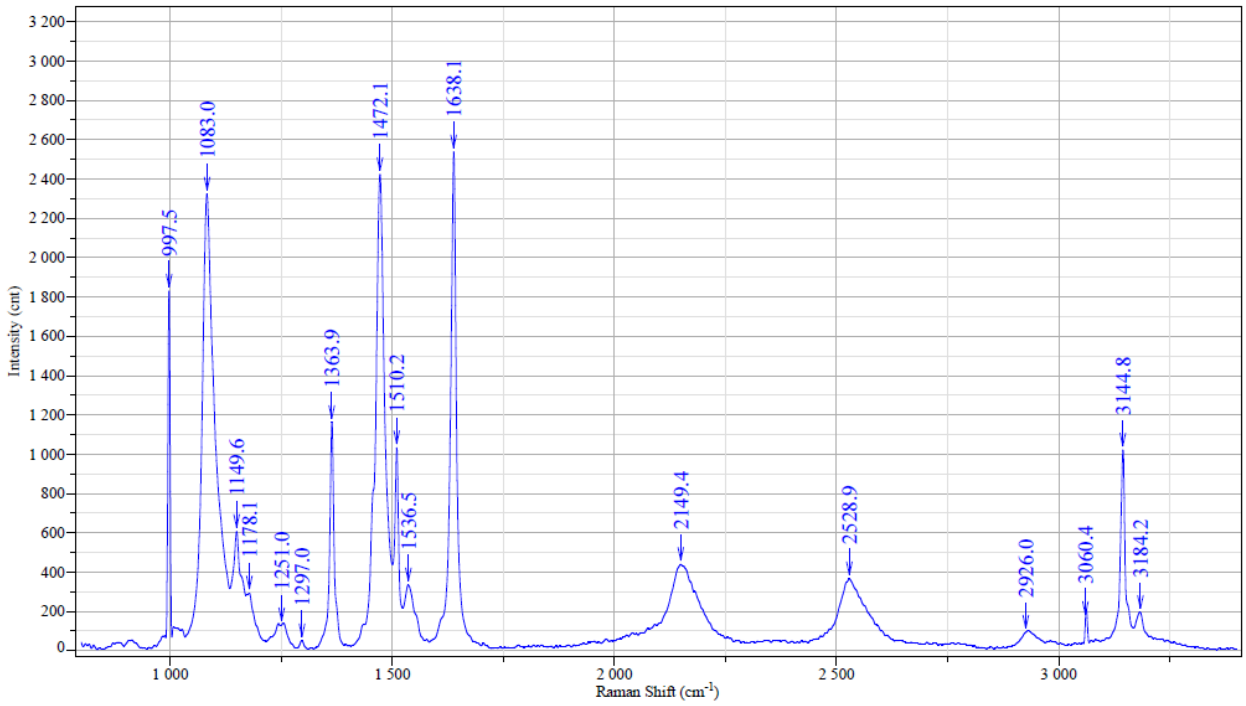

Exposition	10	Slit	100
Accumulation	5 x 4	Operator	Parasar
Laser	632.817	Sample	Cu_acetylene
Spectro	Multi	Remark	
Hole	200	Power	

HORIBA JOBIN YVON

Figure S8. ^{1}H NMR spectrum of $Cu_4(\mu\text{-}[4\text{-Br-}3,5\text{-}(CF_3)_2Pz])_4(\mu\text{-}HC{\equiv}CH)_2$ **(6)** in $CDCl_3$ at room temperature (top) and $Cu_2(\mu\text{-}[4\text{-Br-}3,5\text{-}(CF_3)_2Pz])_2(HC{\equiv}CH)_2$ (**8**) with excess acetylene in CD_2Cl_2 at -70 °C (bottom). Signals at δ 2.07 and 1.55 ppm in the top figure are due to free acetylene and adventitious moisture, respectively.

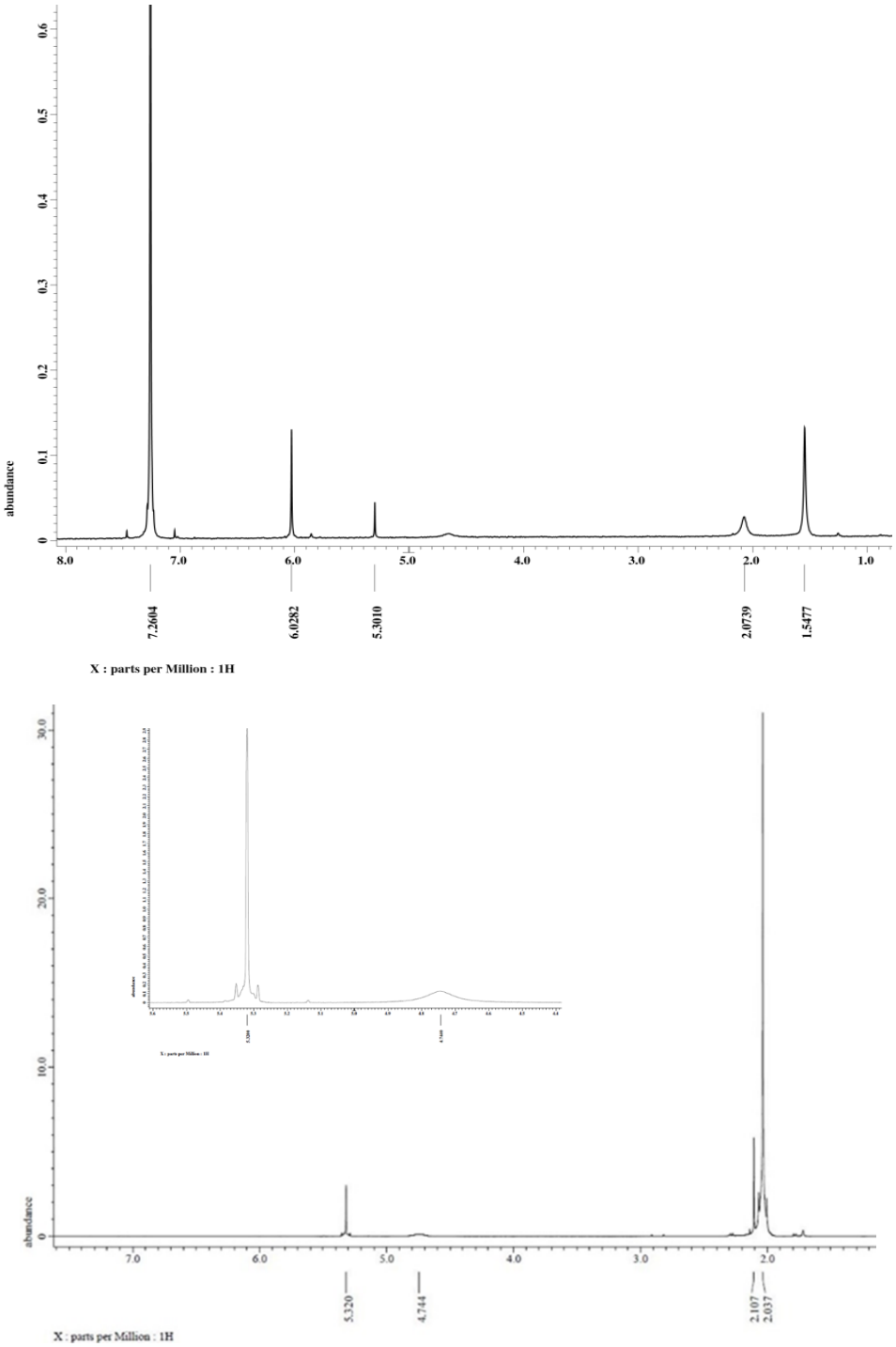

Figure S9. ^{19}F NMR spectrum of $Cu_4(\mu\text{-}[4\text{-Br-}3,5\text{-}(CF_3)_2Pz])_4(\mu\text{-}HC{\equiv}CH)_2$ **(6)** in $CDCl_3$ at room temperature (top) and $Cu_2(\mu\text{-}[4\text{-Br-}3,5\text{-}(CF_3)_2Pz])_2(HC{\equiv}CH)_2$ (**8**) with excess acetylene in CD_2Cl_2 at -70 °C (bottom). The signal for **{**$[4\text{-Br-}3,5\text{-}(CF_3)_2Pz]Cu\}_3$ impurity resulting from some acetylene loss from **6** was observed at -61.2 (br s) in the top figure.

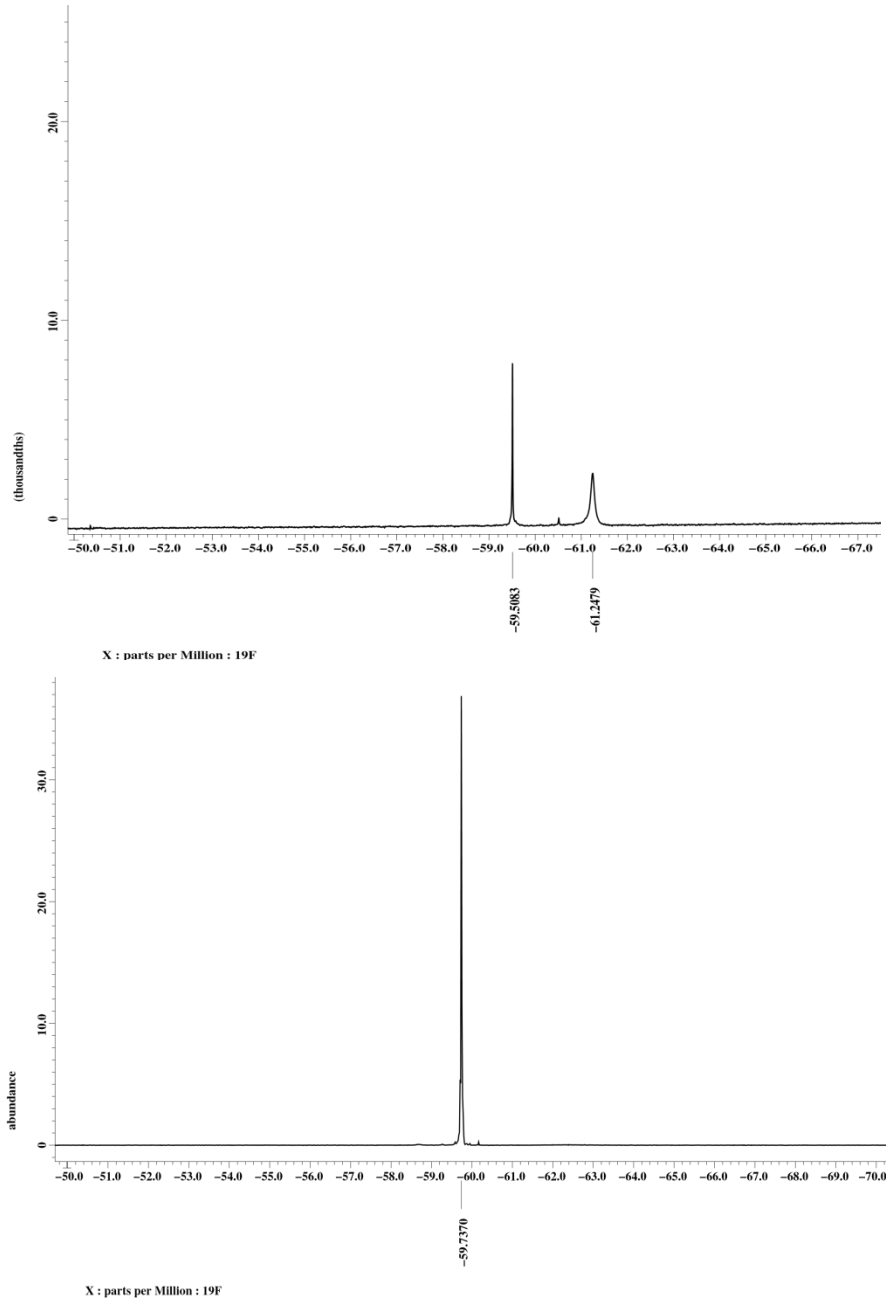

Figure S10. ^{1}H NMR spectra of $Cu_2(\mu\text{-}[4\text{-Br-}3,5\text{-}(CF_3)_2Pz])_2(HC{\equiv}CH)_2$ **(8)** (in CD_2Cl_2) in presence of excess acetylene at various temperatures. Peak at 4.75 ppm (-70 °C) is the signal corresponding to coordinated acetylene.

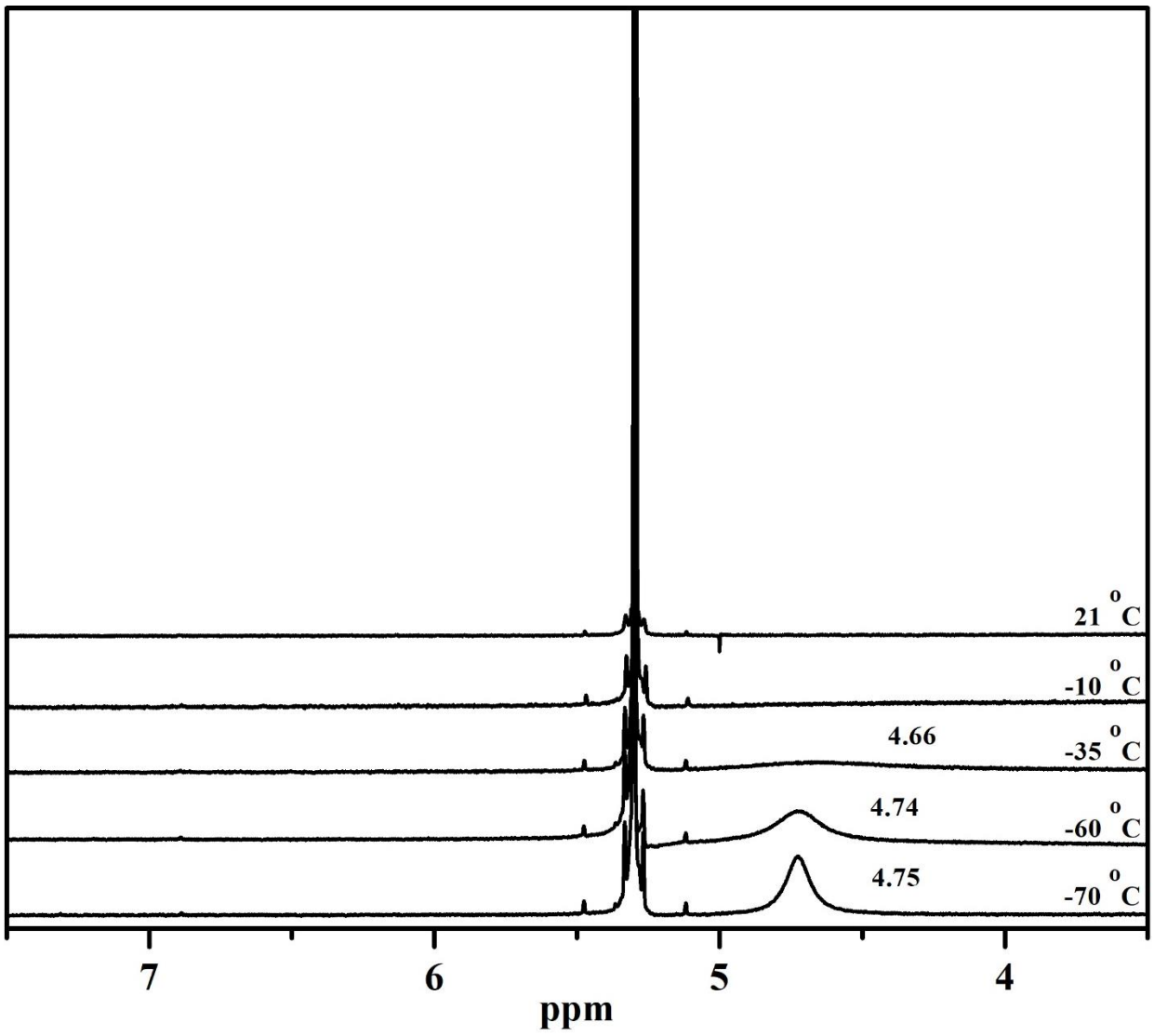

Figure S11. ^{19}F NMR spectra of $Cu_2(\mu\text{-}[4\text{-Br-}3,5\text{-}(CF_3)_2Pz])_2(HC{\equiv}CH)_2$ **(8)** (in CD_2Cl_2) in presence of excess acetylene at various temperatures. Peak at -59.74 ppm (-70 °C) is the signal corresponding to **8**.

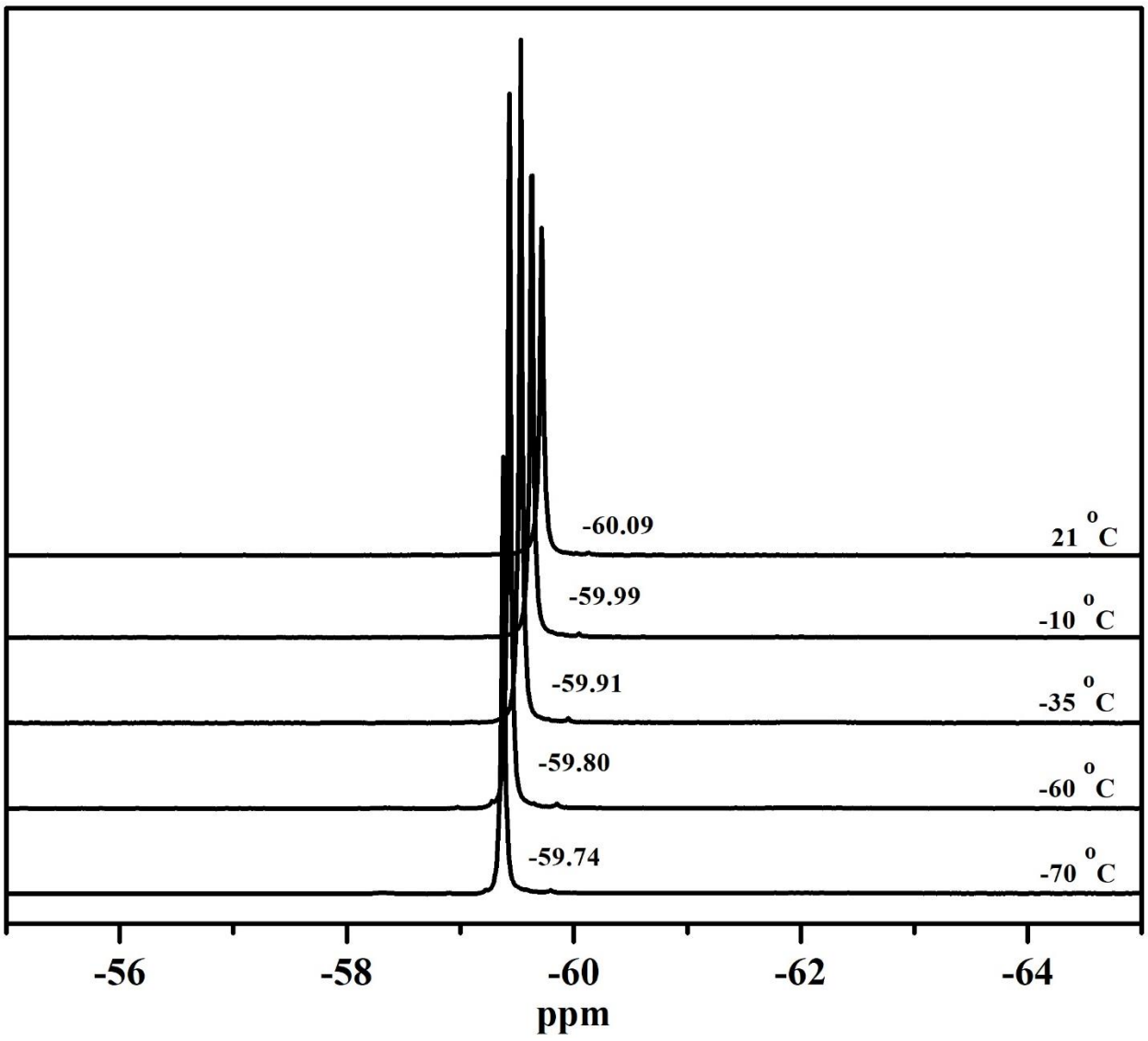

Figure S12. Raman spectrum of solid $Cu_4(\mu\text{-}[4\text{-Br-3,5-}(CF_3)_2Pz])_4(\mu\text{-}HC{\equiv}CH)_2$ **(6)**

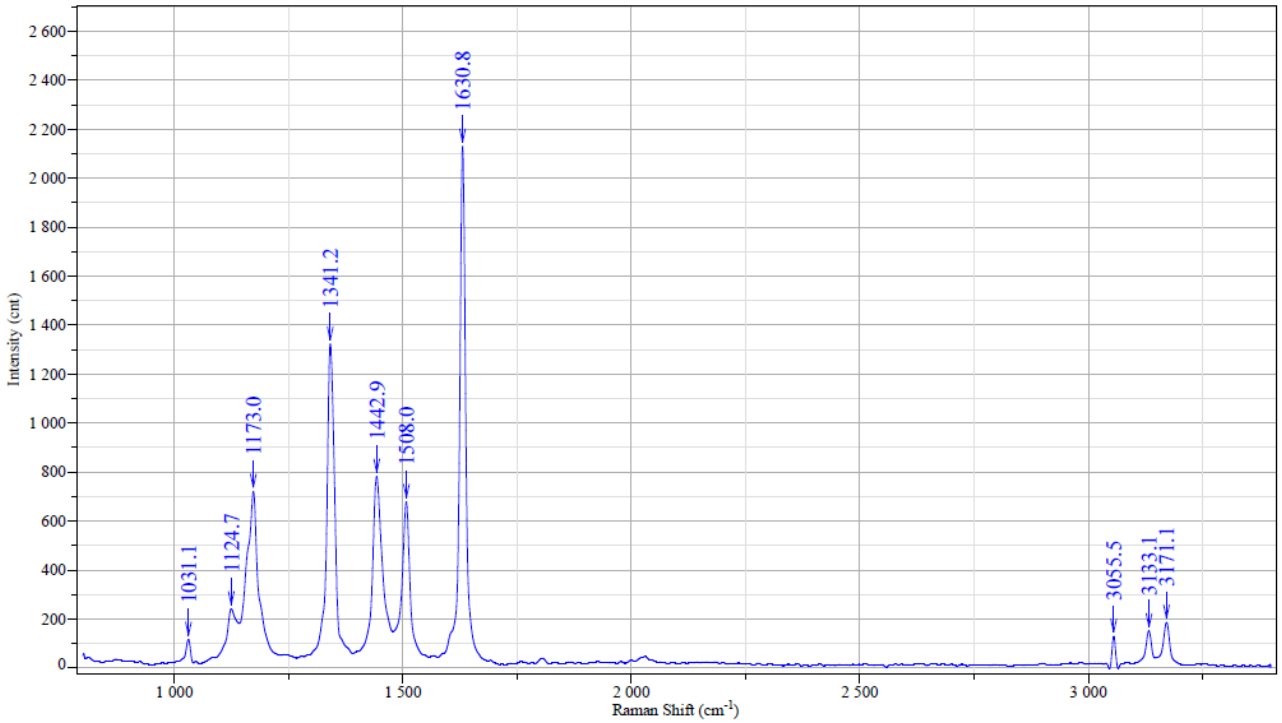

Exposition	10	Slit	100
Accumulation	5 x 4	Operator	Parasar
Laser	632.817	Sample	4Br3,5(CF3)2PZCu3_acetyle
Spectro	Multi	Remark	
Hole	200	Power	

HORIBA JOBIN YVON

Figure S13. Raman spectrum of solid $Cu_2(\mu\text{-}[4\text{-Br-}3,5\text{-}(CF_3)_2Pz])_2(HC{\equiv}CH)_2{\bullet}C_7H_8$ **(8)**

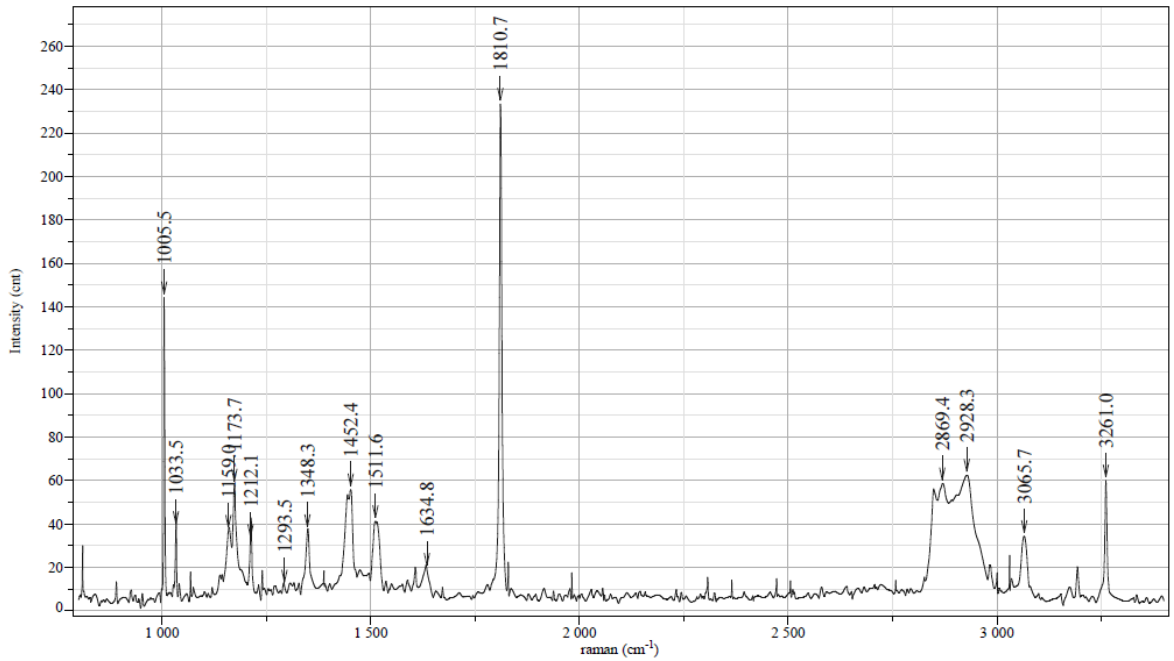

Exposition	5	Slit	100
Accumulation	10 x 4	Operator	
Laser	632.817	Sample	
Spectro	Multi	Remark	
Hole	200	Power	

HORIBA JOBIN YVON

Figure S14. IR spectra of $Cu_2(\mu\text{-}[4\text{-Br-}3,5\text{-}(CF_3)_2Pz])_2(HC{\equiv}CH)_2$ (**8**), and the products resulting from its decomposition with the loss of acetylene at room temperature, in open to air, and the likely formation of $Cu_4(\mu\text{-}[4\text{-Br-}3,5\text{-}(CF_3)_2Pz])_4(\mu\text{-}HC{\equiv}CH)_2$ **(6)**. The peaks at 1810 cm^{-1} and 1634 cm^{-1} correspond to complexes **8** and **6.**

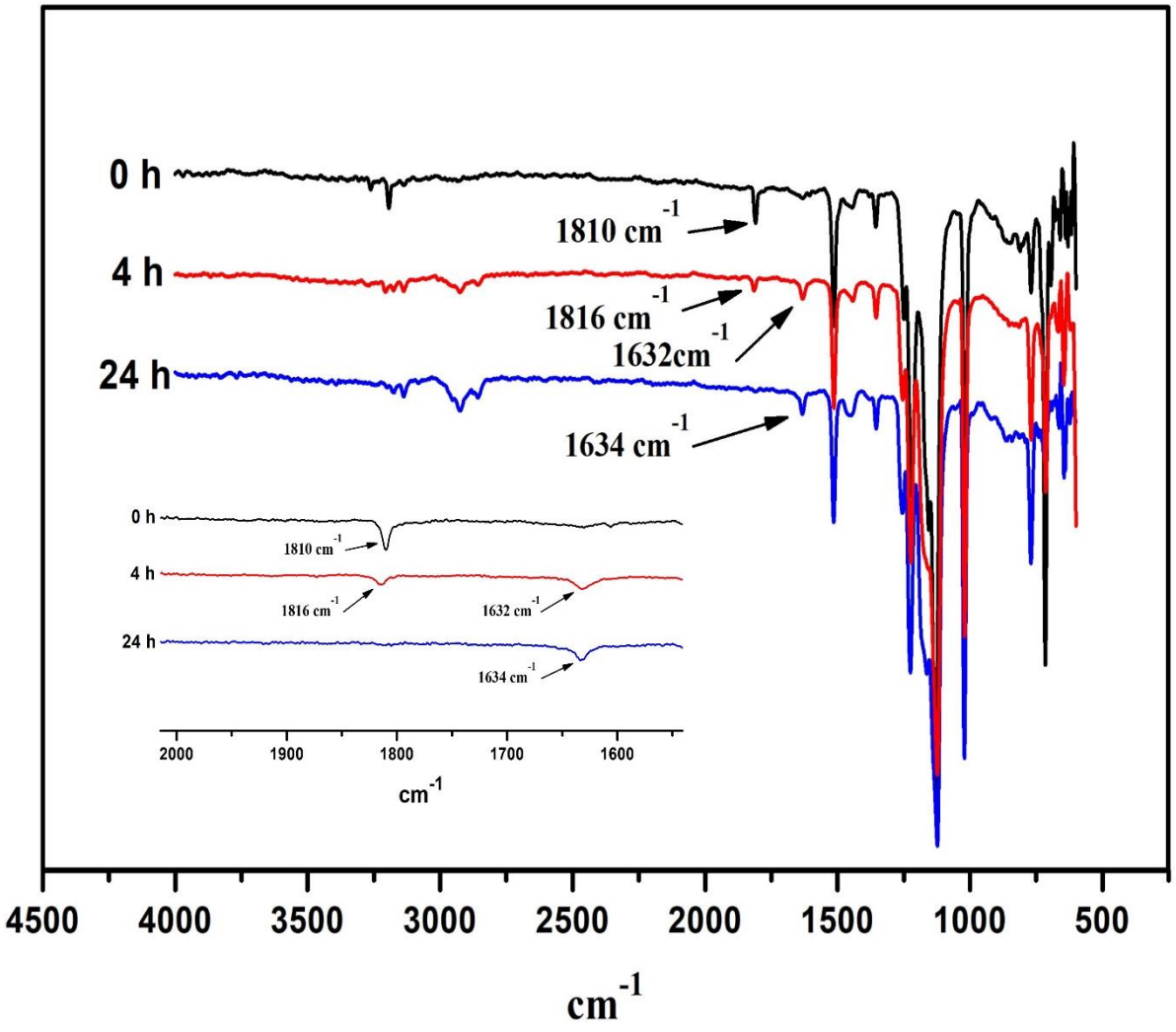

Figure S15. Raman spectra showing the conversion of $Cu_2(\mu\text{-}[4\text{-Br-}3,5\text{-}(CF_3)_2Pz])_2(HC{\equiv}CH)_2$ **(8)** to $Cu_4(\mu\text{-}[4\text{-Br-}3,5\text{-}(CF_3)_2Pz])_4(\mu\text{-}HC{\equiv}CH)_2$ **(6)** with time at room temperature, in open air. The peaks at 1811 cm^{-1} and 1636 cm^{-1} correspond to complexes **8** and **6,** respectively. (Note: Oil coated $Cu_2(\mu\text{-}[4\text{-Br-}3,5\text{-}(CF_3)_2Pz])_2(HC{\equiv}CH)_2{\bullet}C_7H_8$ crystals were used in this study).

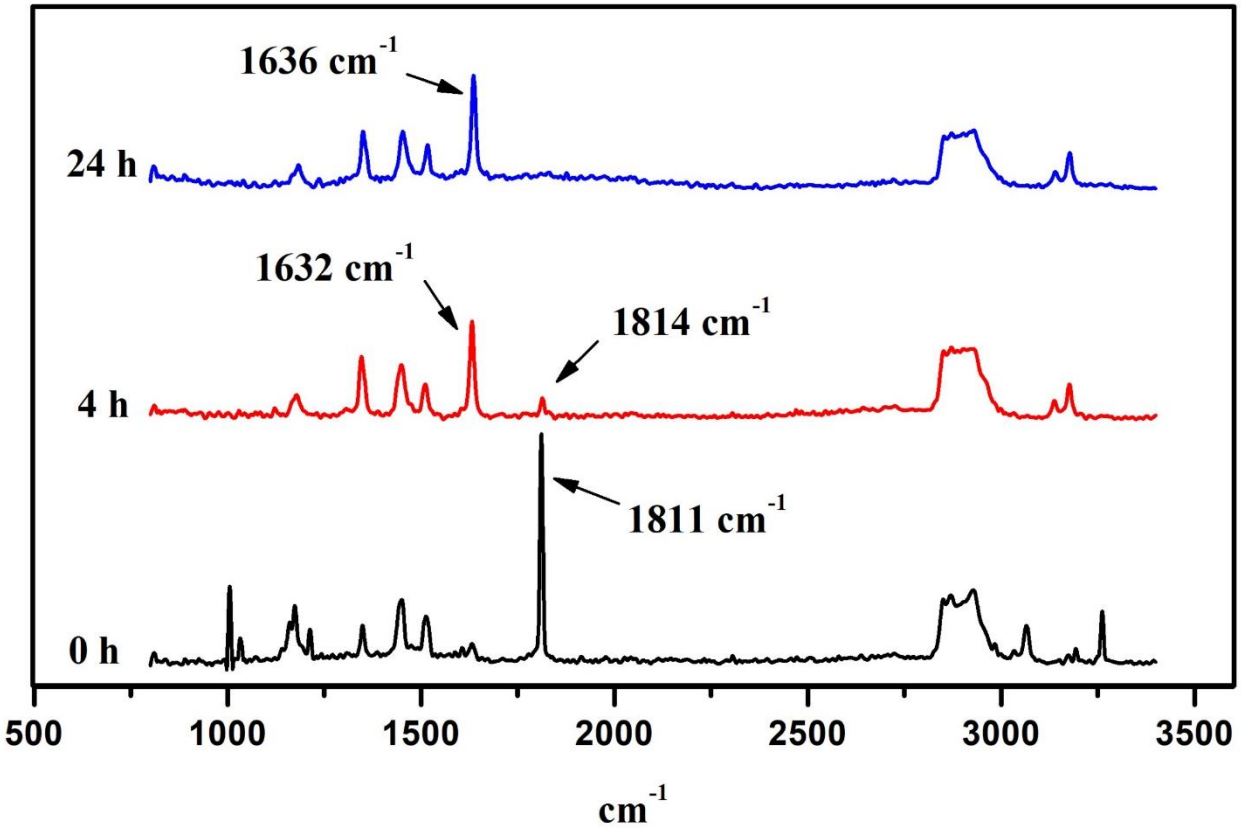

Figure S16. ^{1}H NMR spectrum of $Cu_4(\mu\text{-}[4\text{-}Cl\text{-}3,5\text{-}(CF_3)_2Pz])_4(\mu\text{-}HC{\equiv}CH)_2$ **(7)** in $CDCl_3$ at room temperature. Signals at δ 2.05 and 1.54 ppm are due to free acetylene and adventitious moisture, respectively.

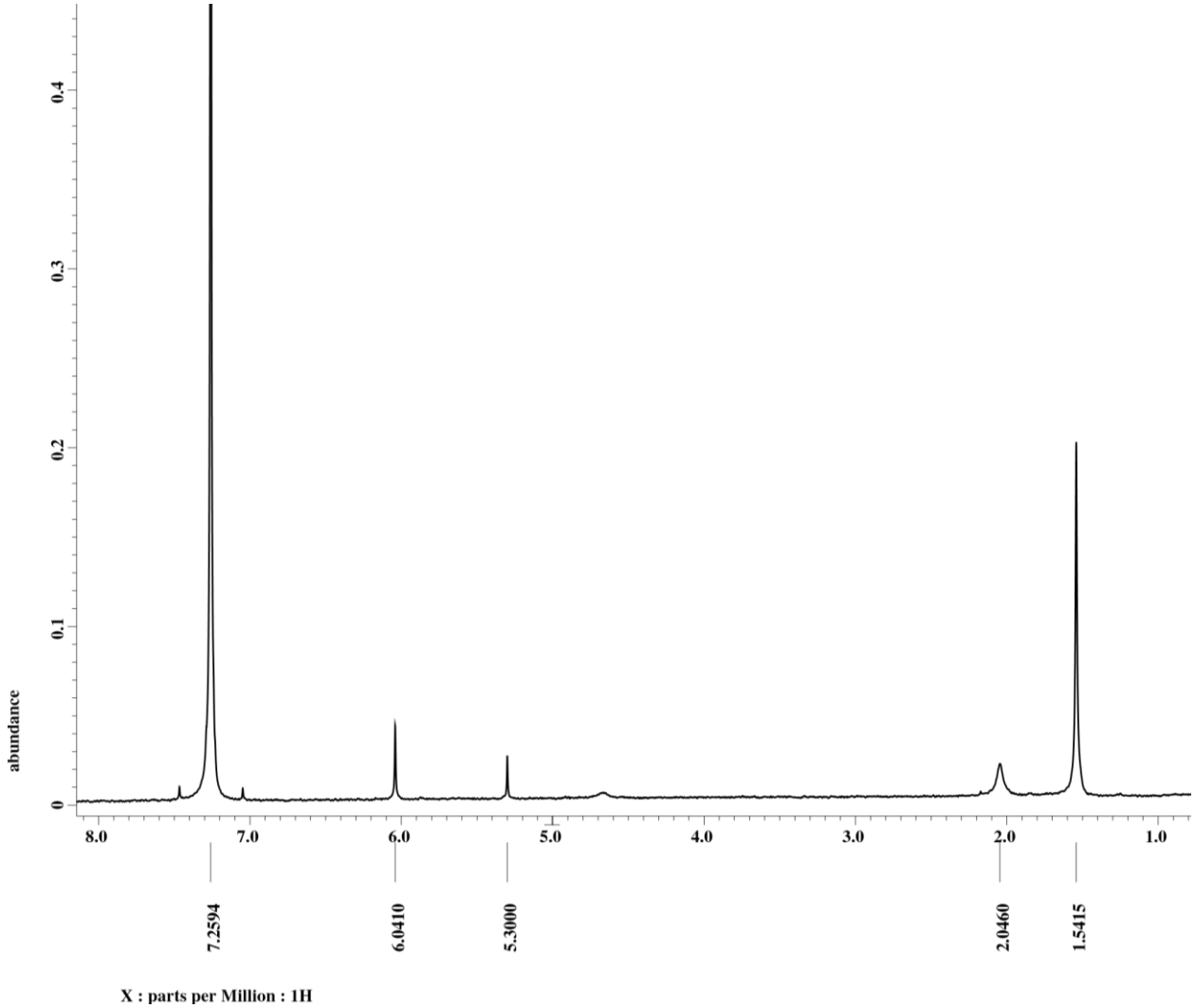

Figure S17. ^{19}F NMR spectrum of $Cu_4(\mu\text{-}[4\text{-}Cl\text{-}3,5\text{-}(CF_3)_2Pz])_4(\mu\text{-}HC{\equiv}CH)_2$ **(7)** in $CDCl_3$ at room temperature. The signal for **{**$[4\text{-}Cl\text{-}3,5\text{-}(CF_3)_2Pz]Cu\}_3$ impurity was observed at -61.1 (br s), which is result of some acetylene loss from **7** in solutions at room temperature.

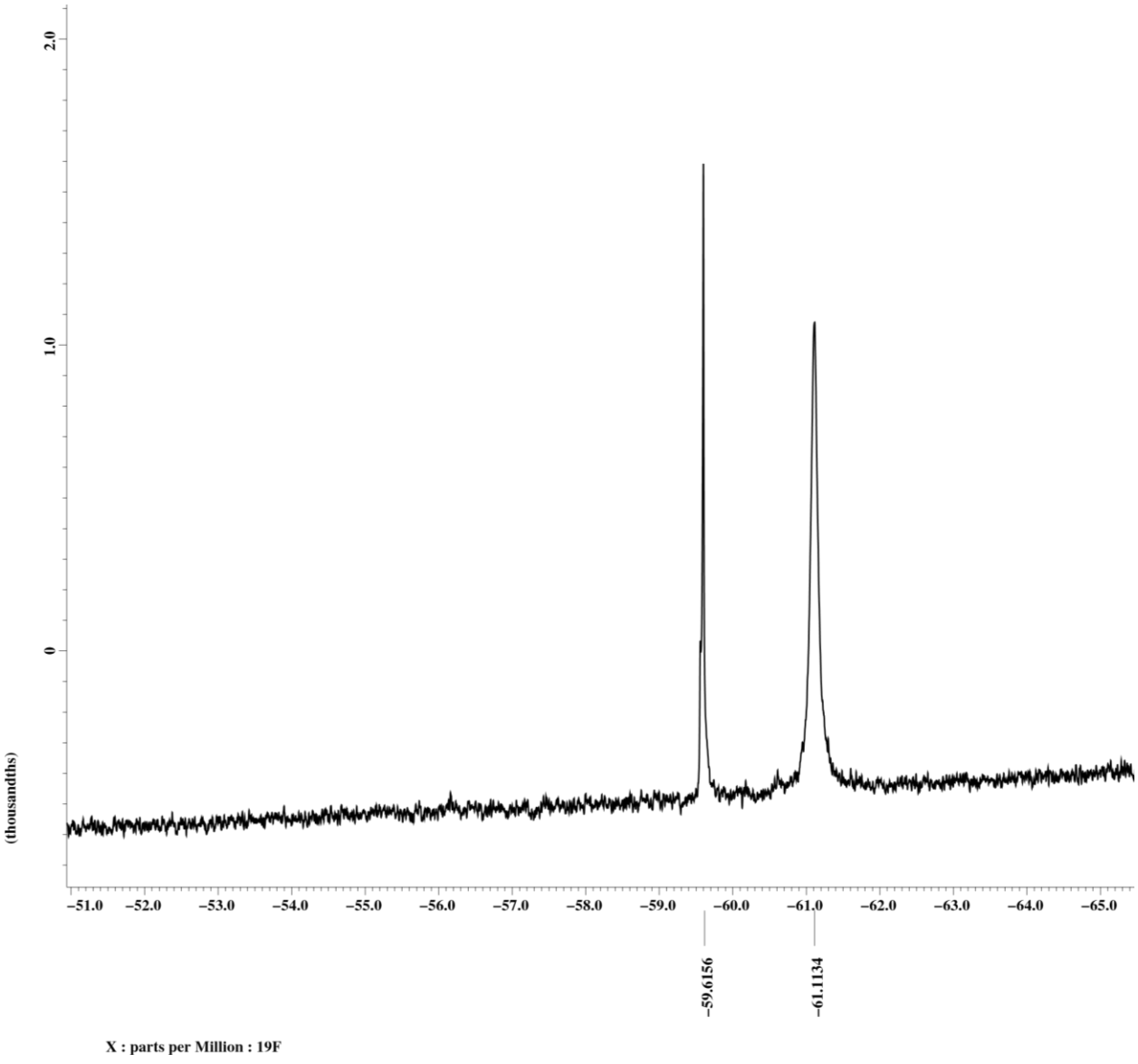

Figure S18. Raman spectrum of solid $Cu_4(\mu\text{-}[4\text{-Cl-3,5-}(CF_3)_2Pz])_4(\mu\text{-}HC{\equiv}CH)_2$ **(7)**

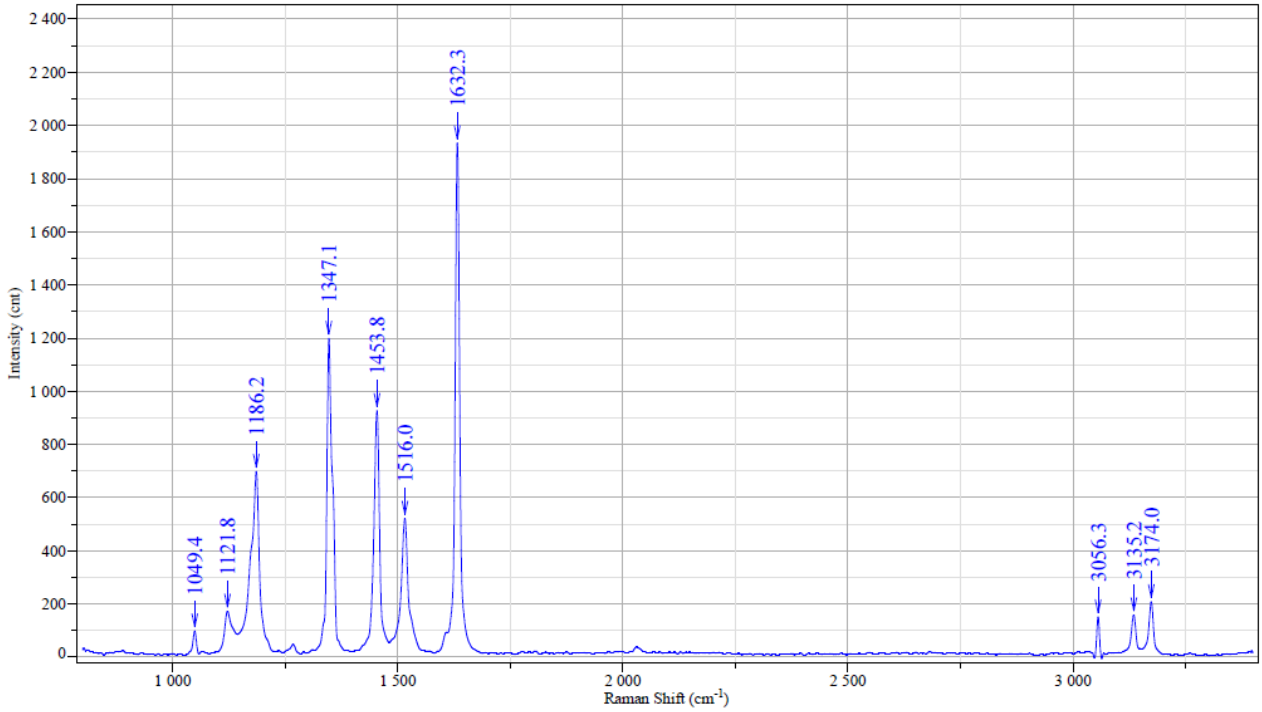

Exposition	10	Slit	100
Accumulation	5 x 4	Operator	Parasar
Laser	632.817	Sample	4Cl3,5(CF3)2PZCu3_acetyle
Spectro	Multi	Remark	
Hole	200	Power	

HORIBA JOBIN YVON

Figure S19. ^{1}H NMR spectrum of $Cu_2(\mu\text{-}[3,5\text{-}(CF_3)_2Pz])_2(HC{\equiv}CPh)_2$ **(9)** in $CDCl_3$ at room temperature.

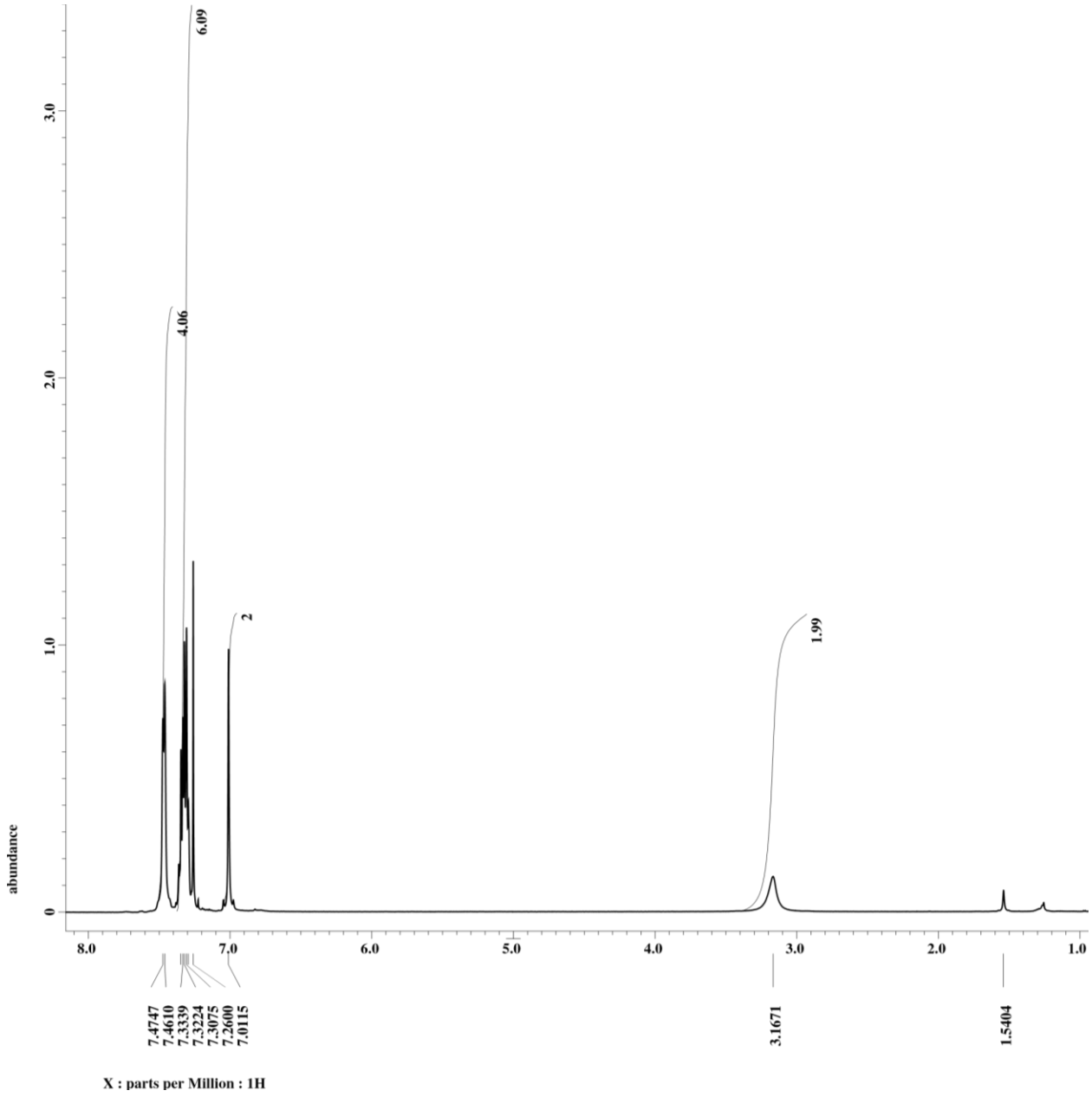

Figure S20. ^{19}F NMR spectrum of $Cu_2(\mu\text{-}[3,5\text{-}(CF_3)_2Pz])_2(HC{\equiv}CPh)_2$ **(9)** in $CDCl_3$ at room temperature.

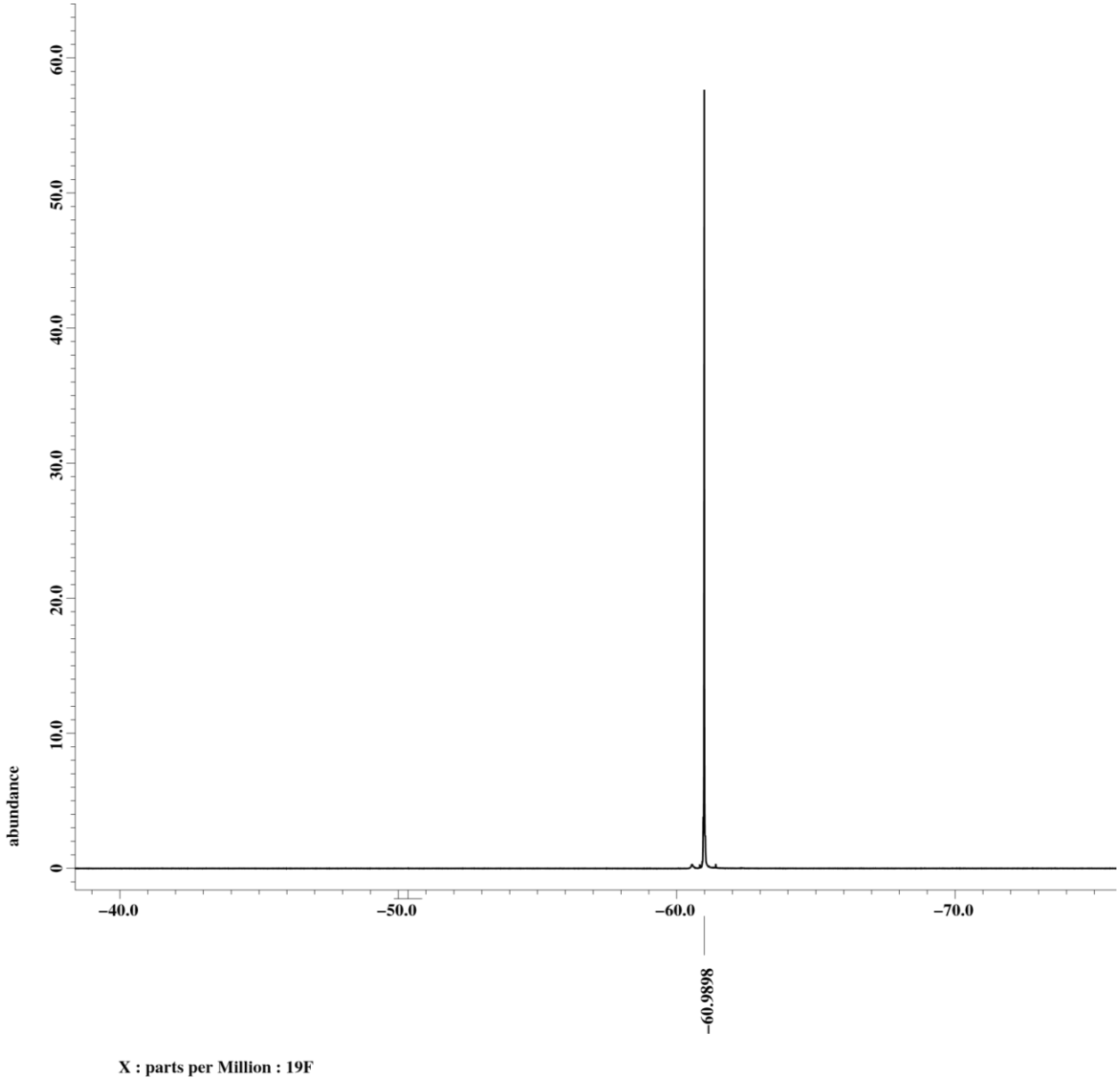

Figure S21. $^{13}C\{^{1}H\}$ NMR spectrum of $Cu_2(\mu\text{-}[3,5\text{-}(CF_3)_2Pz])_2(HC{\equiv}CPh)_2$ **(9)** in CD_2Cl_2 at room temperature.

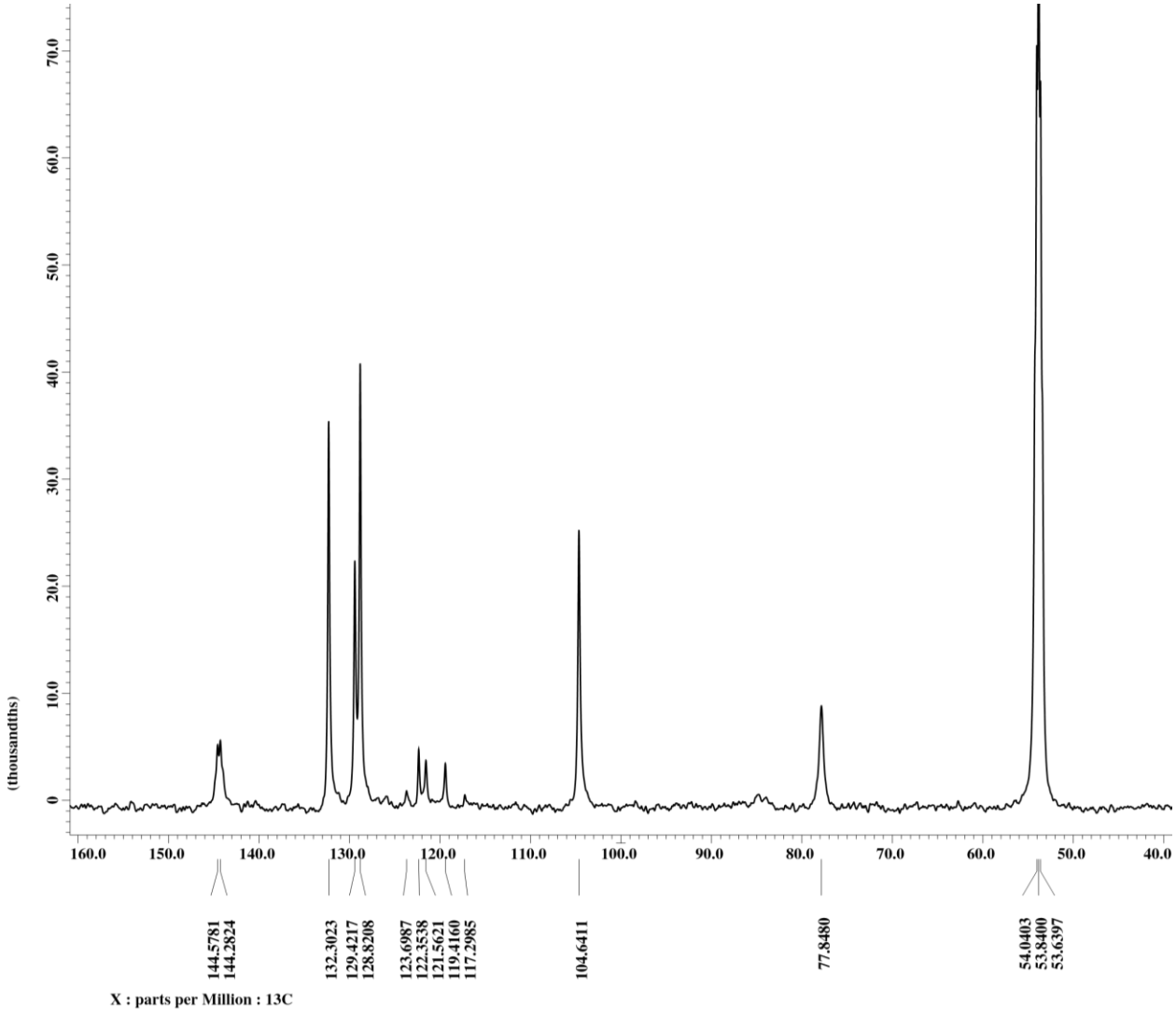

Figure S22. Raman spectrum of solid $Cu_2(\mu\text{-}[3,5\text{-}(CF_3)_2Pz])_2(HC{\equiv}CPh)_2$ **(9)**

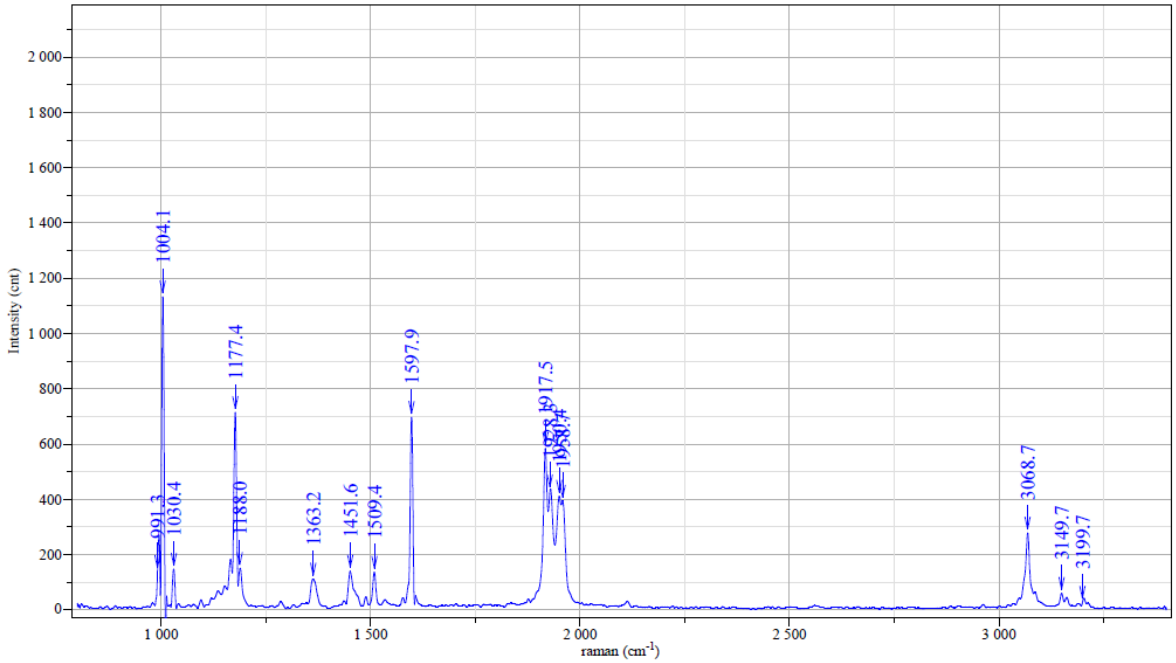

Exposition	5	Slit	100
Accumulation	5 x 4	Operator	
Laser	632.817	Sample	
Spectro	Multi	Remark	
Hole	200	Power	

HORIBA JOBIN YVON

Figure S23. ^{1}H NMR spectrum of $Cu_2(\mu\text{-}[3,5\text{-}(CF_3)_2Pz])_2(HC{\equiv}C(CH_2)_5C{\equiv}CH)$ **(10)** in $CDCl_3$ at room temperature.

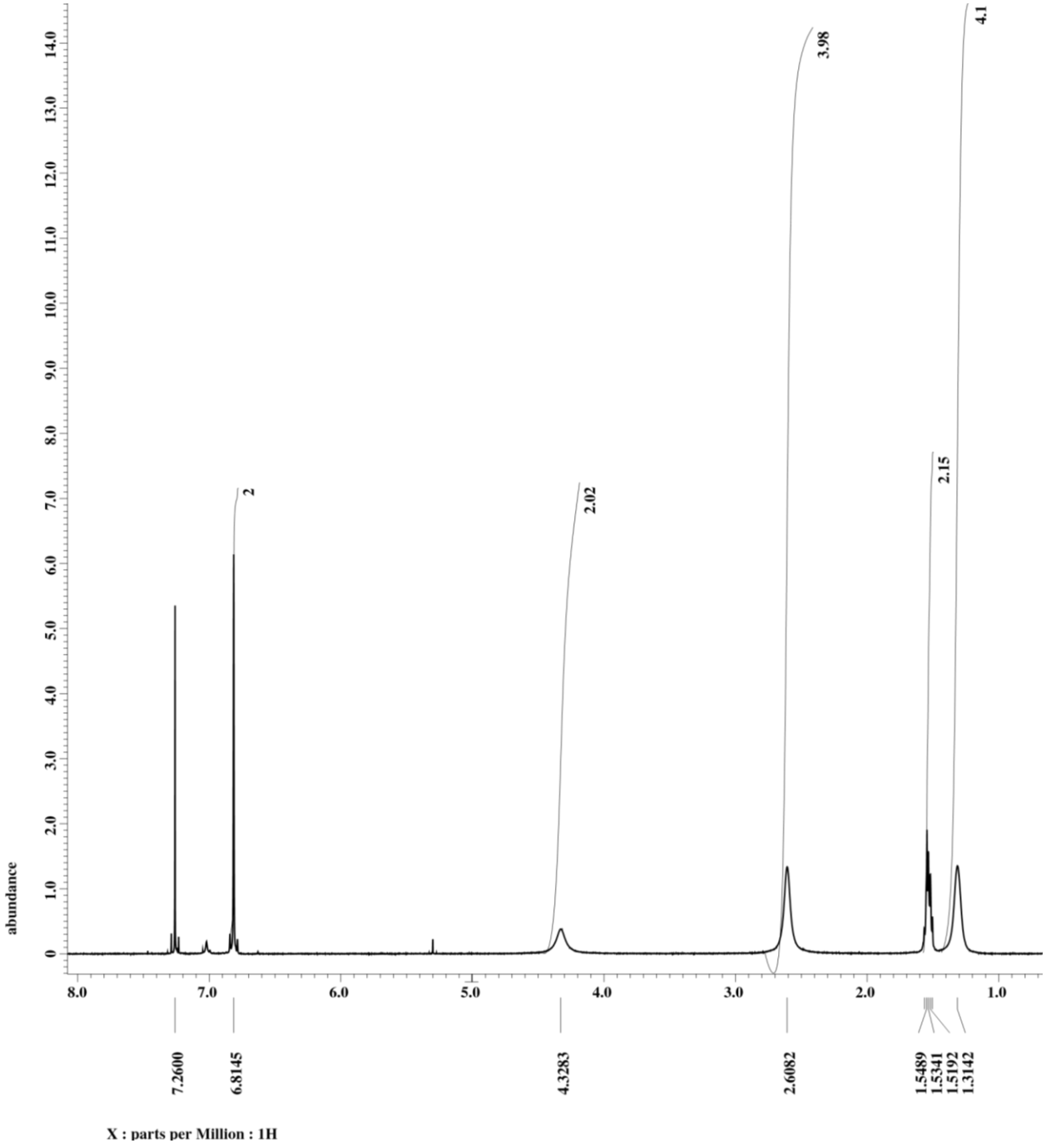

Figure S24. ^{19}F NMR spectrum of $Cu_2(\mu\text{-}[3,5\text{-}(CF_3)_2Pz])_2(HC{\equiv}C(CH_2)_5C{\equiv}CH)$ **(10)** in $CDCl_3$ at room temperature.

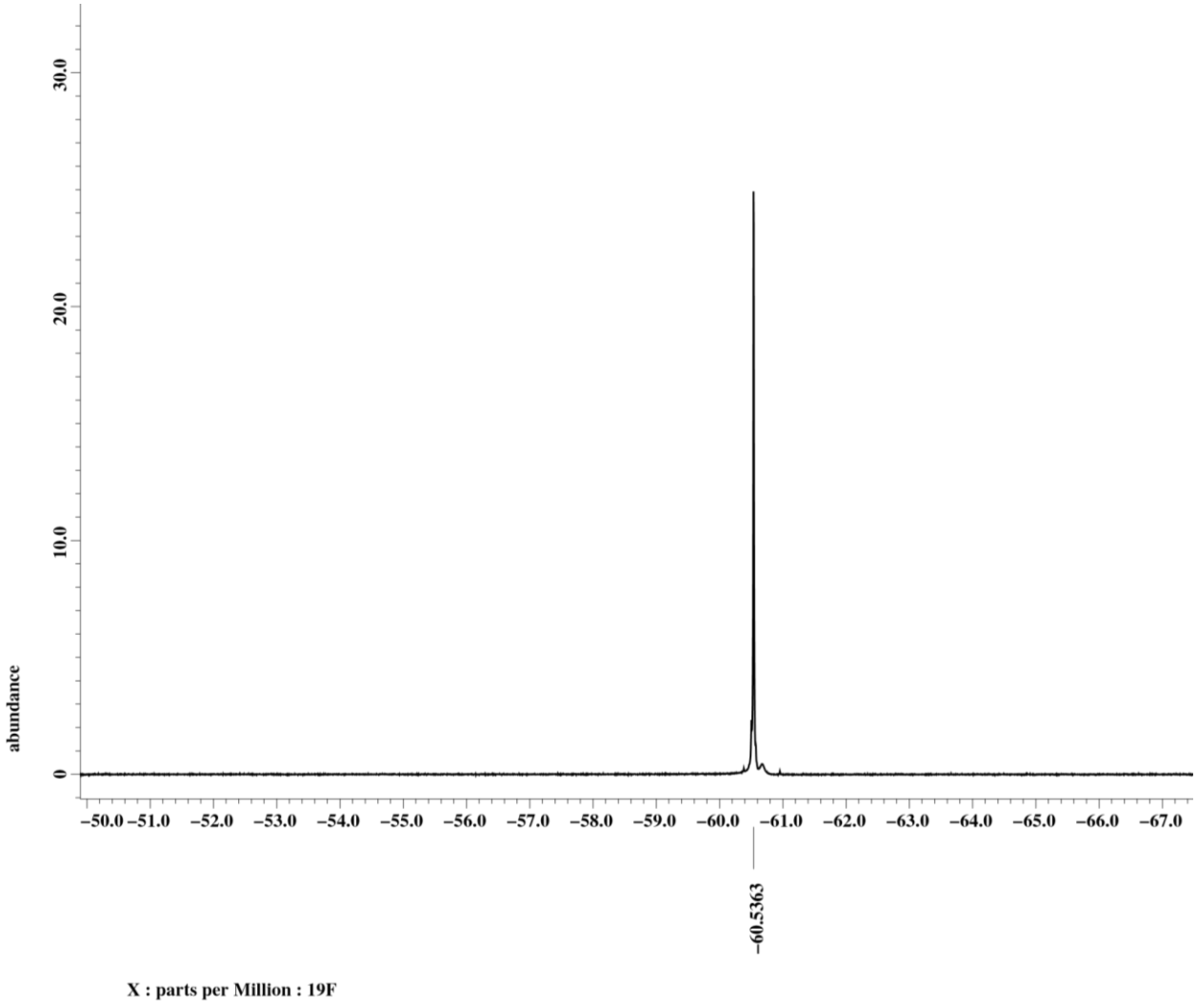

Figure S25. $^{13}C\{^{1}H\}$ NMR spectrum of $Cu_2(\mu\text{-}[3,5\text{-}(CF_3)_2Pz])_2(HC{\equiv}C(CH_2)_5C{\equiv}CH)$ **(10)** in CD_2Cl_2 at room temperature.

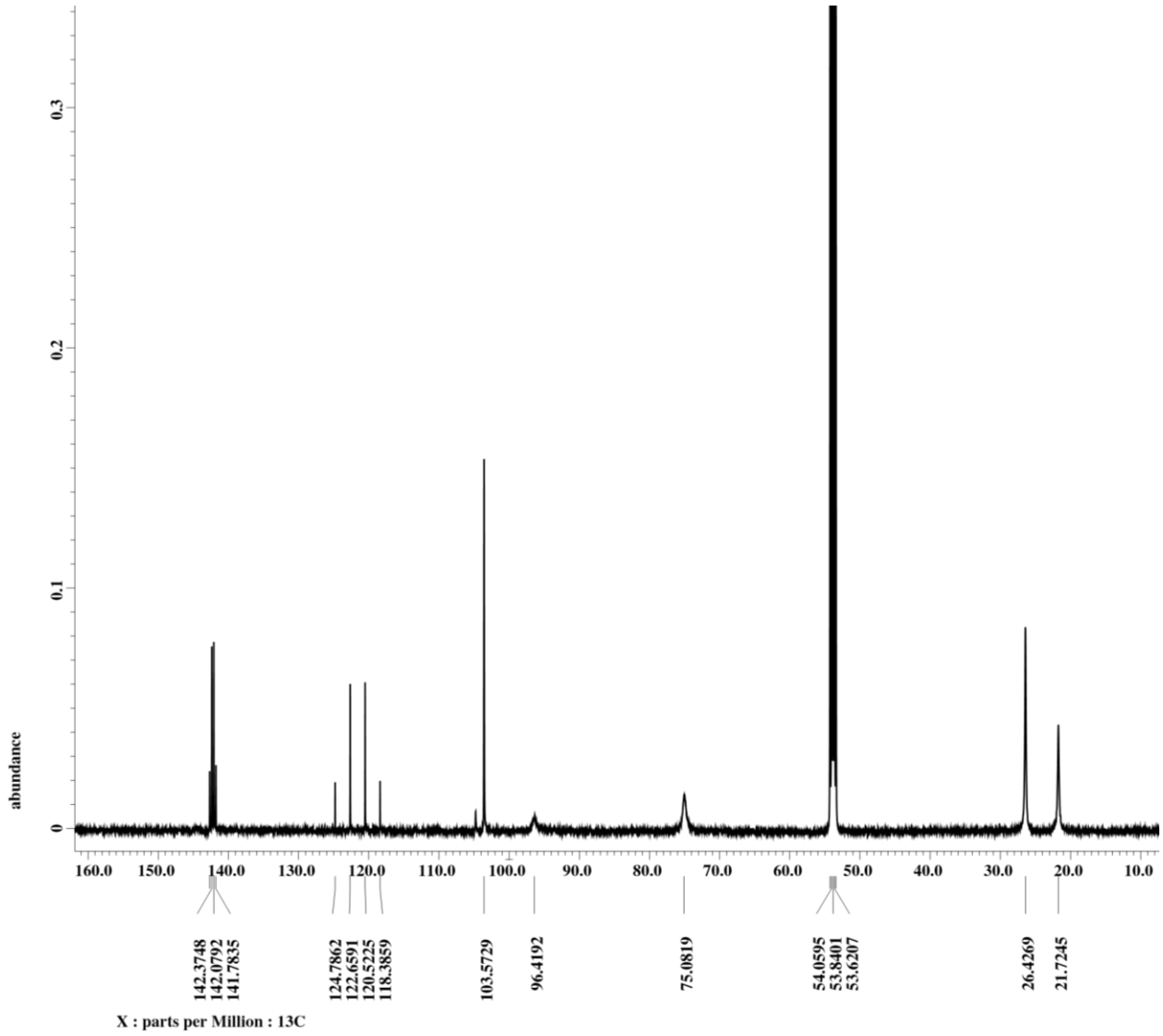

Figure S26. Raman spectrum of solid $Cu_2(\mu\text{-}[3,5\text{-}(CF_3)_2Pz])_2(HC{\equiv}C(CH_2)_5C{\equiv}CH)$ **(10)**

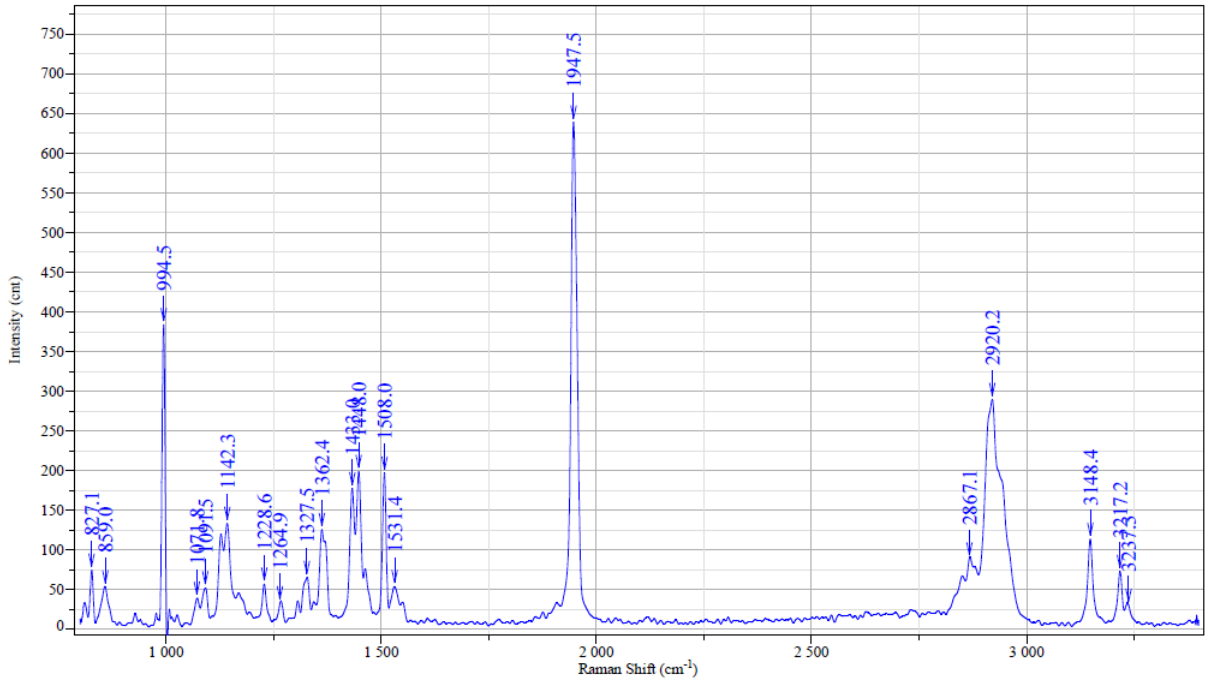

Exposition	5	Slit	100
Accumulation	5 x 4	Operator	Parasar
Laser	632.817	Sample	Cu_1,9Nonadiyne_2:3
Spectro	Multi	Remark	
Hole	200	Power	

HORIBA JOBIN YVON

Figure S27. Raman spectrum of solid $Cu_4(\mu\text{-}[3,5\text{-}(CF_3)_2Pz])_4(HC{\equiv}C(CH_2)_4C{\equiv}CH)_2$ **(11)**

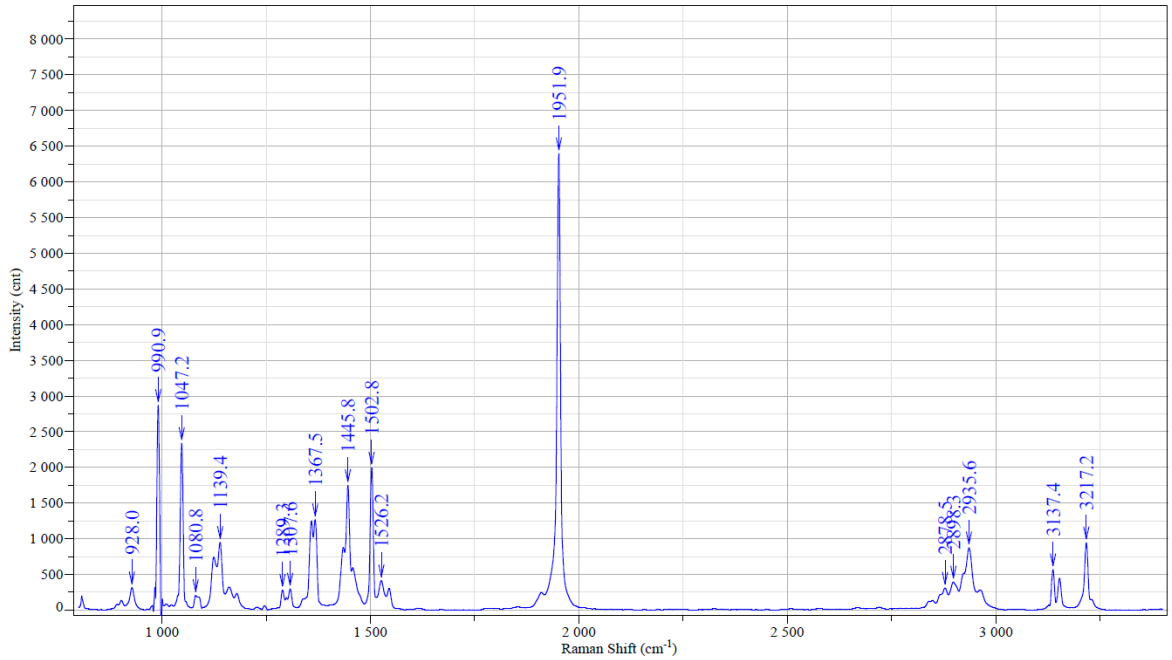

Exposition	10	Slit	100
Accumulation	10 x 4	Operator	Parasar
Laser	632.817	Sample	Cu3_1,7-Octadiyne
Spectro	Multi	Remark	
Hole	200	Power	

HORIBA JOBIN YVON

Figure S28. ^{1}H NMR spectrum of $Cu_4(\mu\text{-}[3,5\text{-}(CF_3)_2Pz])_4(C_2H_5C{\equiv}C(CH_2)_4C{\equiv}CC_2H_5)_2$ **(12)** in $CDCl_3$ at room temperature.

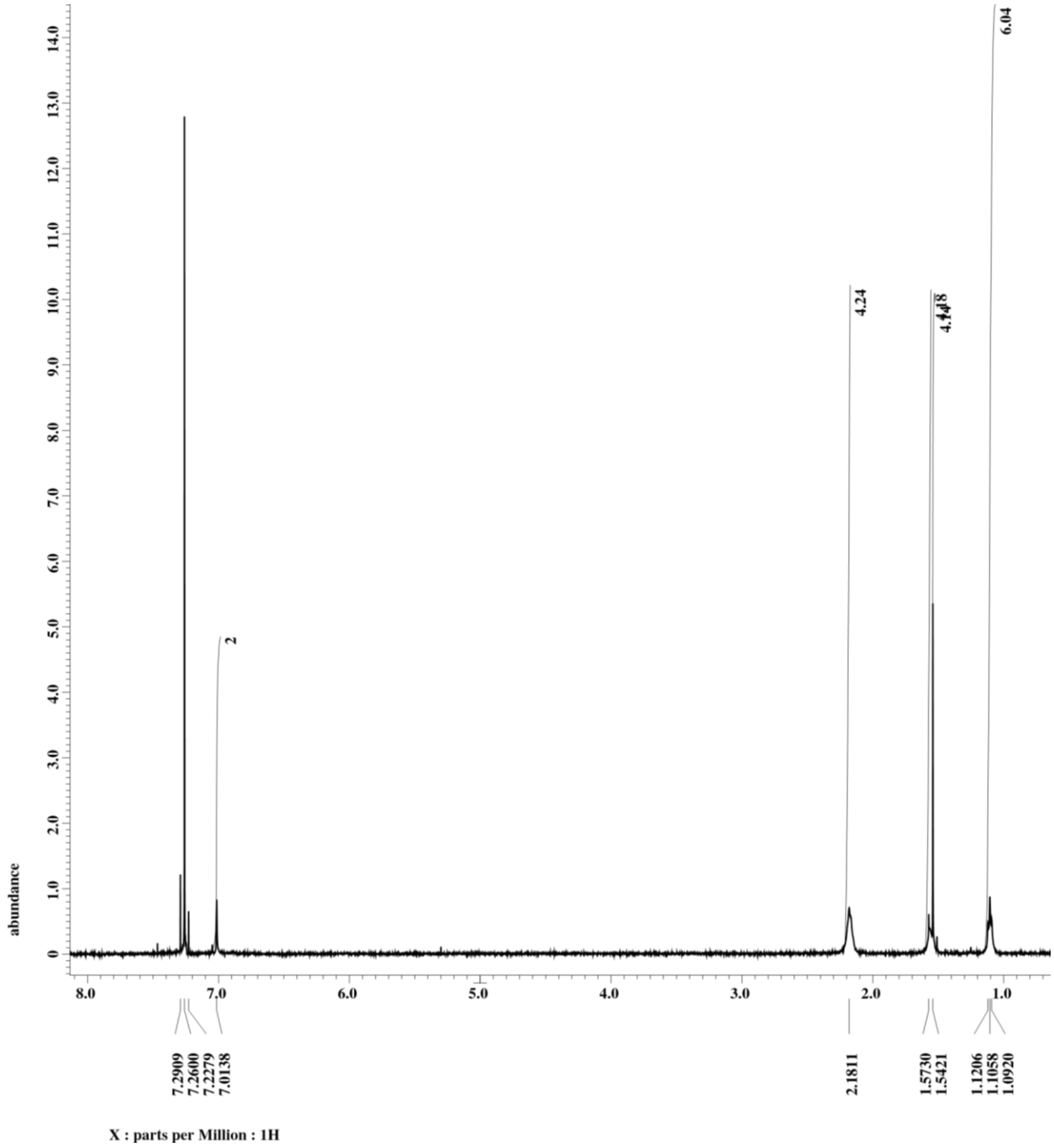

Figure S29. ^{19}F NMR spectrum of $Cu_4(\mu\text{-}[3,5\text{-}(CF_3)_2Pz])_4(C_2H_5C{\equiv}C(CH_2)_4C{\equiv}CC_2H_5)_2$ **(12)** in $CDCl_3$ at room temperature.

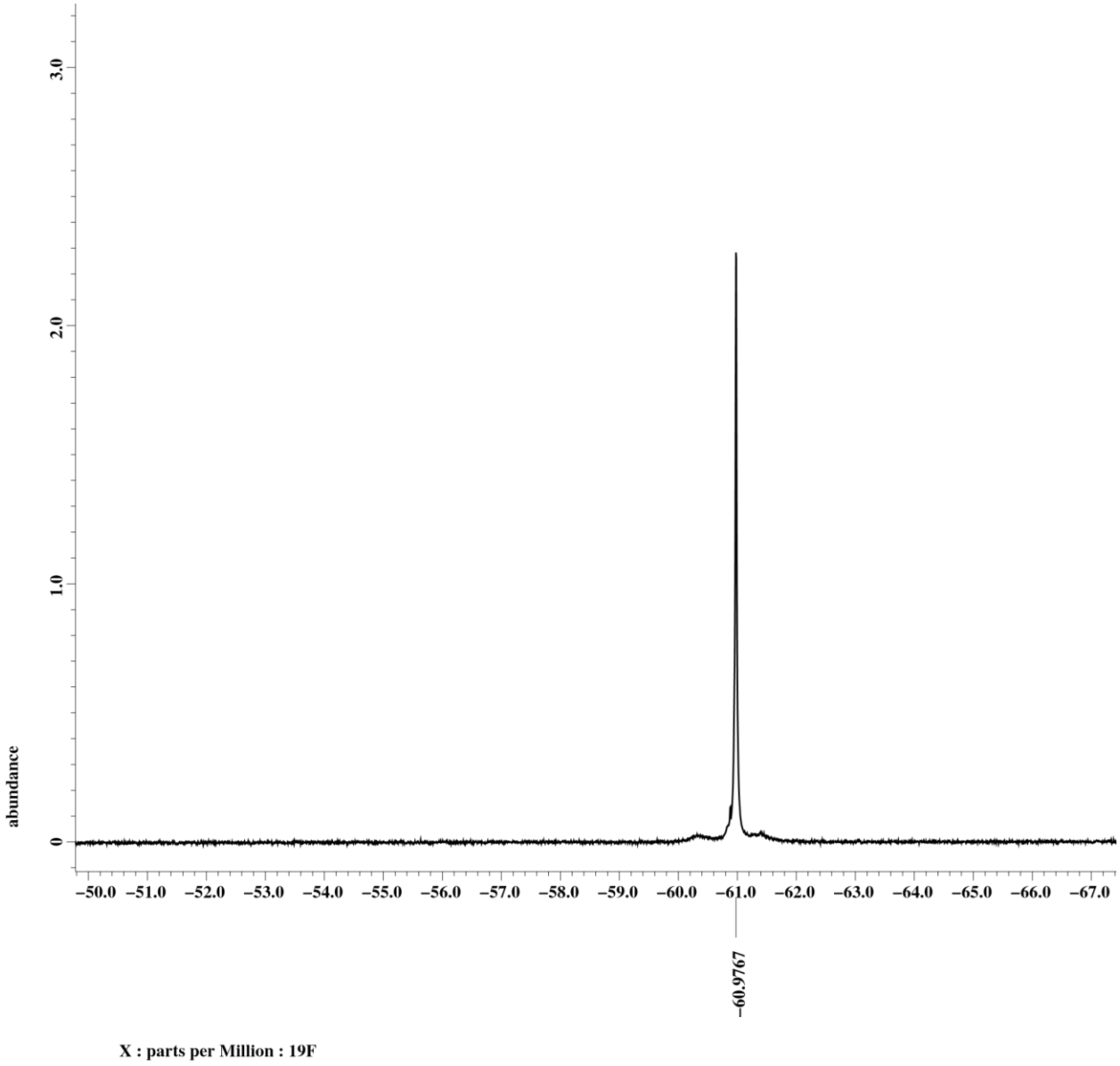

Figure S30. $^{13}C\{^{1}H\}$ NMR spectrum of $Cu_4(\mu\text{-}[3,5\text{-}(CF_3)_2Pz])_4(C_2H_5C{\equiv}C(CH_2)_4C{\equiv}CC_2H_5)_2$ **(12)** in $CDCl_3$ at room temperature.

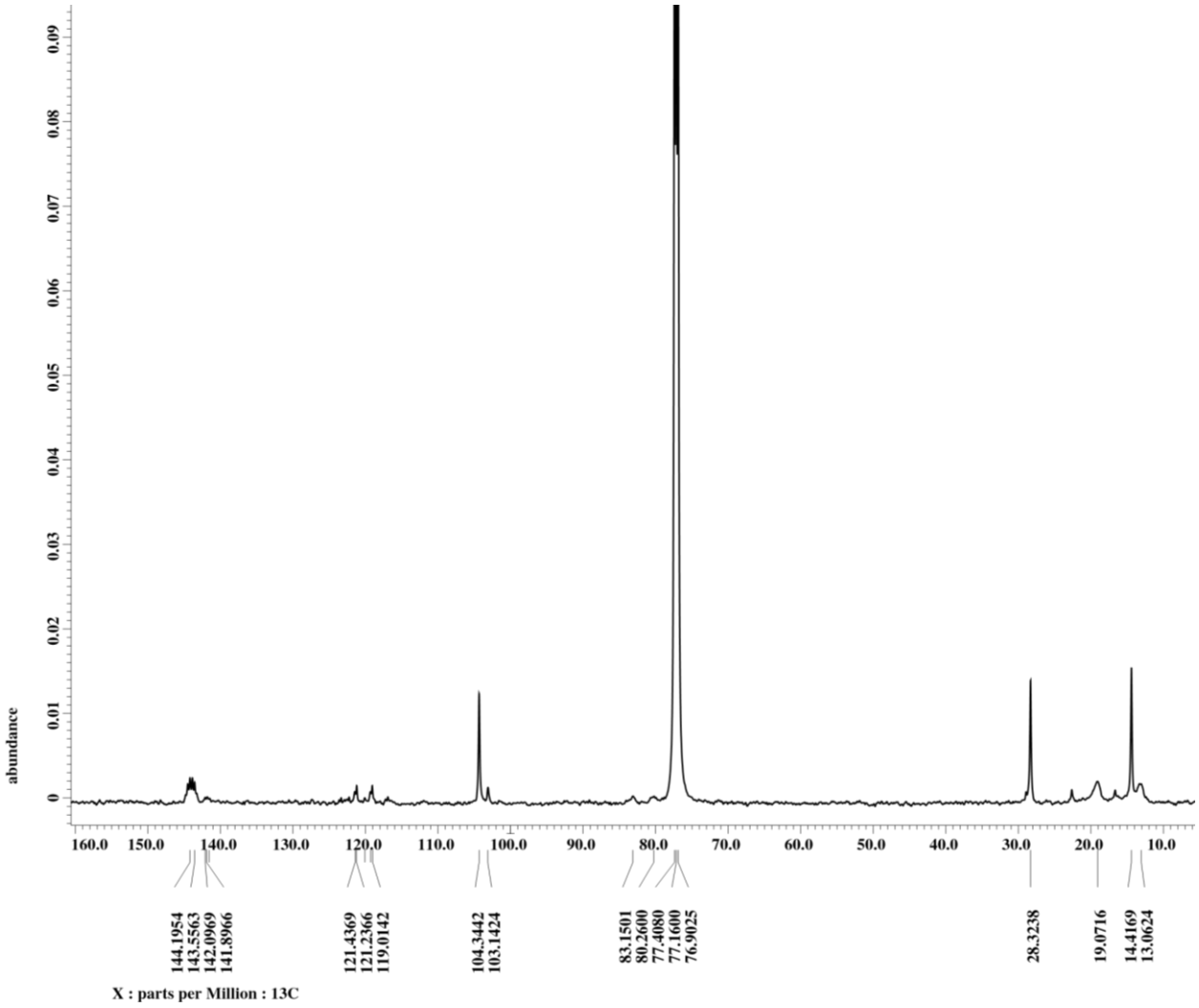

Figure S31. Raman spectrum of solid $Cu_4(\mu\text{-}[3,5\text{-}(CF_3)_2Pz])_4(C_2H_5C{\equiv}C(CH_2)_4C{\equiv}CC_2H_5)_2$ **(12)**

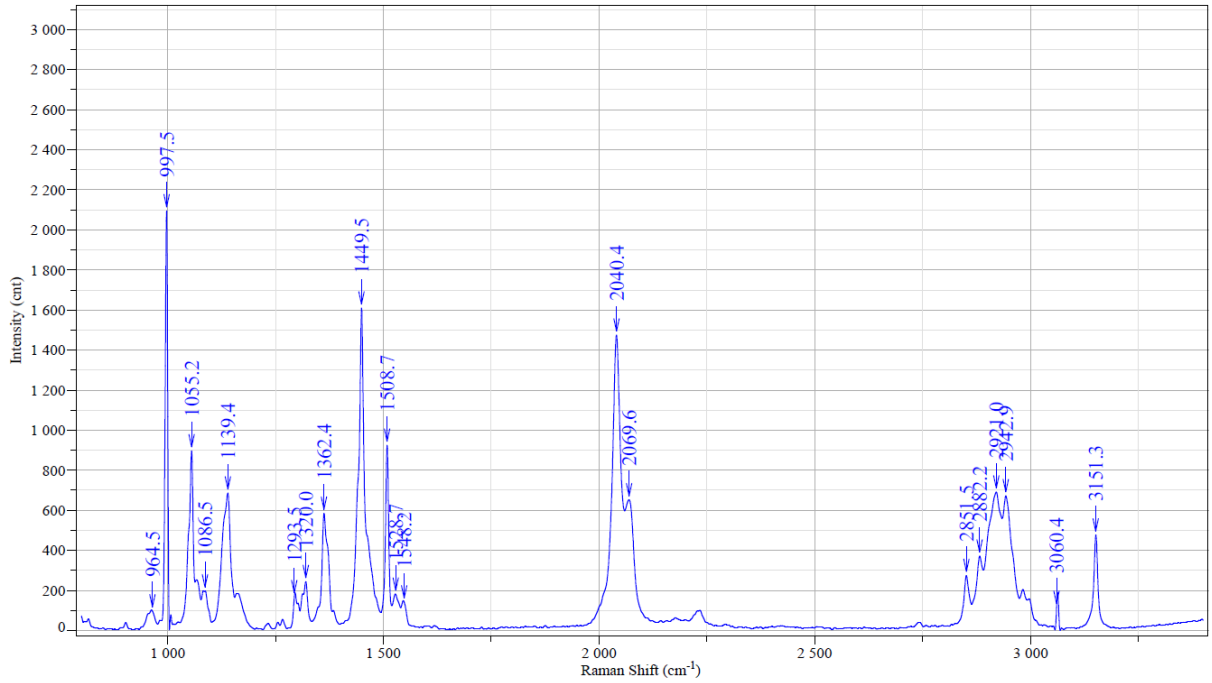

Exposition	10	Slit	100
Accumulation	5 x 4	Operator	Parasar
Laser	632.817	Sample	Cu_Dodecadiene
Spectro	Multi	Remark	
Hole	200	Power	

HORIBA JOBIN YVON

Figure S32. X-ray crystal structure of $Cu_4(\mu\text{-}[3,5\text{-}(CF_3)_2Pz])_4(\mu\text{-}HC{\equiv}CH)_2$ (**4**)

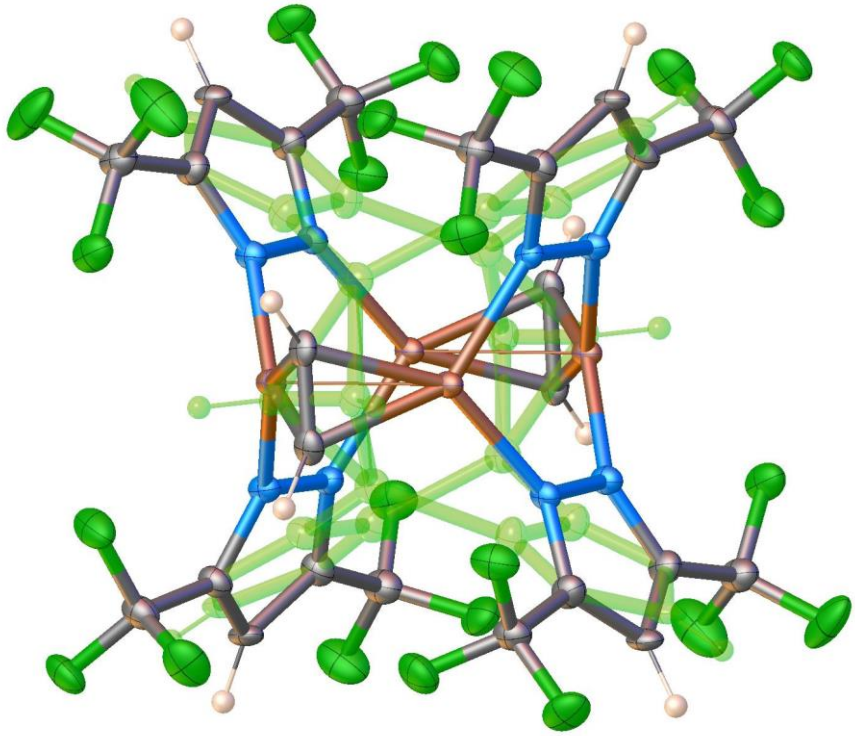

Table S1. Crystal data and structure refinement for $Cu_4(\mu\text{-}[3,5\text{-}(CF_3)_2Pz])_4(\mu\text{-}HC{\equiv}CH)_2$ (**4**)**.**

Identification code	Cu-tAlkynes
Empirical formula	$C_{12}H_4Cu_2F_{12}N_4$
Formula weight	559.27
Temperature/K	100.29
Crystal system	Triclinic
Space group	P-1
a/Å	9.2461(15)
b/Å	9.4479(16)
c/Å	11.1313(18)
α/°	95.590(4)
β/°	113.485(2)
γ/°	104.311(3)
Volume/Å^3	842.9(2)
Z	2
ρ_{calc}g/cm^3	2.204
μ/mm^{-1}	2.657
F(000)	540.0
Crystal size/mm^3	0.2 × 0.08 × 0.08

Radiation	MoKα (λ = 0.71073)
2Θ range for data collection/°	4.918 to 58.294
Index ranges	-12 ≤ h ≤ 12, -12 ≤ k ≤ 12, -15 ≤ l ≤ 15
Reflections collected	18287
Independent reflections	4530 [R_{int} = 0.0363, R_{sigma} = 0.0326]
Data/restraints/parameters	4530/121/362
Goodness-of-fit on F^2	1.043
Final R indexes [I>=2σ (I)]	R_1 = 0.0319, wR_2 = 0.0746
Final R indexes [all data]	R_1 = 0.0412, wR_2 = 0.0787
Largest diff. peak/hole / e $Å^{-3}$	0.48/-0.57

Figure S33. Intially, the two minor occupancy copper atoms (highlighted in green, left figure) appear as peaks slighly heavier than carbon linked to acetylene carbons. This gives the appearance of an unusual four-carbon or four-atom ligand linked to copper sites. After some effort, we realized that those peaks are due to minor occupancy disordered copper, as shown in the complete structure (right figure). The occupancues of the two fragments were refined to 0.877:0.123.

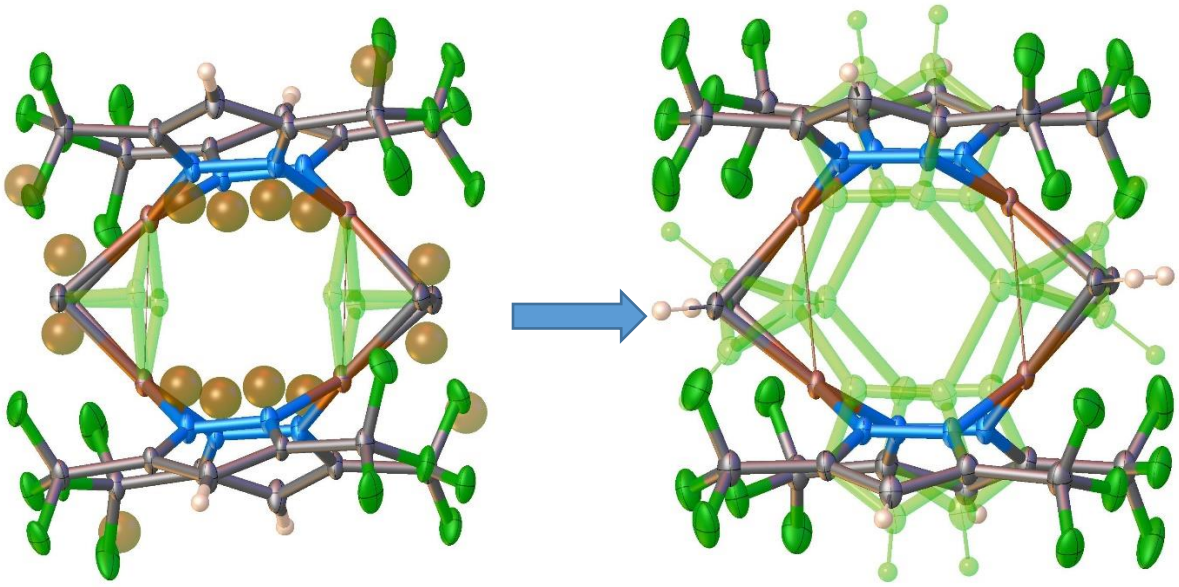

Figure S34. Atom labels of $Cu_4(\mu\text{-}[3,5\text{-}(CF_3)_2Pz])_4(\mu\text{-}HC{\equiv}CH)_2$ (**4**)

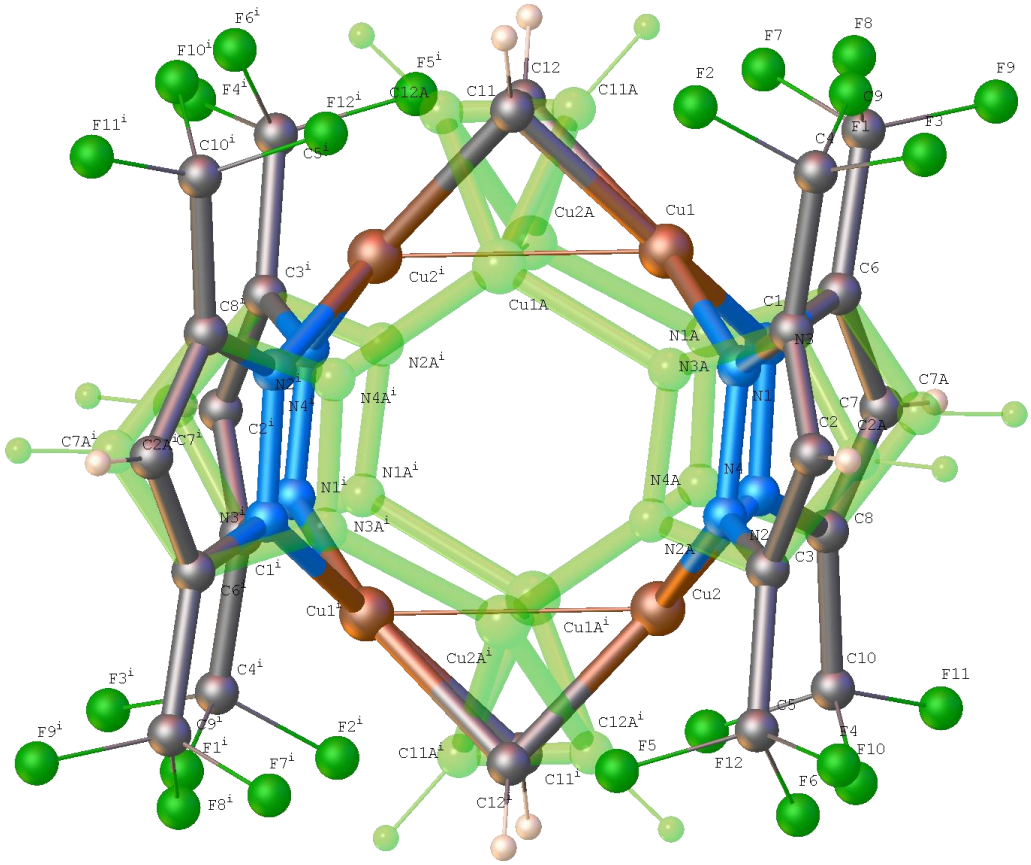

Table S2. Bond Lengths for $Cu_4(\mu\text{-}[3,5\text{-}(CF_3)_2Pz])_4(\mu\text{-}HC{\equiv}CH)_2$ (**4**)

Atom	Atom	Length/Å	Atom	Atom	Length/Å
Cu1	$Cu2^1$	2.6469(6)	F11	C10	1.337(3)
Cu1	N3	1.952(2)	F12	C10	1.343(3)
Cu1	N1	1.949(2)	N3	N4	1.362(3)
Cu1	C11	1.982(3)	N3	C6	1.355(3)
Cu1	C12	1.975(3)	N4	C8	1.361(3)
Cu2	N4	1.970(2)	N1	N2	1.361(3)
Cu2	N2	1.972(2)	N1	C1	1.352(2)
Cu2	$C11^1$	1.996(3)	N2	C3	1.356(2)
Cu2	$C12^1$	1.993(2)	N1A	N2A	1.38(2)
Cu1A	Cu2A	2.676(3)	N1A	C1	1.354(4)
Cu1A	N1A	1.976(12)	N2A	C3	1.349(4)
Cu1A	$N4A^1$	1.909(13)	N3A	N4A	1.36(2)
Cu1A	C11A	1.96(2)	N3A	C6	1.351(4)
Cu1A	C12A	1.96(2)	N4A	C8	1.350(4)

Cu2A	N2A[1]	1.885(12)	C1	C4	1.488(3)
Cu2A	N3A	1.926(12)	C1	C2	1.377(3)
Cu2A	C11A	1.97(2)	C1	C2A	1.379(4)
Cu2A	C12A	1.99(2)	C3	C5	1.492(3)
F1	C4	1.345(3)	C3	C2	1.383(3)
F2	C4	1.343(3)	C3	C2A	1.380(4)
F3	C4	1.333(3)	C6	C9	1.498(3)
F4	C5	1.326(3)	C6	C7	1.381(3)
F5	C5	1.349(3)	C6	C7A	1.379(4)
F6	C5	1.337(3)	C8	C10	1.494(3)
F7	C9	1.328(3)	C8	C7	1.380(3)
F8	C9	1.334(3)	C8	C7A	1.379(4)
F9	C9	1.328(3)	C11	C12	1.269(4)
F10	C10	1.335(3)	C11A	C12A	1.21(3)

[1]1-X,1-Y,1-Z

Table S3. Bond Angles for $Cu_4(\mu\text{-}[3,5\text{-}(CF_3)_2Pz])_4(\mu\text{-}HC{\equiv}CH)_2$ **(4).**

Atom	Atom	Atom	Angle/˚	Atom	Atom	Atom	Angle/˚
N3	Cu1	Cu2[1]	113.06(6)	N1	C1	C2	111.38(18)
N3	Cu1	C11	147.72(10)	N1A	C1	C4	118.9(7)
N3	Cu1	C12	110.48(10)	N1A	C1	C2A	108.0(7)
N1	Cu1	Cu2[1]	113.22(6)	C2	C1	C4	129.74(19)
N1	Cu1	N3	101.71(8)	C2A	C1	C4	132.2(3)
N1	Cu1	C11	110.01(10)	N2	C3	C5	120.44(18)
N1	Cu1	C12	147.29(10)	N2	C3	C2	110.99(18)
C11	Cu1	Cu2[1]	48.52(7)	N2A	C3	C5	112.0(7)
C12	Cu1	Cu2[1]	48.46(7)	N2A	C3	C2A	114.8(7)
C12	Cu1	C11	37.41(12)	C2	C3	C5	128.5(2)
N4	Cu2	Cu1[1]	114.07(6)	C2A	C3	C5	131.9(3)
N4	Cu2	N2	104.37(8)	F1	C4	C1	111.34(19)
N4	Cu2	C11[1]	109.28(10)	F2	C4	F1	105.8(2)
N4	Cu2	C12[1]	146.32(10)	F2	C4	C1	112.8(2)
N2	Cu2	Cu1[1]	112.74(6)	F3	C4	F1	107.66(19)
N2	Cu2	C11[1]	146.02(10)	F3	C4	F2	107.09(19)
N2	Cu2	C12[1]	109.03(10)	F3	C4	C1	111.76(19)
C11[1]	Cu2	Cu1[1]	48.06(8)	F4	C5	F5	107.1(2)
C12[1]	Cu2	Cu1[1]	47.87(8)	F4	C5	F6	108.6(2)
C12[1]	Cu2	C11[1]	37.10(11)	F4	C5	C3	111.25(19)
N1A	Cu1A	Cu2A	111.4(4)	F5	C5	C3	111.9(2)
N4A[1]	Cu1A	Cu2A	115.1(4)	F6	C5	F5	105.40(19)
N4A[1]	Cu1A	N1A	103.9(5)	F6	C5	C3	112.38(19)
N4A[1]	Cu1A	C11A	147.2(8)	N3	C6	C9	120.07(19)

N4A[1]	Cu1A	C12A	111.3(7)	N3	C6	C7	111.27(19)
C11A	Cu1A	Cu2A	47.2(6)	N3A	C6	C9	116.8(7)
C11A	Cu1A	N1A	108.5(8)	N3A	C6	C7A	111.0(7)
C11A	Cu1A	C12A	36.0(9)	C7	C6	C9	128.7(2)
C12A	Cu1A	Cu2A	47.8(6)	C7A	C6	C9	131.2(3)
C12A	Cu1A	N1A	144.4(7)	N4	C8	C10	120.70(19)
N2A[1]	Cu2A	Cu1A	113.1(4)	N4	C8	C7	111.06(19)
N2A[1]	Cu2A	N3A	102.0(5)	N4A	C8	C10	116.7(7)
N2A[1]	Cu2A	C11A	146.1(8)	N4A	C8	C7A	111.0(7)
N2A[1]	Cu2A	C12A	110.7(7)	C7	C8	C10	128.2(2)
N3A	Cu2A	Cu1A	112.8(4)	C7A	C8	C10	131.2(3)
N3A	Cu2A	C11A	111.0(8)	F7	C9	F8	105.9(2)
N3A	Cu2A	C12A	146.3(7)	F7	C9	F9	107.9(2)
C11A	Cu2A	Cu1A	46.8(6)	F7	C9	C6	112.2(2)
C11A	Cu2A	C12A	35.6(9)	F8	C9	C6	112.16(19)
C12A	Cu2A	Cu1A	46.8(6)	F9	C9	F8	106.8(2)
N4	N3	Cu1	118.26(14)	F9	C9	C6	111.6(2)
C6	N3	Cu1	134.29(16)	F10	C10	F11	107.7(2)
C6	N3	N4	107.25(18)	F10	C10	F12	106.24(19)
N3	N4	Cu2	118.92(14)	F10	C10	C8	112.61(18)
C8	N4	Cu2	133.95(15)	F11	C10	F12	106.84(19)
C8	N4	N3	107.13(18)	F11	C10	C8	110.90(19)
N2	N1	Cu1	118.85(14)	F12	C10	C8	112.2(2)
C1	N1	Cu1	133.50(15)	Cu1	C11	Cu2[1]	83.42(9)
C1	N1	N2	107.22(18)	C12	C11	Cu1	71.00(18)
N1	N2	Cu2	118.12(14)	C12	C11	Cu2[1]	71.34(16)
C3	N2	Cu2	134.64(15)	Cu1	C12	Cu2[1]	83.67(9)
C3	N2	N1	107.21(17)	C11	C12	Cu1	71.59(18)
N2A	N1A	Cu1A	110.7(3)	C11	C12	Cu2[1]	71.56(16)
C1	N1A	Cu1A	136.7(10)	Cu1A	C11A	Cu2A	86.0(7)
C1	N1A	N2A	112.1(10)	C12A	C11A	Cu1A	72.1(14)
C3	N2A	Cu2A[1]	131.9(10)	C12A	C11A	Cu2A	73.1(14)
C3	N2A	N1A	101.8(9)	Cu1A	C12A	Cu2A	85.4(8)
N4A	N3A	Cu2A	114.9(4)	C11A	C12A	Cu1A	71.9(14)
C6	N3A	Cu2A	137.6(11)	C11A	C12A	Cu2A	71.3(14)
C6	N3A	N4A	107.3(10)	C1	C2	C3	103.19(19)
C8	N4A	Cu1A[1]	129.7(10)	C8	C7	C6	103.3(2)
C8	N4A	N3A	107.4(9)	C1	C2A	C3	103.3(4)
N1	C1	C4	118.87(19)	C8	C7A	C6	103.4(4)

[1]1-X,1-Y,1-Z

Figure S35. X-ray crystal structure of $Cu_2(\mu\text{-}[4\text{-Br-}3,5\text{-}(CF_3)_2Pz])_2(HC{\equiv}CH)_2{\bullet}$(toluene) (**8**)

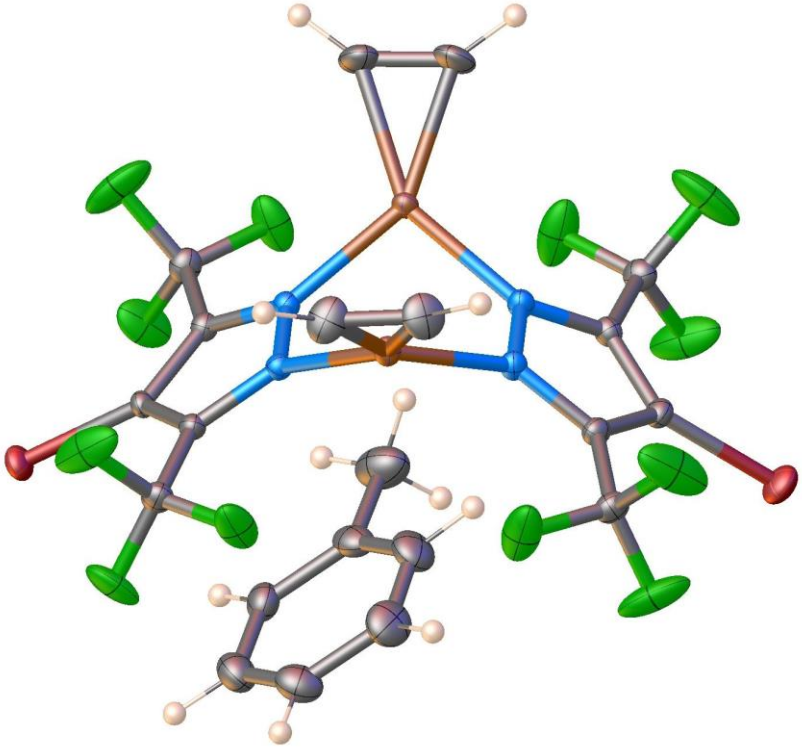

Table S4. Crystal data and structure refinement for $Cu_2(\mu\text{-}[4\text{-Br-}3,5\text{-}(CF_3)_2Pz])_2(HC{\equiv}CH)_2{\bullet}$(toluene) (**8**)**.**

Identification code	Cu-tAlkynes
Empirical formula	$C_{21}H_{12}Br_2Cu_2F_{12}N_4$
Formula weight	835.25
Temperature/K	100.01
Crystal system	orthorhombic
Space group	$Cmc2_1$
a/Å	17.0895(6)
b/Å	15.2842(5)
c/Å	10.1011(3)
α/°	90
β/°	90
γ/°	90
Volume/Å^3	2638.40(15)
Z	4
ρ_{calc}g/cm^3	2.103
μ/mm^{-1}	4.746
F(000)	1608.0

Crystal size/mm^3	0.25 × 0.22 × 0.18
Radiation	MoKα (λ = 0.71073)
2Θ range for data collection/°	6.686 to 66.284
Index ranges	-26 ≤ h ≤ 26, -23 ≤ k ≤ 23, -15 ≤ l ≤ 15
Reflections collected	21352
Independent reflections	5139 [R_{int} = 0.0239, R_{sigma} = 0.0348]
Data/restraints/parameters	5139/123/225
Goodness-of-fit on F^2	1.073
Final R indexes [I>=2σ (I)]	R_1 = 0.0218, wR_2 = 0.0501
Final R indexes [all data]	R_1 = 0.0239, wR_2 = 0.0511
Largest diff. peak/hole / e Å^{-3}	0.34/-0.75

Figure S36. Atom labels of $Cu_2(\mu\text{-}[4\text{-Br-}3,5\text{-}(CF_3)_2Pz])_2(HC{\equiv}CH)_2{\bullet}$(toluene) (**8**)

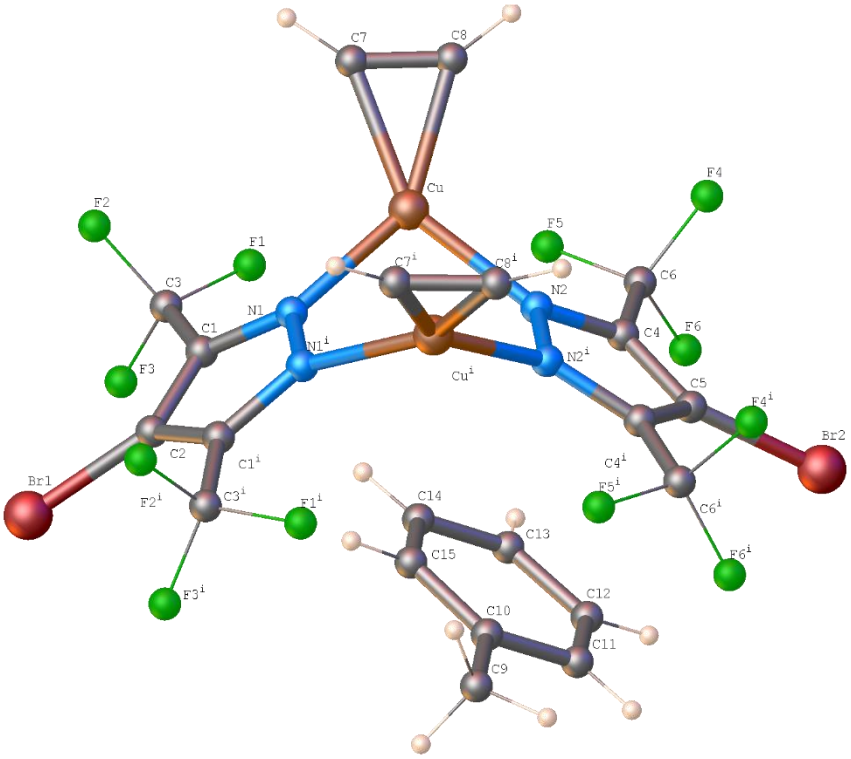

Table S5. Bond Lengths for $Cu_2(\mu\text{-}[4\text{-Br-}3,5\text{-}(CF_3)_2Pz])_2(HC{\equiv}CH)_2{\bullet}$(toluene) (**8**).

Atom	Atom	Length/Å	Atom	Atom	Length/Å
Br1	C2	1.860(3)	N2	N2^1	1.360(3)
Br2	C5	1.863(3)	N2	C4	1.344(3)
Cu	N1	1.9697(18)	C1	C2	1.392(3)
Cu	N2	1.9742(18)	C1	C3	1.491(3)
Cu	C7	1.966(3)	C4	C5	1.387(3)
Cu	C8	1.974(3)	C4	C6	1.489(3)

F1	C3	1.326(3)	C7	C8	1.227(4)
F2	C3	1.316(3)	C9	C10	1.506(10)
F3	C3	1.321(3)	C10	C11	1.392(7)
F4	C6	1.334(3)	C10	C15	1.370(9)
F5	C6	1.326(3)	C11	C12	1.390(9)
F6	C6	1.324(3)	C12	C13	1.378(8)
N1	N1[1]	1.355(3)	C13	C14	1.379(8)
N1	C1	1.346(3)	C14	C15	1.397(12)

[1]1-X,+Y,+Z

Table S6. Bond Angles for $Cu_2(\mu\text{-}[4\text{-Br-}3,5\text{-}(CF_3)_2Pz])_2(HC{\equiv}CH)_2{\bullet}$(toluene) (**8**).

Atom	Atom	Atom	Angle/˚	Atom	Atom	Atom	Angle/˚
N1	Cu	N2	98.94(8)	F3	C3	C1	112.2(2)
N1	Cu	C8	148.24(10)	N2	C4	C5	109.87(18)
C7	Cu	N1	111.96(10)	N2	C4	C6	121.11(19)
C7	Cu	N2	148.68(11)	C5	C4	C6	128.8(2)
C7	Cu	C8	36.29(11)	C4[1]	C5	Br2	127.86(12)
C8	Cu	N2	112.60(10)	C4	C5	Br2	127.86(12)
N1[1]	N1	Cu	117.93(5)	C4[1]	C5	C4	104.3(2)
C1	N1	Cu	133.78(14)	F4	C6	C4	110.95(18)
C1	N1	N1[1]	108.07(11)	F5	C6	F4	106.8(2)
N2[1]	N2	Cu	117.78(5)	F5	C6	C4	112.34(19)
C4	N2	Cu	134.22(14)	F6	C6	F4	106.5(2)
C4	N2	N2[1]	107.99(11)	F6	C6	F5	106.9(2)
N1	C1	C2	110.04(19)	F6	C6	C4	113.0(2)
N1	C1	C3	120.77(19)	C8	C7	Cu	72.19(17)
C2	C1	C3	129.1(2)	C7	C8	Cu	71.52(16)
C1	C2	Br1	128.09(13)	C11	C10	C9	118.8(6)
C1[1]	C2	Br1	128.09(13)	C15	C10	C9	122.6(7)
C1	C2	C1[1]	103.8(3)	C15	C10	C11	118.6(6)
F1	C3	C1	112.00(19)	C12	C11	C10	119.7(5)
F2	C3	F1	106.3(2)	C13	C12	C11	120.8(5)
F2	C3	F3	107.4(3)	C12	C13	C14	120.1(6)
F2	C3	C1	112.4(2)	C13	C14	C15	118.5(6)
F3	C3	F1	106.2(2)	C10	C15	C14	122.2(5)

[1]1-X,+Y,+Z

Figure S37. X-ray crystal structure of $Cu_2(\mu\text{-}[3,5\text{-}(CF_3)_2Pz])_2(HC{\equiv}CPh)_2$ (**9**)

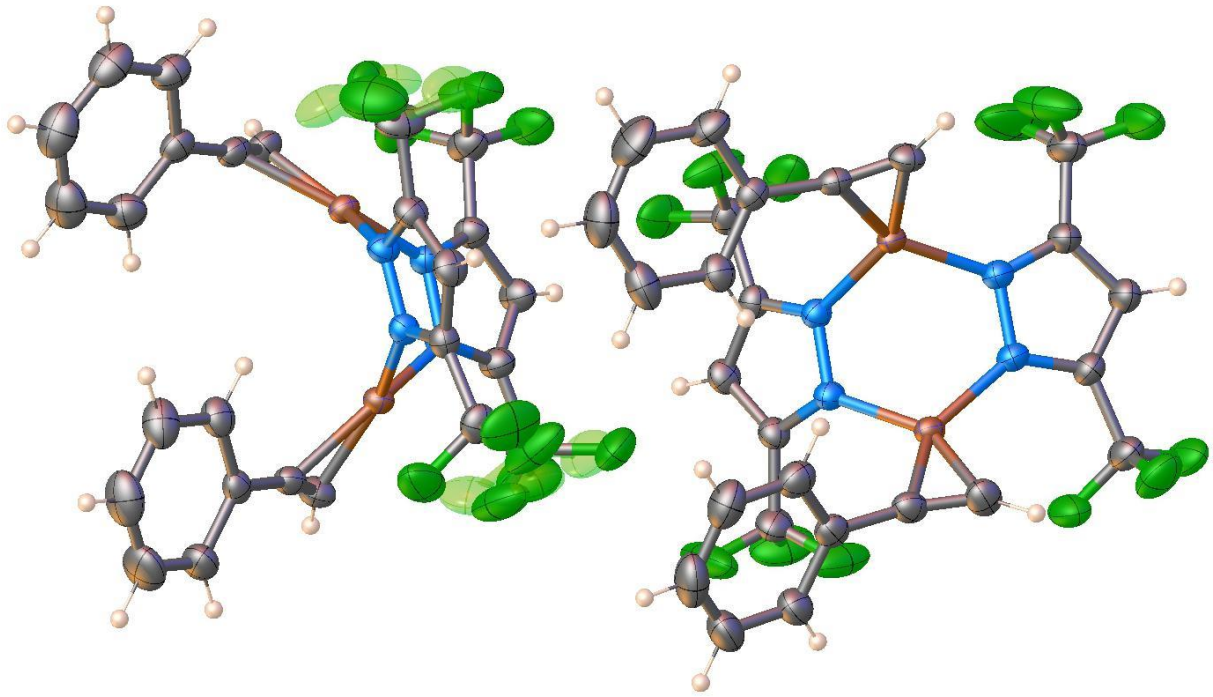

Table S7. Crystal data and structure refinement for $Cu_2(\mu\text{-}[3,5\text{-}(CF_3)_2Pz])_2(HC{\equiv}CPh)_2$ (**9**)**.**

Identification code	Cu-tAlkynes
Empirical formula	$C_{26}H_{14}Cu_2F_{12}N_4$
Formula weight	737.49
Temperature/K	175.0
Crystal system	triclinic
Space group	P-1
a/Å	12.9771(15)
b/Å	13.6360(15)
c/Å	17.588(3)
α/°	71.399(3)
β/°	71.758(2)
γ/°	79.715(2)
Volume/Å^3	2790.7(6)
Z	4
ρ_{calc}g/cm^3	1.755
μ/mm^{-1}	1.629
F(000)	1456.0

Crystal size/mm^3	0.2 × 0.15 × 0.1
Radiation	MoKα (λ = 0.71073)
2Θ range for data collection/°	5.9 to 58.258
Index ranges	-17 ≤ h ≤ 17, -18 ≤ k ≤ 18, -24 ≤ l ≤ 24
Reflections collected	35889
Independent reflections	14970 [R_{int} = 0.0263, R_{sigma} = 0.0330]
Data/restraints/parameters	14970/117/849
Goodness-of-fit on F^2	1.045
Final R indexes [I>=2σ (I)]	R_1 = 0.0465, wR_2 = 0.1289
Final R indexes [all data]	R_1 = 0.0601, wR_2 = 0.1401
Largest diff. peak/hole / e Å^{-3}	1.60/-0.67

Figure S38. Atom labels of $Cu_2(\mu\text{-}[3,5\text{-}(CF_3)_2Pz])_2(HC{\equiv}CPh)_2$ (**9**)

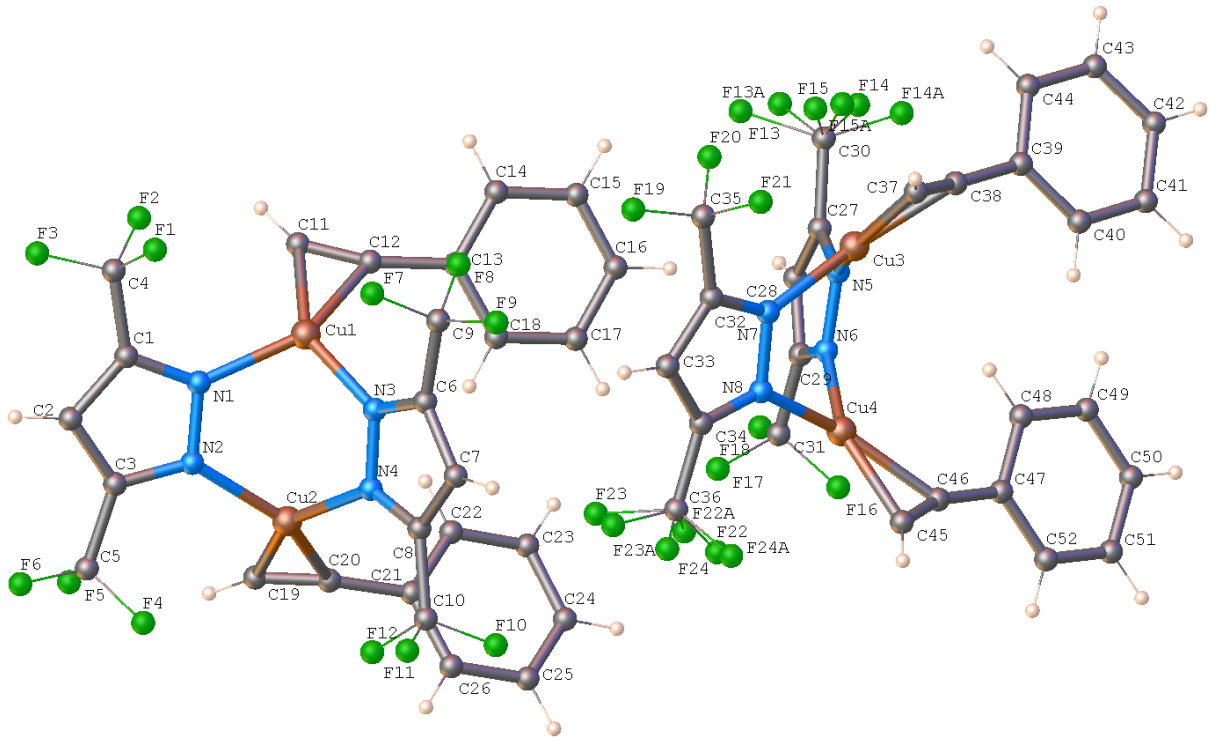

Table S8. Bond Lengths for $Cu_2(\mu\text{-}[3,5\text{-}(CF_3)_2Pz])_2(HC{\equiv}CPh)_2$ (**9**).

Atom	Atom	Length/Å	Atom	Atom	Length/Å
Cu1	N1	1.976(2)	Cu3	C38	2.009(3)
Cu1	N3	1.962(2)	Cu4	N6	1.958(2)
Cu1	C11	1.944(3)	Cu4	N8	1.968(2)
Cu1	C12	1.987(3)	Cu4	C45	1.938(3)

Cu2	N2	1.986(2)	Cu4	C46	1.975(3)
Cu2	N4	1.967(2)	F13	C30	1.464(7)
Cu2	C19	1.944(3)	F14	C30	1.248(8)
Cu2	C20	2.014(3)	F15	C30	1.294(9)
F1	C4	1.298(5)	F16	C31	1.323(4)
F2	C4	1.325(5)	F17	C31	1.313(4)
F3	C4	1.308(4)	F18	C31	1.316(4)
F4	C5	1.332(4)	F19	C35	1.331(4)
F5	C5	1.348(4)	F20	C35	1.328(4)
F6	C5	1.320(4)	F21	C35	1.345(4)
F7	C9	1.320(4)	F22	C36	1.270(6)
F8	C9	1.320(4)	F23	C36	1.403(6)
F9	C9	1.321(3)	F24	C36	1.306(6)
F10	C10	1.279(4)	N5	N6	1.352(3)
F11	C10	1.335(4)	N5	C27	1.342(3)
F12	C10	1.333(4)	N6	C29	1.340(3)
N1	N2	1.357(3)	N7	N8	1.361(3)
N1	C1	1.339(4)	N7	C32	1.346(3)
N2	C3	1.344(3)	N8	C34	1.340(4)
N3	N4	1.349(3)	C27	C28	1.378(4)
N3	C6	1.341(3)	C27	C30	1.491(4)
N4	C8	1.340(3)	C28	C29	1.386(4)
C1	C2	1.387(4)	C29	C31	1.486(4)
C1	C4	1.487(4)	C30	F13A	1.256(5)
C2	C3	1.376(4)	C30	F14A	1.401(6)
C3	C5	1.491(4)	C30	F15A	1.340(6)
C6	C7	1.382(4)	C32	C33	1.378(4)
C6	C9	1.493(4)	C32	C35	1.482(4)
C7	C8	1.382(4)	C33	C34	1.382(4)
C8	C10	1.493(4)	C34	C36	1.489(4)
C11	C12	1.228(4)	C36	F22A	1.352(7)
C12	C13	1.447(4)	C36	F23A	1.232(6)
C13	C14	1.396(4)	C36	F24A	1.351(7)
C13	C18	1.388(4)	C37	C38	1.221(4)
C14	C15	1.392(5)	C38	C39	1.450(4)
C15	C16	1.371(7)	C39	C40	1.388(4)
C16	C17	1.379(6)	C39	C44	1.401(4)
C17	C18	1.389(4)	C40	C41	1.382(5)
C19	C20	1.225(4)	C41	C42	1.386(6)
C20	C21	1.446(4)	C42	C43	1.386(6)
C21	C22	1.397(4)	C43	C44	1.380(5)
C21	C26	1.396(4)	C45	C46	1.231(4)
C22	C23	1.384(5)	C46	C47	1.453(4)

C23	C24	1.380(6)	C47	C48	1.395(4)
C24	C25	1.375(6)	C47	C52	1.386(4)
C25	C26	1.389(5)	C48	C49	1.385(4)
Cu3	N5	1.969(2)	C49	C50	1.379(6)
Cu3	N7	1.984(2)	C50	C51	1.377(6)
Cu3	C37	1.947(3)	C51	C52	1.381(5)

Table S9. Bond Angles for $Cu_2(\mu\text{-}[3,5\text{-}(CF_3)_2Pz])_2(HC{\equiv}CPh)_2$ (**9**).

Atom	Atom	Atom	Angle/˚	Atom	Atom	Atom	Angle/˚
N1	Cu1	C12	146.91(10)	N6	Cu4	N8	98.88(9)
N3	Cu1	N1	99.77(9)	N6	Cu4	C46	112.62(10)
N3	Cu1	C12	111.63(10)	N8	Cu4	C46	146.94(10)
C11	Cu1	N1	112.02(11)	C45	Cu4	N6	149.19(11)
C11	Cu1	N3	147.93(11)	C45	Cu4	N8	111.71(11)
C11	Cu1	C12	36.38(12)	C45	Cu4	C46	36.66(12)
N2	Cu2	C20	143.63(11)	N6	N5	Cu3	116.53(16)
N4	Cu2	N2	100.57(9)	C27	N5	Cu3	134.93(19)
N4	Cu2	C20	114.73(11)	C27	N5	N6	107.1(2)
C19	Cu2	N2	108.86(11)	N5	N6	Cu4	118.13(16)
C19	Cu2	N4	150.52(11)	C29	N6	Cu4	133.68(19)
C19	Cu2	C20	36.01(13)	C29	N6	N5	108.0(2)
N2	N1	Cu1	115.36(17)	N8	N7	Cu3	118.59(17)
C1	N1	Cu1	136.77(19)	C32	N7	Cu3	134.27(19)
C1	N1	N2	107.7(2)	C32	N7	N8	107.1(2)
N1	N2	Cu2	118.71(17)	N7	N8	Cu4	115.74(17)
C3	N2	Cu2	133.89(19)	C34	N8	Cu4	136.45(19)
C3	N2	N1	107.2(2)	C34	N8	N7	107.7(2)
N4	N3	Cu1	117.70(16)	N5	C27	C28	111.3(3)
C6	N3	Cu1	134.17(19)	N5	C27	C30	120.5(3)
C6	N3	N4	108.0(2)	C28	C27	C30	128.1(3)
N3	N4	Cu2	116.90(16)	C27	C28	C29	102.9(2)
C8	N4	Cu2	134.84(19)	N6	C29	C28	110.6(2)
C8	N4	N3	107.3(2)	N6	C29	C31	120.0(2)
N1	C1	C2	110.8(2)	C28	C29	C31	129.4(3)
N1	C1	C4	121.2(3)	F13	C30	C27	105.1(4)
C2	C1	C4	128.0(3)	F14	C30	F13	101.4(6)
C3	C2	C1	103.0(3)	F14	C30	F15	111.6(8)
N2	C3	C2	111.3(2)	F14	C30	C27	116.8(6)
N2	C3	C5	120.8(3)	F15	C30	F13	101.3(6)
C2	C3	C5	127.9(3)	F15	C30	C27	117.6(6)

F1	C4	F2	102.3(4)	F13A	C30	C27	114.5(4)
F1	C4	F3	110.3(4)	F13A	C30	F14A	103.4(4)
F1	C4	C1	113.4(3)	F13A	C30	F15A	113.4(5)
F2	C4	C1	113.2(3)	F14A	C30	C27	109.6(3)
F3	C4	F2	104.6(3)	F15A	C30	C27	112.2(4)
F3	C4	C1	112.2(3)	F15A	C30	F14A	102.4(4)
F4	C5	F5	105.8(3)	F16	C31	C29	113.1(3)
F4	C5	C3	112.0(3)	F17	C31	F16	105.2(3)
F5	C5	C3	112.0(3)	F17	C31	F18	108.1(3)
F6	C5	F4	109.2(3)	F17	C31	C29	112.7(3)
F6	C5	F5	106.2(3)	F18	C31	F16	105.6(3)
F6	C5	C3	111.4(3)	F18	C31	C29	111.7(3)
N3	C6	C7	110.7(2)	N7	C32	C33	111.1(2)
N3	C6	C9	120.1(2)	N7	C32	C35	121.1(3)
C7	C6	C9	129.2(3)	C33	C32	C35	127.7(3)
C6	C7	C8	102.9(2)	C32	C33	C34	103.2(2)
N4	C8	C7	111.1(2)	N8	C34	C33	110.9(2)
N4	C8	C10	121.3(3)	N8	C34	C36	121.3(3)
C7	C8	C10	127.5(3)	C33	C34	C36	127.8(3)
F7	C9	F8	106.0(3)	F19	C35	F21	105.5(3)
F7	C9	F9	107.7(3)	F19	C35	C32	111.1(3)
F7	C9	C6	111.9(3)	F20	C35	F19	109.3(3)
F8	C9	F9	106.1(3)	F20	C35	F21	105.8(3)
F8	C9	C6	113.2(2)	F20	C35	C32	112.5(3)
F9	C9	C6	111.5(3)	F21	C35	C32	112.3(3)
F10	C10	F11	107.9(4)	F22	C36	F23	106.2(5)
F10	C10	F12	106.6(3)	F22	C36	F24	108.9(6)
F10	C10	C8	114.1(3)	F22	C36	C34	117.3(3)
F11	C10	C8	112.3(2)	F23	C36	C34	110.3(3)
F12	C10	F11	103.8(3)	F24	C36	F23	97.7(5)
F12	C10	C8	111.4(3)	F24	C36	C34	114.3(4)
C12	C11	Cu1	73.72(18)	F22A	C36	C34	110.0(4)
C11	C12	Cu1	69.90(18)	F23A	C36	C34	112.3(4)
C11	C12	C13	160.7(3)	F23A	C36	F22A	119.5(7)
C13	C12	Cu1	128.9(2)	F23A	C36	F24A	102.9(7)
C14	C13	C12	119.3(3)	F24A	C36	C34	107.6(4)
C18	C13	C12	121.1(3)	F24A	C36	F22A	103.2(6)
C18	C13	C14	119.4(3)	C38	C37	Cu3	74.82(19)
C15	C14	C13	119.2(3)	C37	C38	Cu3	69.27(19)
C16	C15	C14	121.0(4)	C37	C38	C39	162.4(3)
C15	C16	C17	120.0(3)	C39	C38	Cu3	128.0(2)
C16	C17	C18	119.9(4)	C40	C39	C38	119.8(3)
C13	C18	C17	120.4(3)	C40	C39	C44	119.8(3)

C20	C19	Cu2	75.1(2)	C44	C39	C38	120.3(3)
C19	C20	Cu2	68.87(19)	C41	C40	C39	120.0(3)
C19	C20	C21	162.2(3)	C40	C41	C42	120.5(4)
C21	C20	Cu2	128.5(2)	C43	C42	C41	119.5(3)
C22	C21	C20	119.0(3)	C44	C43	C42	120.7(3)
C26	C21	C20	121.1(3)	C43	C44	C39	119.6(3)
C26	C21	C22	119.7(3)	C46	C45	Cu4	73.35(18)
C23	C22	C21	120.1(3)	C45	C46	Cu4	69.99(18)
C24	C23	C22	119.9(4)	C45	C46	C47	160.0(3)
C25	C24	C23	120.3(4)	C47	C46	Cu4	129.5(2)
C24	C25	C26	120.8(4)	C48	C47	C46	120.9(3)
C25	C26	C21	119.2(3)	C52	C47	C46	119.1(3)
N5	Cu3	N7	100.98(9)	C52	C47	C48	119.9(3)
N5	Cu3	C38	114.12(11)	C49	C48	C47	119.5(3)
N7	Cu3	C38	143.86(11)	C50	C49	C48	120.2(4)
C37	Cu3	N5	149.81(11)	C51	C50	C49	120.2(3)
C37	Cu3	N7	109.16(11)	C50	C51	C52	120.3(3)
C37	Cu3	C38	35.91(12)	C51	C52	C47	119.9(3)

Figure S39. X-ray crystal structure of $Cu_2(\mu\text{-}[3,5\text{-}(CF_3)_2Pz])_2(HC{\equiv}C(CH_2)_5C{\equiv}CH)$ (**10**)

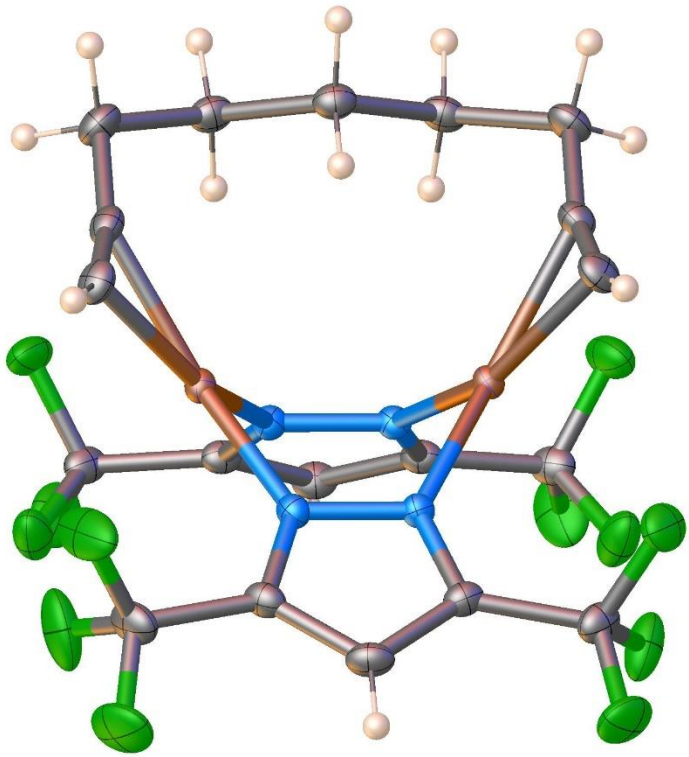

Table S10. Crystal data and structure refinement for $Cu_2(\mu\text{-}[3,5\text{-}(CF_3)_2Pz])_2(HC{\equiv}C(CH_2)_5C{\equiv}CH)$ (**10**)**.**

Identification code	Cu-tAlkynes
Empirical formula	$C_{19}H_{14}Cu_2F_{12}N_4$
Formula weight	653.42
Temperature/K	100.0
Crystal system	monoclinic
Space group	$P2_1/n$
a/Å	11.0850(4)
b/Å	14.3949(5)
c/Å	14.0223(4)
α/°	90
β/°	90.7460(10)
γ/°	90
Volume/Å^3	2237.31(13)
Z	4
ρ_{calc}g/cm^3	1.940
μ/mm^{-1}	2.017
F(000)	1288.0

Crystal size/mm^3	0.26 × 0.22 × 0.14
Radiation	MoKα (λ = 0.71073)
2Θ range for data collection/°	5.66 to 66.46
Index ranges	-17 ≤ h ≤ 16, -22 ≤ k ≤ 22, -21 ≤ l ≤ 21
Reflections collected	36294
Independent reflections	8553 [R_{int} = 0.0223, R_{sigma} = 0.0200]
Data/restraints/parameters	8553/0/342
Goodness-of-fit on F^2	1.060
Final R indexes [I>=2σ (I)]	R_1 = 0.0279, wR_2 = 0.0704
Final R indexes [all data]	R_1 = 0.0352, wR_2 = 0.0740
Largest diff. peak/hole / e Å^{-3}	0.45/-0.84

Figure S40. Atom labels of $Cu_2(\mu\text{-}[3,5\text{-}(CF_3)_2Pz])_2(HC{\equiv}C(CH_2)_5C{\equiv}CH)$ (**10**)

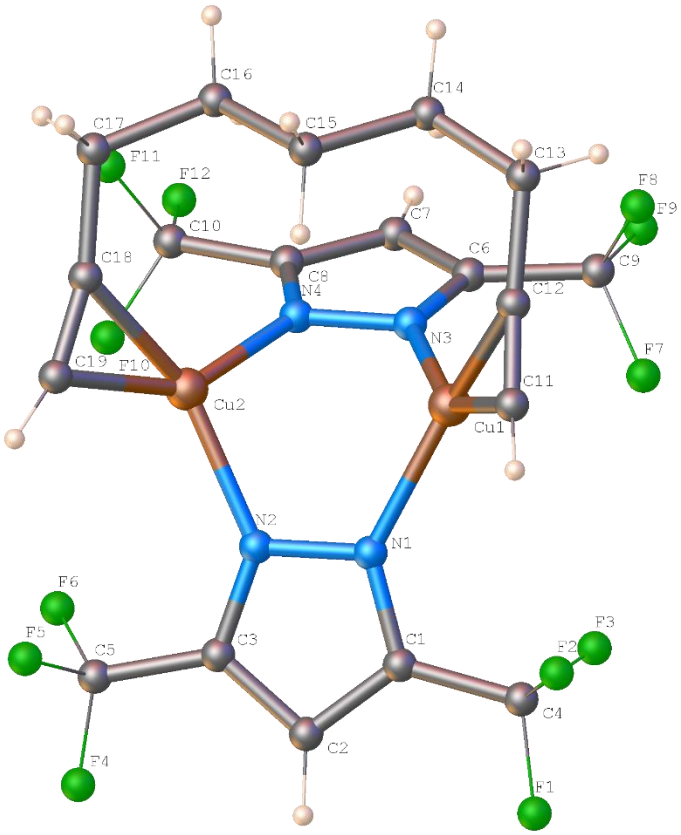

Table S11. Bond Lengths for $Cu_2(\mu\text{-}[3,5\text{-}(CF_3)_2Pz])_2(HC{\equiv}C(CH_2)_5C{\equiv}CH)$ (**10**).

Atom	Atom	Length/Å	Atom	Atom	Length/Å
Cu1	N1	1.9858(10)	N1	C1	1.3449(15)
Cu1	N3	1.9630(10)	N2	C3	1.3436(15)
Cu1	C11	1.9527(13)	N3	N4	1.3528(14)

Cu1	C12	2.0053(12)	N3	C6	1.3422(15)
Cu2	N2	1.9967(10)	N4	C8	1.3443(15)
Cu2	N4	1.9658(10)	C1	C2	1.3833(18)
Cu2	C18	2.0108(13)	C1	C4	1.4843(19)
Cu2	C19	1.9574(13)	C2	C3	1.3831(19)
F1	C4	1.3413(16)	C3	C5	1.4864(19)
F2	C4	1.3409(16)	C6	C7	1.3903(18)
F3	C4	1.3322(17)	C6	C9	1.4901(19)
F4	C5	1.3293(18)	C7	C8	1.3897(18)
F5	C5	1.3352(18)	C8	C10	1.4894(19)
F6	C5	1.329(2)	C11	C12	1.2279(19)
F7	C9	1.3398(17)	C12	C13	1.4853(18)
F8	C9	1.3311(16)	C13	C14	1.534(2)
F9	C9	1.3276(16)	C14	C15	1.5256(18)
F10	C10	1.3371(17)	C15	C16	1.5249(19)
F11	C10	1.3308(15)	C16	C17	1.534(2)
F12	C10	1.3402(15)	C17	C18	1.4832(19)
N1	N2	1.3572(14)	C18	C19	1.2296(19)

Table S12. Bond Angles for $Cu_2(\mu\text{-}[3,5\text{-}(CF_3)_2Pz])_2(HC{\equiv}C(CH_2)_5C{\equiv}CH)$ **(10).**

Atom	Atom	Atom	Angle/˚	Atom	Atom	Atom	Angle/˚
N1	Cu1	C12	145.25(5)	F4	C5	C3	111.26(13)
N3	Cu1	N1	97.92(4)	F5	C5	C3	112.64(12)
N3	Cu1	C12	114.39(5)	F6	C5	F4	107.56(14)
C11	Cu1	N1	111.08(5)	F6	C5	F5	106.56(15)
C11	Cu1	N3	150.47(5)	F6	C5	C3	111.97(12)
C11	Cu1	C12	36.12(6)	N3	C6	C7	110.89(11)
N2	Cu2	C18	145.07(5)	N3	C6	C9	119.87(11)
N4	Cu2	N2	98.34(4)	C7	C6	C9	129.24(11)
N4	Cu2	C18	113.99(5)	C8	C7	C6	102.83(11)
C19	Cu2	N2	111.77(5)	N4	C8	C7	110.73(11)
C19	Cu2	N4	149.70(5)	N4	C8	C10	119.71(11)
C19	Cu2	C18	36.07(6)	C7	C8	C10	129.56(11)
N2	N1	Cu1	116.64(7)	F7	C9	C6	111.97(11)
C1	N1	Cu1	135.79(9)	F8	C9	F7	105.66(13)
C1	N1	N2	107.48(10)	F8	C9	C6	113.03(11)
N1	N2	Cu2	116.41(7)	F9	C9	F7	107.55(12)
C3	N2	Cu2	136.17(9)	F9	C9	F8	107.30(11)
C3	N2	N1	107.40(10)	F9	C9	C6	110.98(12)
N4	N3	Cu1	116.56(7)	F10	C10	F12	107.41(12)
C6	N3	Cu1	135.66(9)	F10	C10	C8	112.08(11)

C6	N3	N4	107.71(10)	F11	C10	F10	106.04(12)
N3	N4	Cu2	117.43(7)	F11	C10	F12	106.97(11)
C8	N4	Cu2	134.60(9)	F11	C10	C8	113.12(11)
C8	N4	N3	107.84(10)	F12	C10	C8	110.87(12)
N1	C1	C2	111.06(11)	C12	C11	Cu1	74.28(8)
N1	C1	C4	120.09(11)	C11	C12	Cu1	69.61(8)
C2	C1	C4	128.81(12)	C11	C12	C13	161.54(13)
C3	C2	C1	102.86(11)	C13	C12	Cu1	128.44(9)
N2	C3	C2	111.19(11)	C12	C13	C14	114.26(11)
N2	C3	C5	120.17(12)	C15	C14	C13	114.26(11)
C2	C3	C5	128.64(12)	C16	C15	C14	112.10(11)
F1	C4	C1	110.89(12)	C15	C16	C17	114.26(11)
F2	C4	F1	106.33(11)	C18	C17	C16	115.19(11)
F2	C4	C1	112.89(11)	C17	C18	Cu2	129.36(9)
F3	C4	F1	107.63(12)	C19	C18	Cu2	69.60(8)
F3	C4	F2	106.63(12)	C19	C18	C17	160.71(13)
F3	C4	C1	112.12(11)	C18	C19	Cu2	74.33(8)
F4	C5	F5	106.51(13)				

Figure S41. X-ray crystal structure of $Cu_4(\mu\text{-}[3,5\text{-}(CF_3)_2Pz])_4(HC{\equiv}C(CH_2)_4C{\equiv}CH)_2$ (**11**)

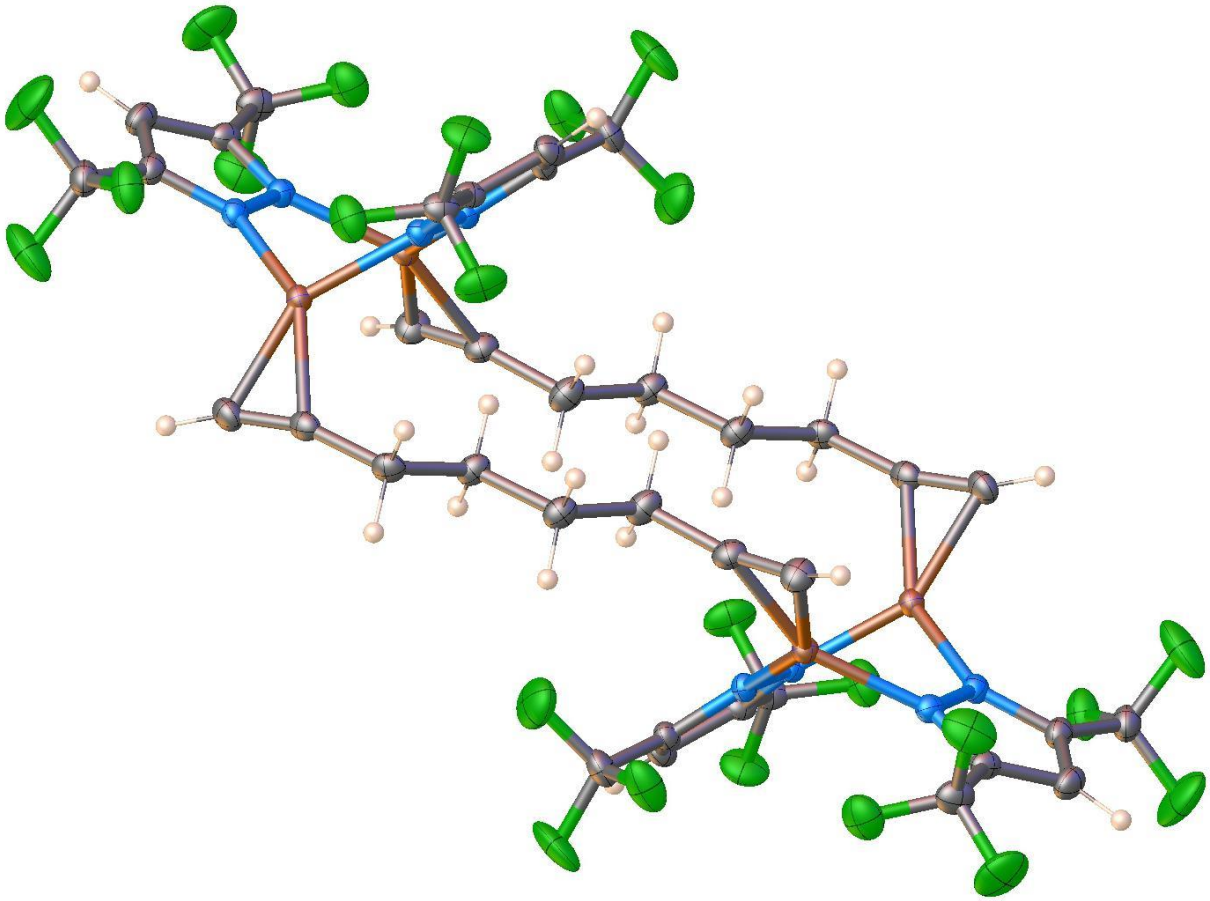

Table S13. Crystal data and structure refinement for $Cu_4(\mu\text{-}[3,5\text{-}(CF_3)_2Pz])_4(HC{\equiv}C(CH_2)_4C{\equiv}CH)_2$ (**11**).

Identification code	Cu-tAlkynes
Empirical formula	$C_{18}H_{12}Cu_2F_{12}N_4$
Formula weight	639.40
Temperature/K	100.0
Crystal system	triclinic
Space group	P-1
a/Å	10.4189(5)
b/Å	10.4808(5)
c/Å	12.2860(6)
α/°	92.068(2)

β/°	110.195(2)
γ/°	115.740(2)
Volume/Å^3	1106.40(9)
Z	2
ρ_{calc}g/cm^3	1.919
μ/mm^{-1}	2.037
F(000)	628.0
Crystal size/mm^3	0.25 × 0.25 × 0.08
Radiation	MoKα (λ = 0.71073)
2Θ range for data collection/°	6.304 to 65.444
Index ranges	-15 ≤ h ≤ 15, -15 ≤ k ≤ 15, -18 ≤ l ≤ 18
Reflections collected	14149
Independent reflections	7904 [R_{int} = 0.0224, R_{sigma} = 0.0387]
Data/restraints/parameters	7904/0/333
Goodness-of-fit on F^2	1.020
Final R indexes [I>=2σ (I)]	R_1 = 0.0362, wR_2 = 0.0874
Final R indexes [all data]	R_1 = 0.0536, wR_2 = 0.0963
Largest diff. peak/hole / e Å^{-3}	0.90/-0.72

Figure S42. Atom labels of $Cu_4(\mu\text{-}[3,5\text{-}(CF_3)_2Pz])_4(HC{\equiv}C(CH_2)_4C{\equiv}CH)_2$ (**11**)

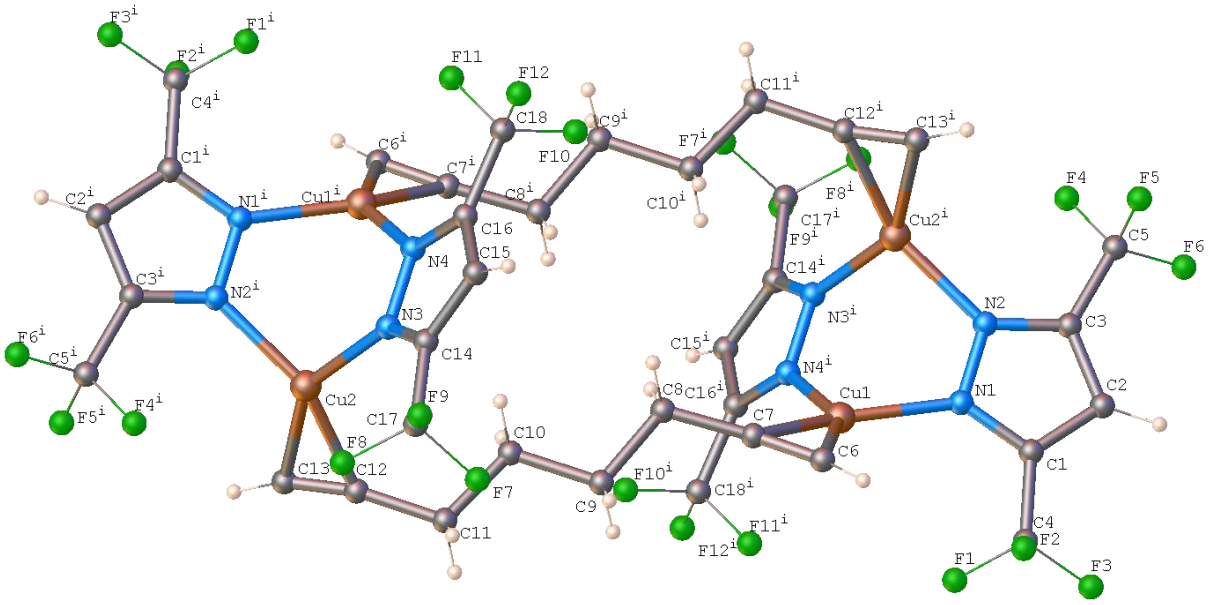

Table S14. Bond Lengths for $Cu_4(\mu\text{-}[3,5\text{-}(CF_3)_2Pz])_4(HC{\equiv}C(CH_2)_4C{\equiv}CH)_2$ **(11).**

Atom	Atom	Length/Å	Atom	Atom	Length/Å
Cu1	N1	1.9716(17)	N1	C1	1.344(3)
Cu1	N4[1]	1.9752(16)	N2	C3	1.342(3)
Cu1	C6	1.957(2)	N3	N4	1.356(2)
Cu1	C7	1.990(2)	N3	C14	1.344(2)
Cu2	N2[1]	1.9838(17)	N4	C16	1.341(2)
Cu2	N3	1.9693(17)	C1	C2	1.388(3)
Cu2	C12	1.994(2)	C1	C4	1.481(3)
Cu2	C13	1.959(2)	C2	C3	1.390(3)
F1	C4	1.340(3)	C3	C5	1.487(3)
F2	C4	1.344(3)	C6	C7	1.219(3)
F3	C4	1.329(3)	C7	C8	1.481(3)
F4	C5	1.336(3)	C8	C9	1.530(3)
F5	C5	1.324(3)	C9	C10	1.521(3)
F6	C5	1.330(3)	C10	C11	1.527(3)
F7	C17	1.347(3)	C11	C12	1.480(3)
F8	C17	1.334(3)	C12	C13	1.220(3)
F9	C17	1.336(2)	C14	C15	1.381(3)
F10	C18	1.336(3)	C14	C17	1.484(3)
F11	C18	1.332(3)	C15	C16	1.391(3)
F12	C18	1.334(3)	C16	C18	1.484(3)
N1	N2	1.355(2)			

[1]1-X,1-Y,1-Z

Table S15. Bond Angles for $Cu_4(\mu\text{-}[3,5\text{-}(CF_3)_2Pz])_4(HC{\equiv}C(CH_2)_4C{\equiv}CH)_2$ **(11).**

Atom	Atom	Atom	Angle/˚	Atom	Atom	Atom	Angle/˚
N1	Cu1	N4[1]	100.29(7)	F4	C5	C3	112.03(18)
N1	Cu1	C7	146.56(8)	F5	C5	F4	106.0(2)
N4[1]	Cu1	C7	111.41(8)	F5	C5	F6	107.5(2)
C6	Cu1	N1	112.13(9)	F5	C5	C3	113.2(2)
C6	Cu1	N4[1]	147.31(9)	F6	C5	F4	106.6(2)
C6	Cu1	C7	35.98(9)	F6	C5	C3	111.1(2)
N2[1]	Cu2	C12	147.72(8)	C7	C6	Cu1	73.47(14)
N3	Cu2	N2[1]	99.78(7)	C6	C7	Cu1	70.55(14)
N3	Cu2	C12	110.87(8)	C6	C7	C8	163.4(2)
C13	Cu2	N2[1]	112.63(9)	C8	C7	Cu1	125.75(16)
C13	Cu2	N3	146.77(9)	C7	C8	C9	113.57(18)
C13	Cu2	C12	35.94(9)	C10	C9	C8	110.03(17)
N2	N1	Cu1	116.37(13)	C9	C10	C11	113.00(17)

C1	N1	Cu1	135.92(15)	C12	C11	C10	112.37(17)
C1	N1	N2	107.70(17)	C11	C12	Cu2	125.30(15)
N1	N2	Cu2[1]	116.88(13)	C13	C12	Cu2	70.45(14)
C3	N2	Cu2[1]	135.42(15)	C13	C12	C11	163.9(2)
C3	N2	N1	107.66(17)	C12	C13	Cu2	73.61(14)
N4	N3	Cu2	115.71(12)	N3	C14	C15	110.93(18)
C14	N3	Cu2	136.71(14)	N3	C14	C17	120.88(18)
C14	N3	N4	107.48(16)	C15	C14	C17	128.09(18)
N3	N4	Cu1[1]	117.65(12)	C14	C15	C16	103.20(17)
C16	N4	Cu1[1]	134.19(14)	N4	C16	C15	110.49(18)
C16	N4	N3	107.90(16)	N4	C16	C18	120.75(18)
N1	C1	C2	110.87(19)	C15	C16	C18	128.75(19)
N1	C1	C4	120.3(2)	F7	C17	C14	111.70(19)
C2	C1	C4	128.8(2)	F8	C17	F7	106.18(19)
C1	C2	C3	102.83(19)	F8	C17	F9	107.55(19)
N2	C3	C2	110.9(2)	F8	C17	C14	113.09(18)
N2	C3	C5	120.44(19)	F9	C17	F7	106.23(18)
C2	C3	C5	128.6(2)	F9	C17	C14	111.67(18)
F1	C4	F2	105.5(2)	F10	C18	C16	112.5(2)
F1	C4	C1	112.76(19)	F11	C18	F10	105.7(2)
F2	C4	C1	112.2(2)	F11	C18	F12	107.1(2)
F3	C4	F1	107.1(2)	F11	C18	C16	112.30(18)
F3	C4	F2	107.2(2)	F12	C18	F10	107.4(2)
F3	C4	C1	111.7(2)	F12	C18	C16	111.5(2)

[1]1-X,1-Y,1-Z

Figure S43. X-ray crystal structure of $Cu_4(\mu\text{-}[3,5\text{-}(CF_3)_2Pz])_4(C_2H_5C{\equiv}C(CH_2)_4C{\equiv}CC_2H_5)_2$ (**12**)

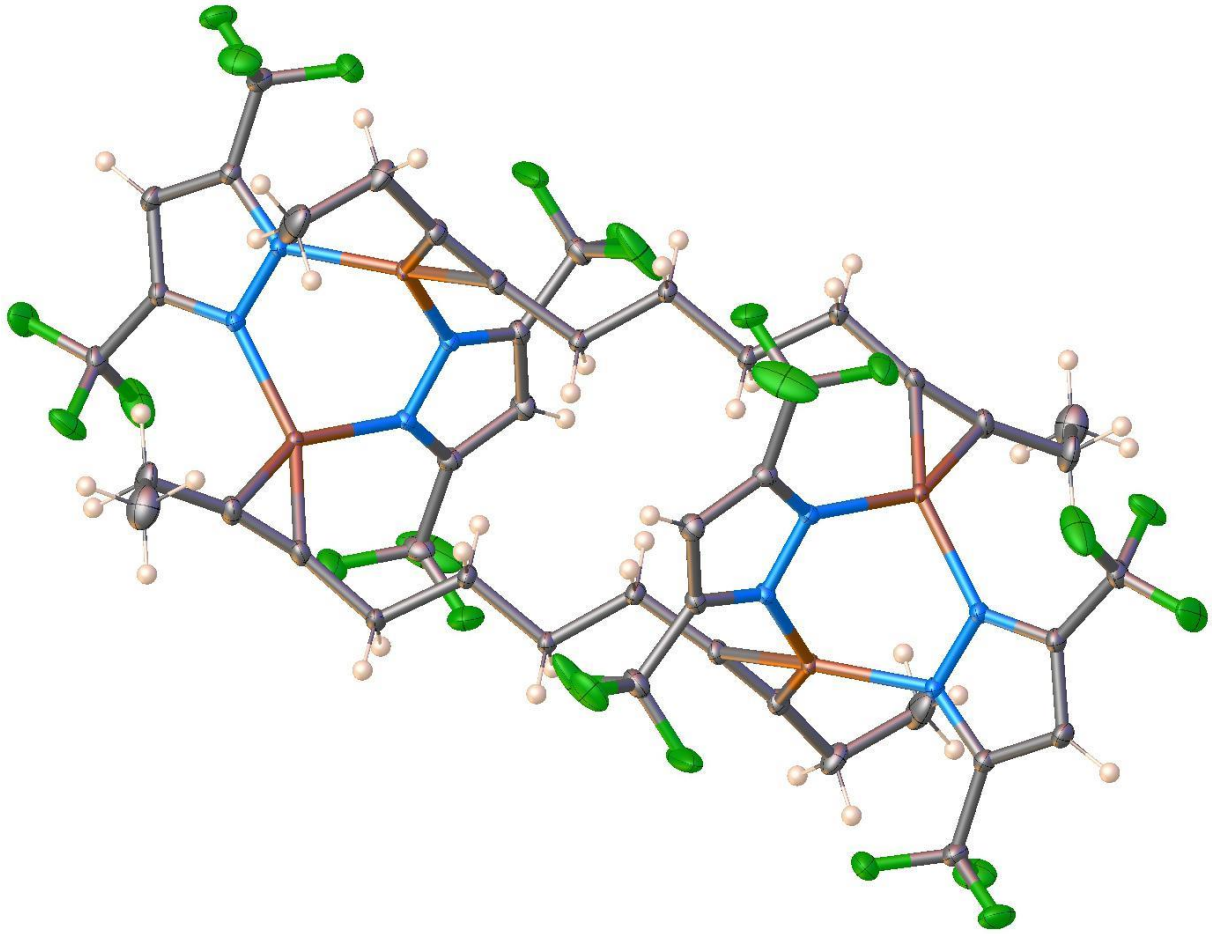

Table S16. Crystal data and structure refinement for $Cu_4(\mu\text{-}[3,5\text{-}(CF_3)_2Pz])_4(C_2H_5C{\equiv}C(CH_2)_4C{\equiv}CC_2H_5)_2$ **(12).**

Identification code	Cu-tAlkynes
Empirical formula	$C_{22}H_{20}Cu_2F_{12}N_4$
Formula weight	695.50
Temperature/K	100.0
Crystal system	triclinic
Space group	P-1
a/Å	8.4602(3)
b/Å	9.2660(4)
c/Å	17.3777(7)
α/°	97.7580(10)
β/°	90.3530(10)
γ/°	107.1170(10)

Volume/Å^3	1288.50(9)
Z	2
ρ_{calc}g/cm^3	1.793
μ/mm^{-1}	1.757
F(000)	692.0
Crystal size/mm^3	0.24 × 0.13 × 0.025
Radiation	MoKα (λ = 0.71073)
2Θ range for data collection/°	5.51 to 60.828
Index ranges	-12 ≤ h ≤ 12, -13 ≤ k ≤ 13, -24 ≤ l ≤ 24
Reflections collected	17811
Independent reflections	7741 [R_{int} = 0.0196, R_{sigma} = 0.0265]
Data/restraints/parameters	7741/0/363
Goodness-of-fit on F^2	1.041
Final R indexes [I>=2σ (I)]	R_1 = 0.0274, wR_2 = 0.0655
Final R indexes [all data]	R_1 = 0.0337, wR_2 = 0.0685
Largest diff. peak/hole / e Å^{-3}	0.66/-0.64

Figure S44. Atom labels of $Cu_4(\mu\text{-}[3,5\text{-}(CF_3)_2Pz])_4(C_2H_5C{\equiv}C(CH_2)_4C{\equiv}CC_2H_5)_2$ (**12**)

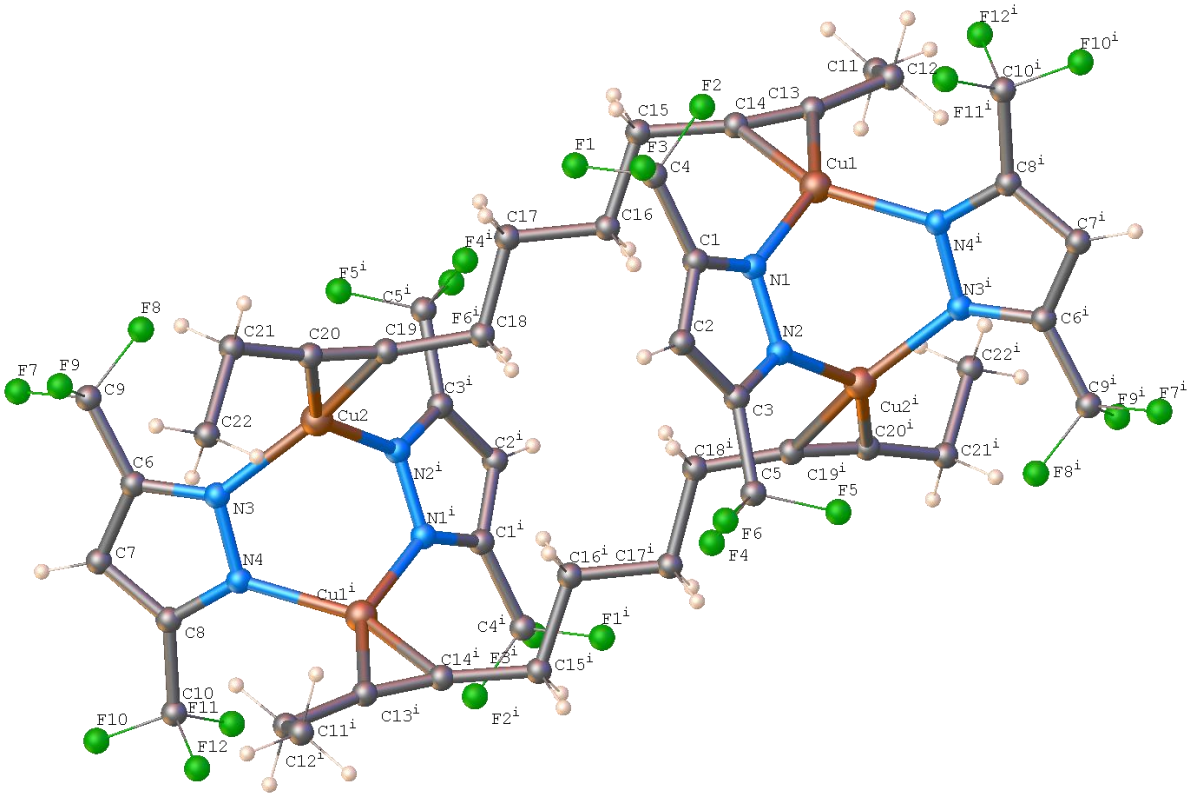

Table S17. Bond Lengths for $Cu_4(\mu\text{-}[3,5\text{-}(CF_3)_2Pz])_4(C_2H_5C{\equiv}C(CH_2)_4C{\equiv}CC_2H_5)_2$ **(12).**

Atom	Atom	Length/Å	Atom	Atom	Length/Å
Cu1	N1	1.9799(12)	N4	Cu1[1]	1.9816(12)
Cu1	N4[1]	1.9816(12)	N4	C8	1.3425(18)
Cu1	C14	1.9841(15)	F3	C4	1.323(2)
Cu1	C13	1.9770(15)	F5	C5	1.322(2)
Cu2	N3	1.9731(12)	C19	C18	1.4819(19)
Cu2	N2[1]	1.9915(12)	C19	C20	1.234(2)
Cu2	C19	1.9704(14)	C14	C15	1.481(2)
Cu2	C20	1.9908(14)	C14	C13	1.233(2)
F8	C9	1.3351(18)	C8	C7	1.390(2)
F12	C10	1.3274(19)	C8	C10	1.487(2)
F2	C4	1.330(2)	C15	C16	1.5303(19)
F9	C9	1.344(2)	C18	C17	1.5332(19)
F7	C9	1.3363(18)	C6	C9	1.484(2)
F10	C10	1.3330(18)	C6	C7	1.387(2)
F6	C5	1.3282(19)	C3	C2	1.386(2)
F1	C4	1.343(2)	C3	C5	1.484(2)
F11	C10	1.3310(19)	C13	C12	1.486(2)
F4	C5	1.328(2)	C1	C2	1.385(2)
N3	N4	1.3549(16)	C1	C4	1.486(2)
N3	C6	1.3445(18)	C20	C21	1.478(2)
N1	N2	1.3554(16)	C16	C17	1.5227(19)
N1	C1	1.3413(18)	C21	C22	1.523(3)
N2	Cu2[1]	1.9915(12)	C12	C11	1.505(3)
N2	C3	1.3433(18)			

[1]1-X,1-Y,1-Z

TableS18. Bond Angles for $Cu_4(\mu\text{-}[3,5\text{-}(CF_3)_2Pz])_4(C_2H_5C{\equiv}C(CH_2)_4C{\equiv}CC_2H_5)_2$ **(12).**

Atom	Atom	Atom	Angle/˚	Atom	Atom	Atom	Angle/˚
N1	Cu1	N4[1]	97.89(5)	C2	C3	C5	128.73(14)
N1	Cu1	C14	113.33(5)	C14	C13	Cu1	72.18(10)
N4[1]	Cu1	C14	147.53(6)	C14	C13	C12	163.06(16)
C13	Cu1	N1	149.06(6)	C12	C13	Cu1	124.68(12)
C13	Cu1	N4[1]	111.53(6)	N1	C1	C2	111.07(12)
C13	Cu1	C14	36.26(6)	N1	C1	C4	120.87(13)

N3	Cu2	N2[1]	97.80(5)	C2	C1	C4	128.06(13)
N3	Cu2	C20	118.36(6)	C19	C20	Cu2	70.94(9)
C19	Cu2	N3	153.16(6)	C19	C20	C21	162.03(15)
C19	Cu2	N2[1]	107.14(6)	C21	C20	Cu2	126.90(11)
C19	Cu2	C20	36.31(6)	C17	C16	C15	113.56(12)
C20	Cu2	N2[1]	143.43(5)	F8	C9	F9	106.04(13)
N4	N3	Cu2	114.39(9)	F8	C9	F7	107.97(14)
C6	N3	Cu2	136.84(10)	F8	C9	C6	112.52(13)
C6	N3	N4	107.68(11)	F9	C9	C6	112.37(13)
N2	N1	Cu1	114.13(9)	F7	C9	F9	106.47(13)
C1	N1	Cu1	138.13(10)	F7	C9	C6	111.12(13)
C1	N1	N2	107.55(11)	C6	C7	C8	102.83(13)
N1	N2	Cu2[1]	116.83(9)	C16	C17	C18	110.06(11)
C3	N2	Cu2[1]	135.38(10)	F12	C10	F10	106.66(13)
C3	N2	N1	107.62(11)	F12	C10	F11	106.83(14)
N3	N4	Cu1[1]	116.79(9)	F12	C10	C8	113.18(13)
C8	N4	Cu1[1]	135.53(10)	F10	C10	C8	110.95(13)
C8	N4	N3	107.65(11)	F11	C10	F10	106.69(14)
C18	C19	Cu2	125.59(10)	F11	C10	C8	112.14(13)
C20	C19	Cu2	72.75(9)	C1	C2	C3	102.86(13)
C20	C19	C18	161.30(15)	F2	C4	F1	105.75(14)
C15	C14	Cu1	124.74(10)	F2	C4	C1	112.45(13)
C13	C14	Cu1	71.56(10)	F1	C4	C1	111.95(14)
C13	C14	C15	163.40(15)	F3	C4	F2	107.74(15)
N4	C8	C7	110.93(13)	F3	C4	F1	107.18(15)
N4	C8	C10	120.35(13)	F3	C4	C1	111.43(14)
C7	C8	C10	128.63(13)	C20	C21	C22	112.23(15)
C14	C15	C16	112.06(12)	F6	C5	F4	105.68(13)
C19	C18	C17	113.97(11)	F6	C5	C3	111.26(13)
N3	C6	C9	120.94(13)	F4	C5	C3	112.79(14)
N3	C6	C7	110.90(13)	F5	C5	F6	107.07(15)
C7	C6	C9	128.13(13)	F5	C5	F4	107.67(16)
N2	C3	C2	110.89(13)	F5	C5	C3	112.00(13)
N2	C3	C5	120.34(13)	C13	C12	C11	112.71(15)

[1]1-X,1-Y,1-Z

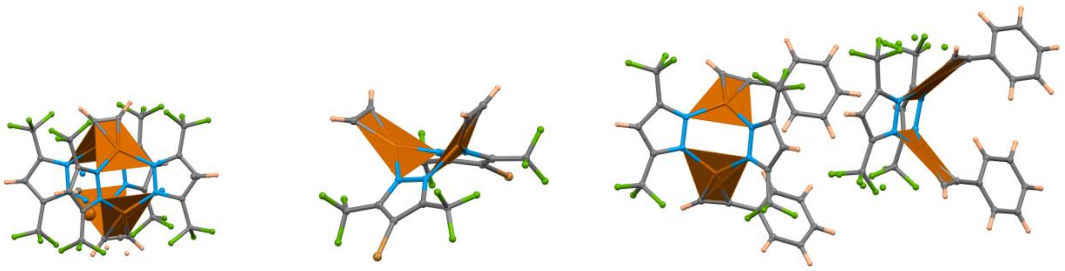

Compound **4** Compound **8** Compound **9**

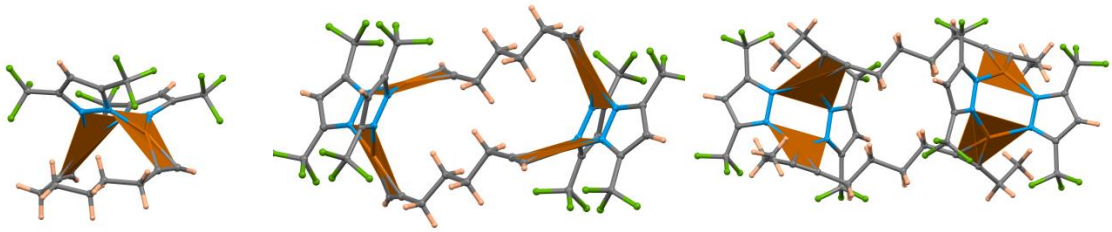

Compound **10** Compound **11** Compound **12**

Figure S45. Views showing the co-planar arrangement of N_2Cu and CuC_2(alkyne) planes of compounds **4, 8-12**

Carboxylation of Terminal Alkynes using {[3,5-$(CF_3)_2$Pz]Cu}$_3$ catalyst.

Product Characterization

Phenylpropiolic acid

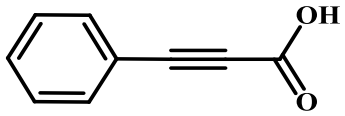

^{1}H NMR (in $(CD_3)_2CO$): δ 14.14 (br, s, 1H, COOH), 7.60–7.57 (m, 1H, Ar-H), 7.49–7.42 (m, 2H, Ar-H), 7.32 (br, s, 2H, Ar-H) ppm.

Reference: Yu, D.; Zhang, Y., Copper- and copper–N-heterocyclic carbene-catalyzed C─H activating carboxylation of terminal alkynes with CO_2 at ambient conditions. *Proc. Natl. Acad. Sci. U. S. A.* **2010**, *107*, 20184-20189.

1,4-diphenyl buta-1,3-diyne

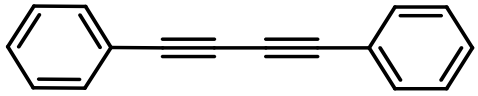

^{1}H NMR (in $CDCl_3$): δ 7.56-7.51 (m, 4 H), 7.40-7.28 (m, 6 H) ppm.

Reference: Wang, D.; Li, J.; Li, N.; Gao, T.; Hou, S.; Chen, B., An efficient approach to homocoupling of terminal alkynes: Solvent-free synthesis of 1,3-diynes using catalytic Cu(II) and base. *Green Chem.* **2010**, *12*, 45-48.

4-Methylphenylpropiolic acid

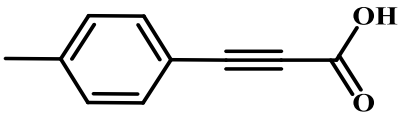

^{1}H NMR (in $CDCl_3$): δ 10.55 (br s, 1H, COOH) 7.51 (d, *J* = 8.0 Hz, 2H, Ar-H), 7.20 (d, *J* = 8.0 Hz, 2H, Ar-H), 2.39 (s, 3H, CH_3) ppm.

Reference: Gooßen, L. J.; Rodríguez, N.; Manjolinho, F.; Lange, P. P., Synthesis of propiolic acids via copper-catalyzed insertion of carbon dioxide into the C-H bond of terminal alkynes. *Adv. Synth. Catal.* **2010**, *352*, 2913-2917.

1,4-Bis(*p*-methylphenyl)buta-1,3-diyne

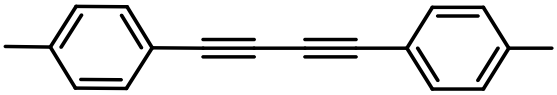

^{1}H NMR (in $CDCl_3$): δ 7.40 (d, *J* = 8.4 Hz, 4H), 7.12 (d, *J* = 8.2 Hz, 4H), 2.34 (s, 6H) ppm.

Reference: Wang, D.; Li, J.; Li, N.; Gao, T.; Hou, S.; Chen, B., An efficient approach to homocoupling of terminal alkynes: Solvent-free synthesis of 1,3-diynes using catalytic Cu(II) and base. *Green Chem.* **2010**, *12*, 45-48.

(4-chlorophenyl)propiolic acid

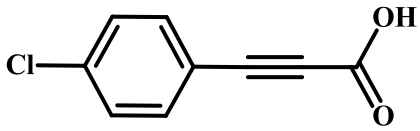

^{1}H NMR (in $CDCl_3$): δ 13.64 (br, s, 1H, COOH) 7.61 (d, *J* = 5.6 Hz, 2H, Ar-H), 7.52 (d, *J* = 5.6 Hz, 2H, Ar-H) ppm.

Reference: Yu, D.; Zhang, Y., Copper- and copper–N-heterocyclic carbene-catalyzed C─H activating carboxylation of terminal alkynes with CO_2 at ambient conditions. *Proc. Natl. Acad. Sci. U. S. A.* **2010**, *107*, 20184-20189.

1,4-bis(4-chlorophenyl) buta-1,3-diyne

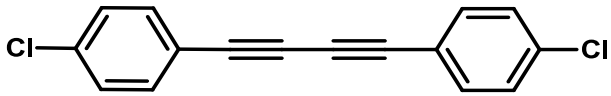

^{1}H NMR (in $CDCl_3$): δ 7.55-7.47 (m, 4 H), 7.07-7.01 (m, 4 H) ppm.

Reference: Yin, W.; He, C.; Chen, M.; Zhang, H; Lei, A., A nickel-catalyzed oxidative coupling reactions of two different terminal alkynes using O_2 as the oxidant at room temperature: facile syntheses of unsymmetric 1,3-diynes. *Org. Lett.* **2009**, *11*, 709-712.

Azide-Alkyne Cycloaddition using $\{[3,5\text{-}(CF_3)_2Pz]Cu\}_3$ catalyst

Product Characterization

Entry	Alkyne	Solvent	Reaction Temperature (°C)	Reaction Time (h)	% Yield*
1	Acetylene	dichloromethane	RT	12	99
2	Phenylacetylene	dichloromethane	RT	12	99
3	1-Octyne	dichloromethane	RT	12	99
4	1,8-Nonadiyne	benzene	80	12	99

*Calculated NMR yield using 1,3,5-Tris(trifluoromethyl)benzene as internal standard.

1-*p*-Tolyl-1*H*-1,2,3-triazole

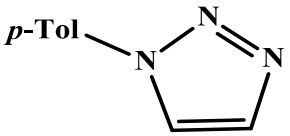

^{1}H NMR (in $CDCl_3$): δ 2.40 (s, 3H), 7.30 (d, *J* = 7.75 Hz, 2H), 7.60 (d, *J* = 7.70 Hz, 2H), 7.83 (s, 1H), 7.99 (s, 1H) ppm. $^{13}C\{^1H\}$ NMR (in $CDCl_3$): δ 21.2, 120.7, 122.1, 130.3, 134.5, 134.9, 139.0 ppm. HRMS calculated for $C_9H_{10}N_3^+$: 160.0870, found: 160.0853.

Reference: Song, R.; Deng, C.; Xie, Y.; Li, J., Solvent-free copper/iron co-catalyzed N-arylation reactions of nitrogen-containing heterocycles with trimethoxysilanes in air. *Tetrahedron Lett.* **2007**, *48*, 7845-7848.

Figure S46. ^{1}H NMR spectrum of 1-*p*-Tolyl-1*H*-1,2,3-triazole in $CDCl_3$ at the room temperature.

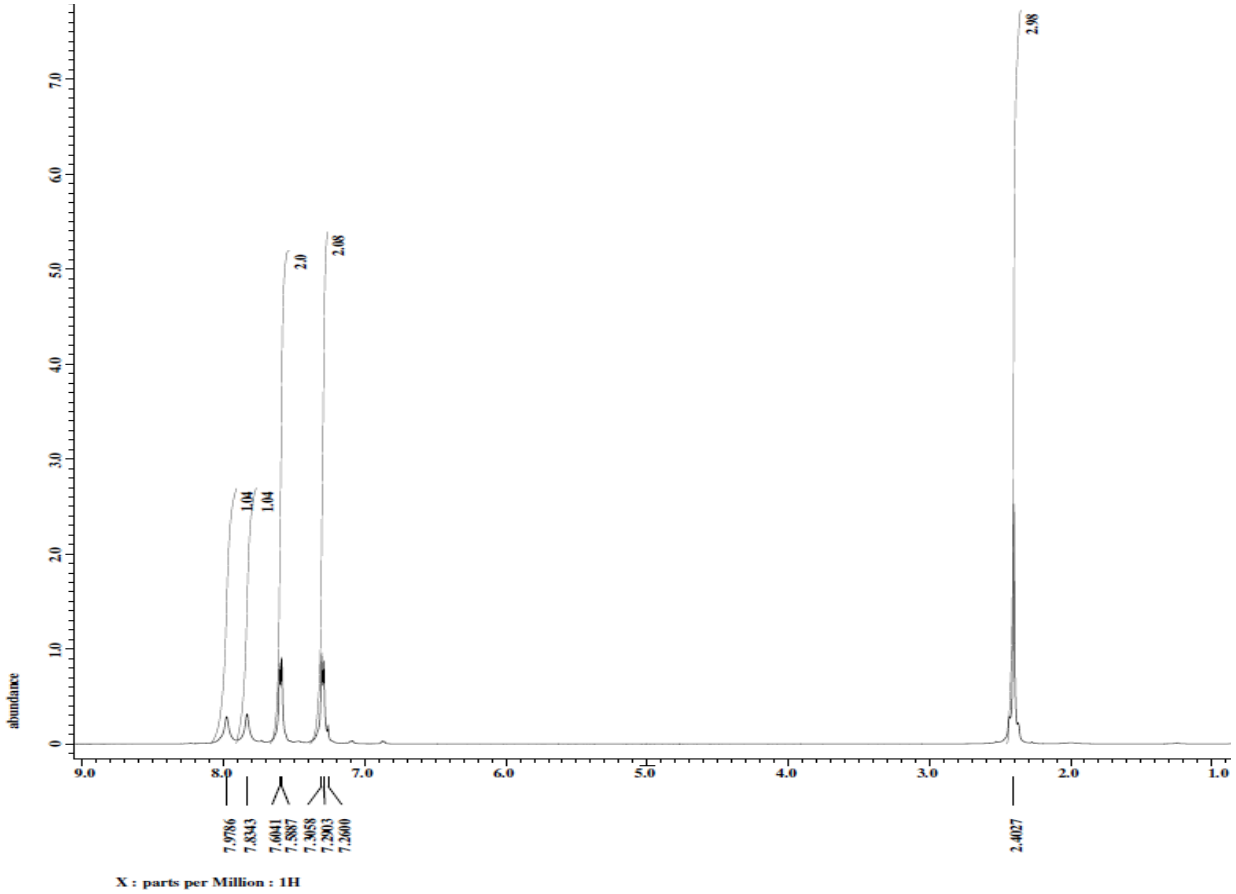

Figure S47. $^{13}C\{^{1}H\}$ NMR spectrum of 1-*p*-Tolyl-1*H*-1,2,3-triazole in $CDCl_3$ at the room temperature.

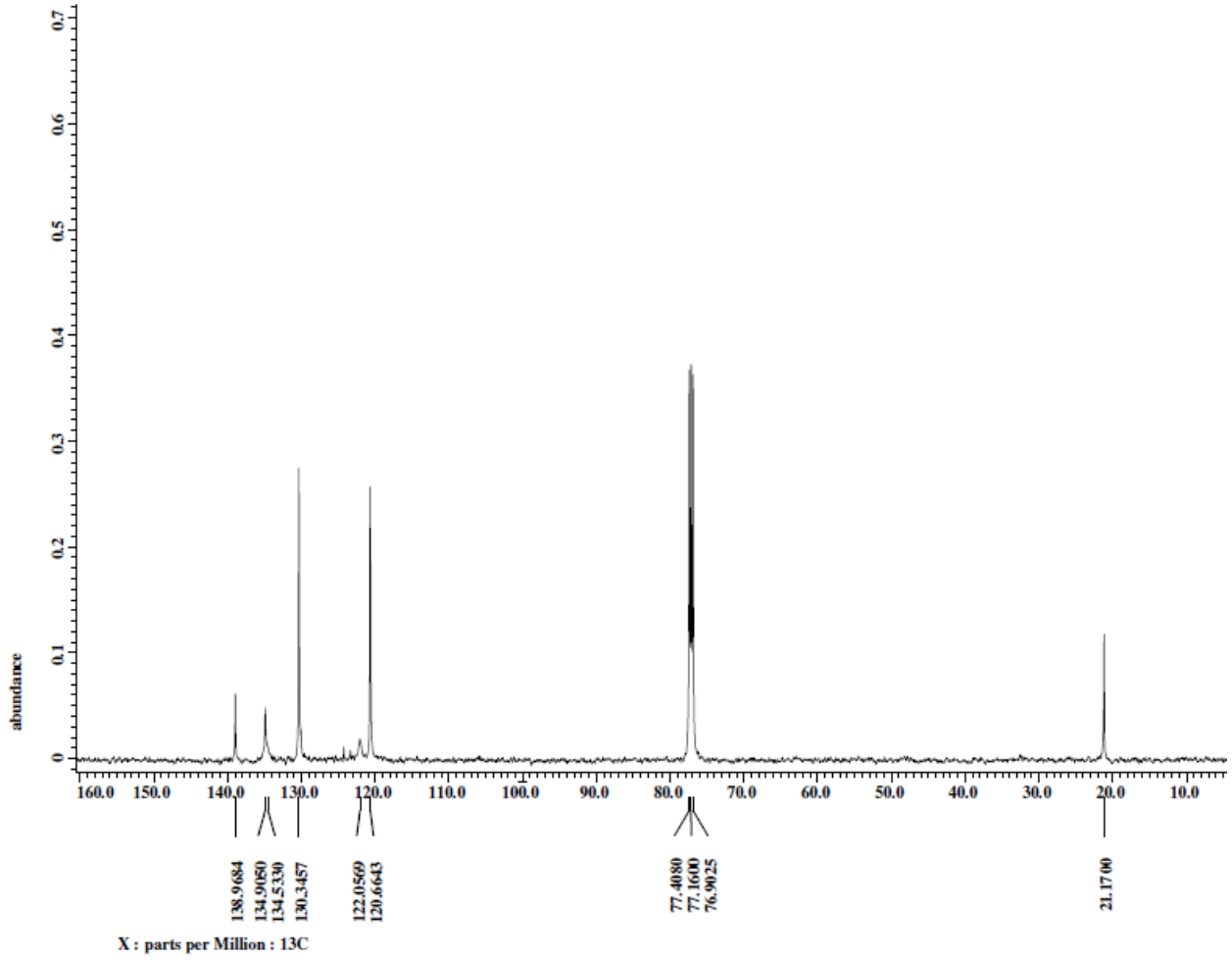

1-*p*-Tolyl-4-phenyl-1*H*-1,2,3-triazole

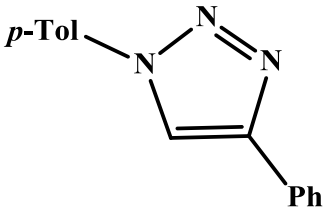

^{1}H NMR (in $CDCl_3$): δ 2.41 (s, 3H), 7.30-7.36 (m, 3H), 7.44 (t, *J* = 6.90 Hz, 2H), 7.64 (d, *J* = 7.45 Hz, 2H), 7.90 (d, *J* = 6.90 Hz, 2H), 8.15 (s, 1H) ppm. ^{13}C{^{1}H} NMR (in $CDCl_3$): δ 21.2, 117.8, 120.5, 125.9, 128.4, 129.0,130.3, 134.8, 139.0, 148.3 ppm. HRMS calculated for $C_{15}H_{14}N_3^+$: 236.1183, found: 236.1153.

Reference: Meng, X.; Xu, X.; Gao, T.; Chen, B., Zn/C-Catalyzed Cycloaddition of Azides and Aryl Alkynes. *Eur. J. Org. Chem.* **2010**, *2010*, 5409-5414.

Figure S48. ^{1}H NMR spectrum of 1-*p*-Tolyl-4-phenyl-1*H*-1,2,3-triazole in $CDCl_3$ at the room temperature.

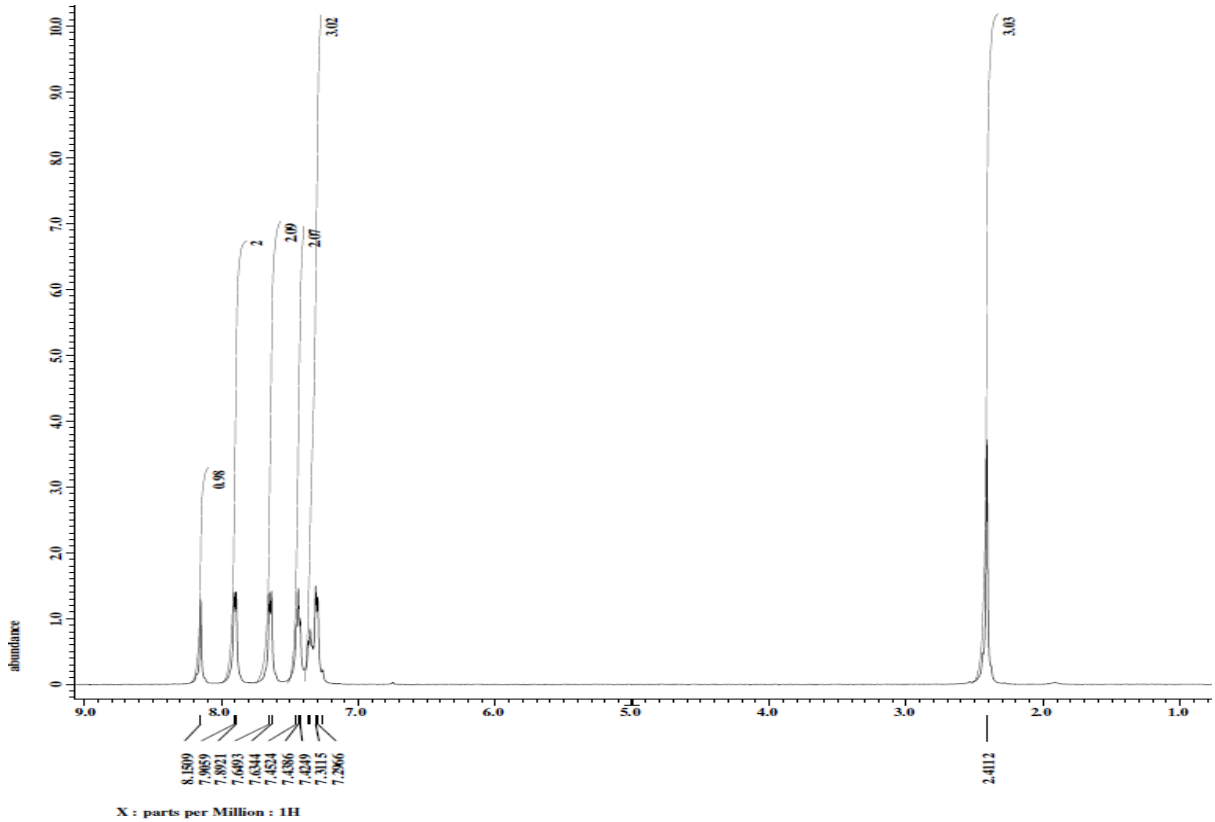

Figure S49. $^{13}C\{^{1}H\}$ NMR spectrum of 1-*p*-Tolyl-4-phenyl-1*H*-1,2,3-triazole in $CDCl_3$ at the room temperature.

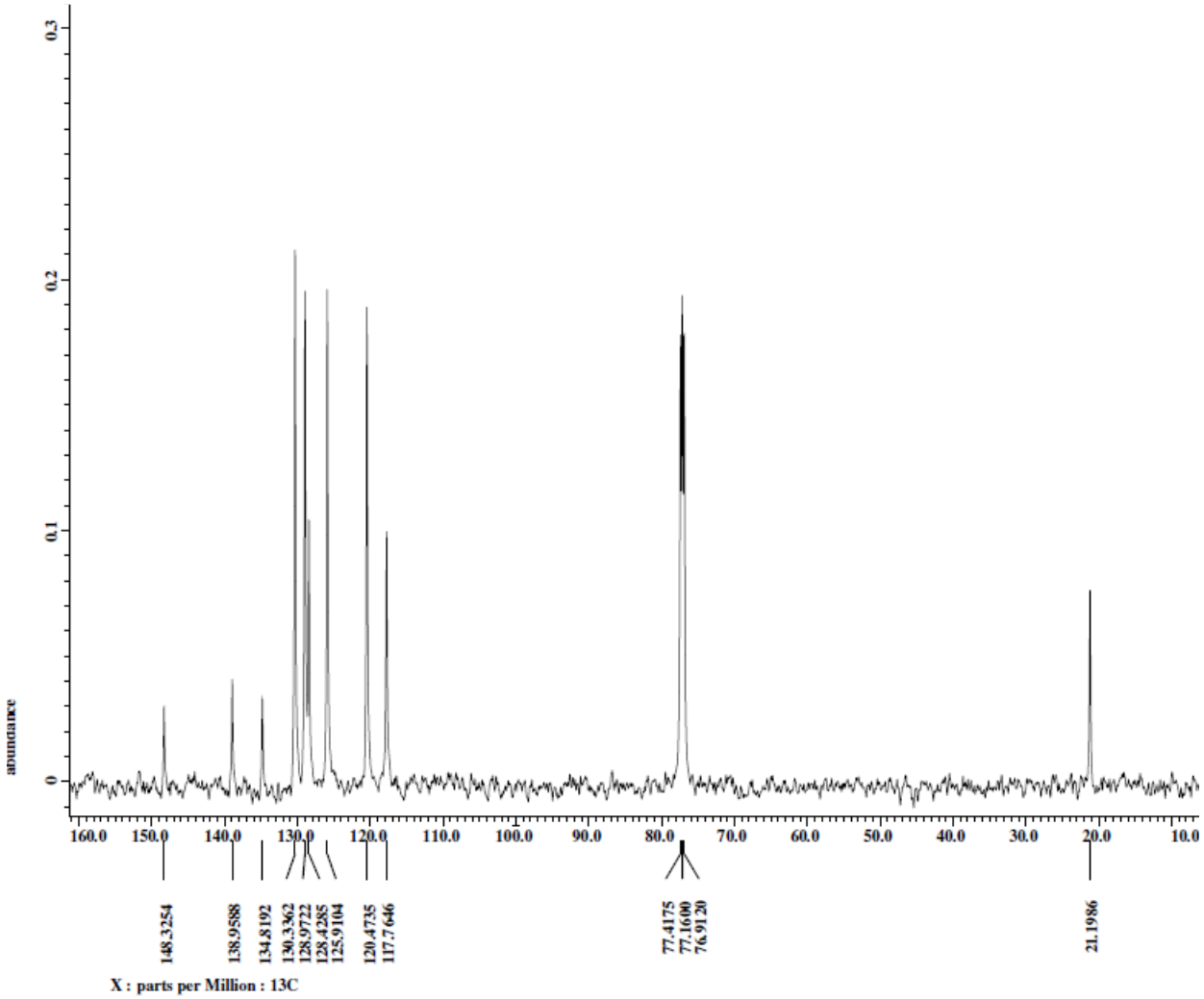

4-hexyl-1-(*p*-tolyl)-1*H*-1,2,3-triazole

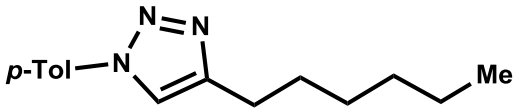

^{1}H NMR (in $CDCl_3$): δ 0.85 (t, *J* = 6.87 Hz, 3H), 1.26-1.29 (m, 4H), 1.33-1.37 (m, 2H), 1.65-1.71 (m, 2H), 2.35 (s, 3H), 2.73 (t, *J* = 7.45 Hz, 2H), 7.23 (d, *J* = 8.02 Hz, 2H), 7.55 (d, *J* = 8.02 Hz, 2H), 7.68 (s, 1H) ppm. ^{13}C{^{1}H} NMR (in $CDCl_3$): δ 14.1, 21.0, 22.6, 25.7, 29.0, 29.4, 31.6, 118.9, 120.2, 130.1, 135.0, 138.4, 149.0 ppm.

Figure S50. ^{1}H NMR spectrum of 4-hexyl-1-(*p*-tolyl)-1*H*-1,2,3-triazole in $CDCl_3$ at room temperature

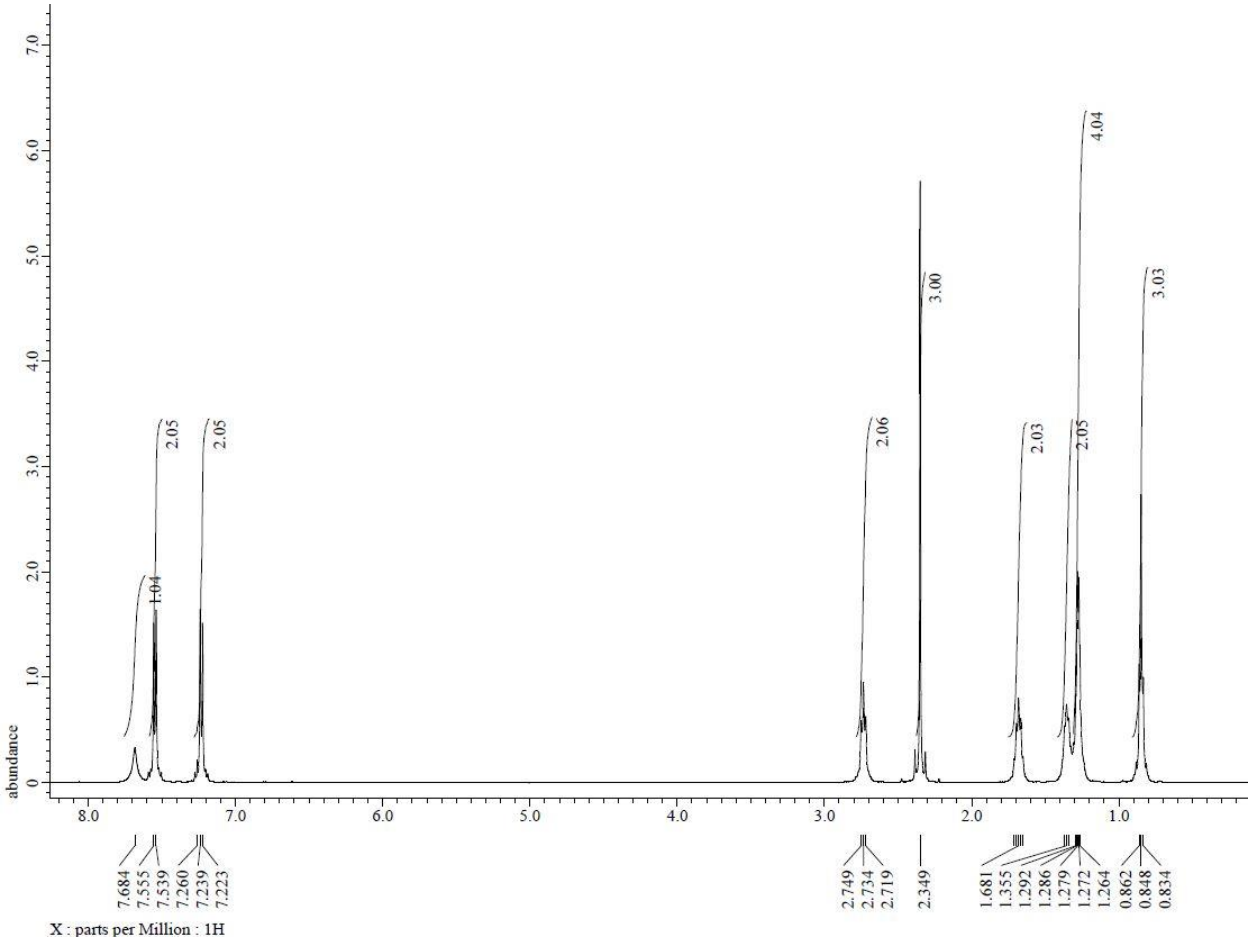

Figure S51. $^{13}C\{^{1}H\}$ NMR spectrum of 4-hexyl-1-(*p*-tolyl)-1*H*-1,2,3-triazole in $CDCl_3$ at the room temperature.

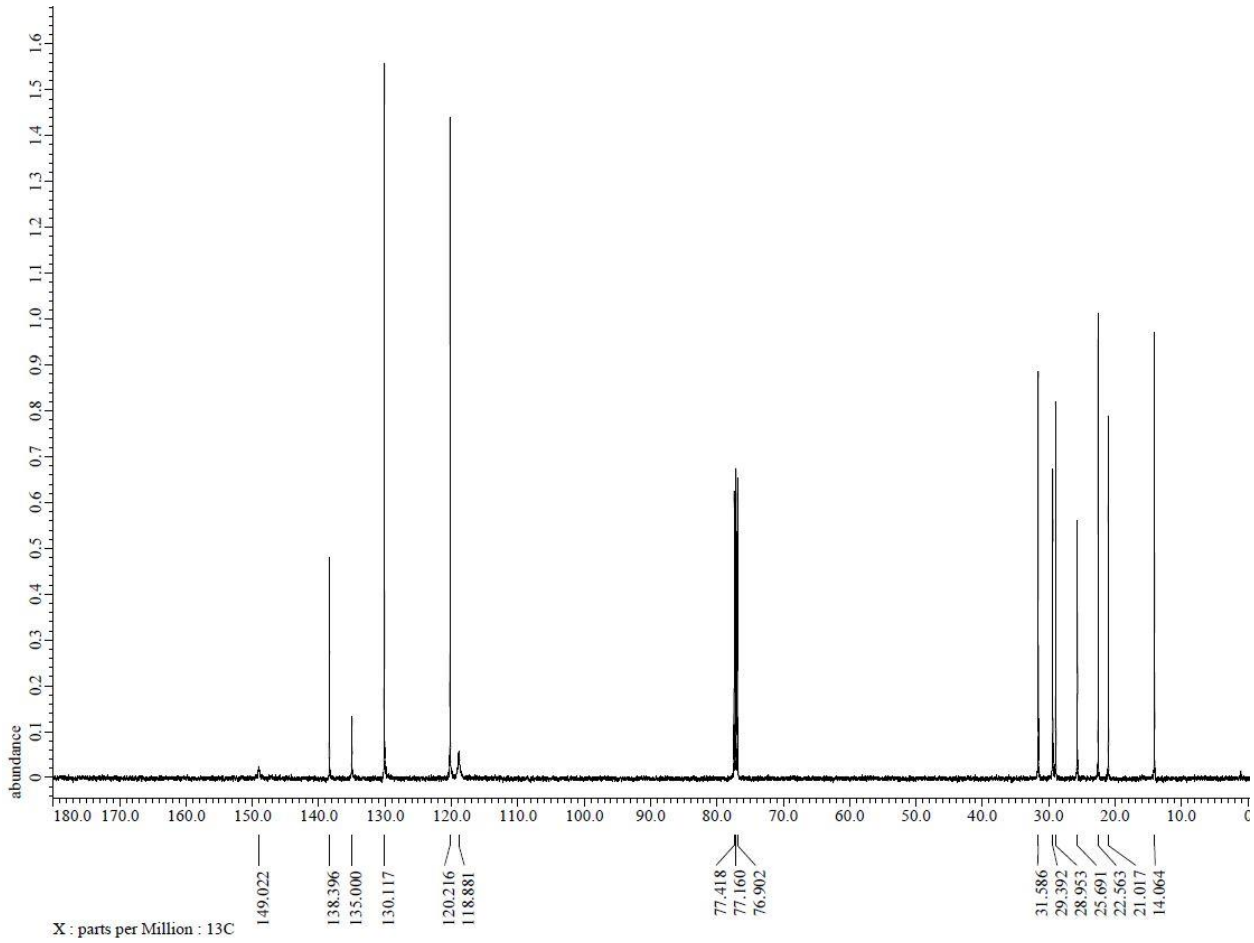

1-p-Tolyl-4-(5-(1-p-tolyl-1*H*-1,2,3-triazol-4-yl)pentyl)-1*H*-1,2,3-triazole

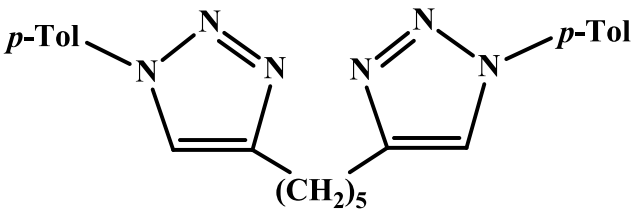

^{1}H NMR (in $CDCl_3$): δ 1.5 (m, *J* = 7.20 Hz, 2H), 1.79 (m, *J* = 7.40 Hz, 2H), 2.39 (s, 3H), 2.80 (m, *J* = 7.30, 2H), 7.28 (d, *J* = 7.45 Hz, 2H), 7.57 (d, *J* = 8.0 Hz, 2H) ppm. ^{13}C{^{1}H} NMR (in $CDCl_3$): δ 21.2, 25.5, 28.6, 29.1, 119.1, 120.4, 130.2, 135.0, 138.5, 148.8 ppm. HRMS calculated for $C_{23}H_{27}N_6^+$: 387.2292, found: 387.2242.

Figure S52. ^{1}H NMR spectrum of 1-*p*-tolyl-4-(5-(1-p-tolyl-1*H*-1,2,3-triazol-4-yl)pentyl)-1*H*-1,2,3-triazole in $CDCl_3$ at the room temperature.

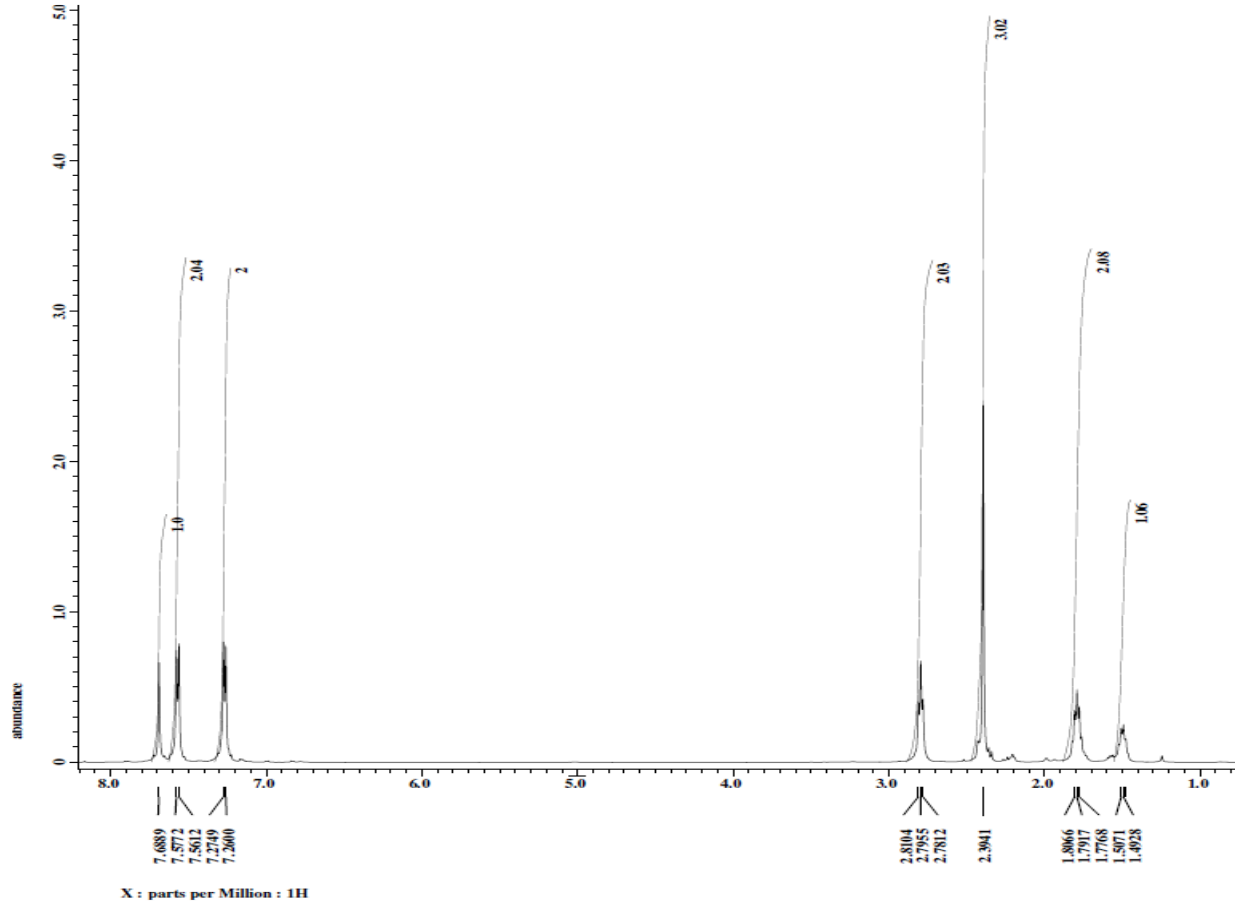

Figure S53. $^{13}C\{^{1}H\}$ NMR spectrum of 1-*p*-tolyl-4-(5-(1-p-tolyl-1*H*-1,2,3-triazol-4-yl)pentyl)-1*H*-1,2,3-triazole in $CDCl_3$ at the room temperature.

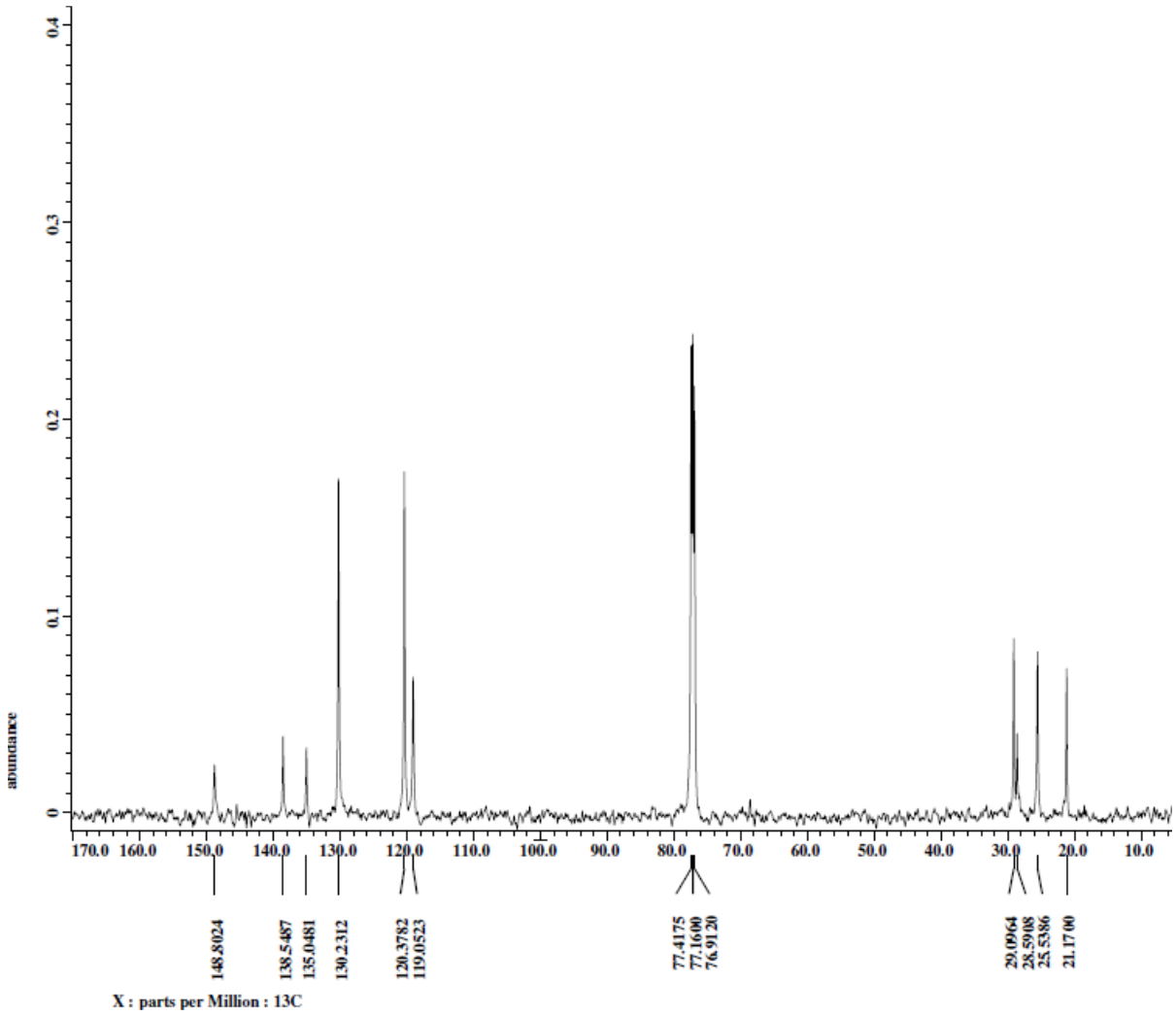

Base-free Hydrothiolation of Alkynes: Product Characterization

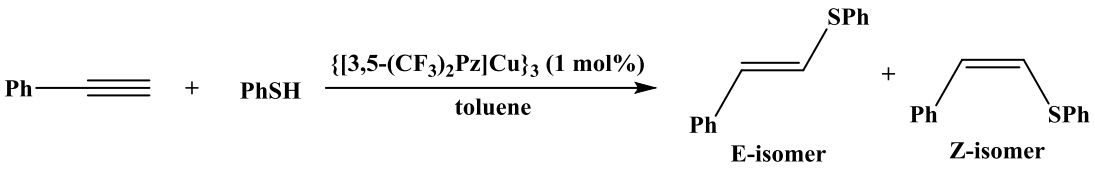

Entry	Catalyst	Temp (ºC)	Time (h)	Under CO_2 (E:Z)	Under N_2 (E:Z)	Overall % yield under CO_2	Overall % yield under N_2	References
1	$\{[3,5\text{-}(CF_3)_2Pz]Cu\}_3$	RT	3	63:37	50:50	70	56	This work
2	*No catalyst*	*RT*	*3*	*30:70*	*70:30*	*42*	*37*	*This work*
3	$\{[3,5\text{-}(CF_3)_2Pz]Cu\}_3$	0	3	26:74	10:90	65	48	This work
4	$\{[3,5\text{-}(CF_3)_2Pz]Cu\}_3$	90	3	30:70	56:44	78	62	This work
5	$\{[3,5\text{-}(CF_3)_2Pz]Cu\}_3$	90	16	78:22	34:66	90	81	This work
6[a]	*CuI/K_2CO_3 (see conditions below)*	*90*	*16*	*10:90*	*84:16*	*92*	*68*	*[a](see below)*

[a]Reaction conditions: phenylacetylene (0.5 mmol), thiophenol (0.75 mmol), CuI (5 mol%), K_2CO_3 (0.6 mmol), H_2O (25 μL) and DMSO (3 mL); Riduan, S. N.; Ying, J. Y.; Zhang, Y., Carbon dioxide mediated stereoselective copper-catalyzed reductive coupling of alkynes and thiols. *Org. Lett.* **2012**, *14*, 1780-1783

Phenyl(styryl)sulfane

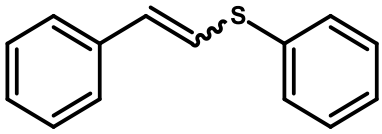

^{1}H NMR (in $CDCl_3$) δ 7.56 – 7.22 (m, 20H), 6.90 (d, 1H, *J* = 15.0 Hz), 6.75 (d, 1H, *J* = 15.0 Hz), 6.61 (d, 1H, *J* = 10.8 Hz), 6.52 (d, 1H, *J* = 10.8 Hz) ppm.

Reference: Riduan, S. N.; Ying, J. Y.; Zhang, Y., Carbon dioxide mediated stereoselective copper-catalyzed reductive coupling of alkynes and thiols. *Org. Lett.* **2012**, *14*, 1780-1783.

Figure S54. ^{1}H NMR spectrum of Phenyl(styryl)sulfane in $CDCl_3$ at the room temperature. Entry 4 CO_2 atm. Isolated as light yellow oil in 90% yield, E/Z ratio: 78:22 (expanded and full spectrum).

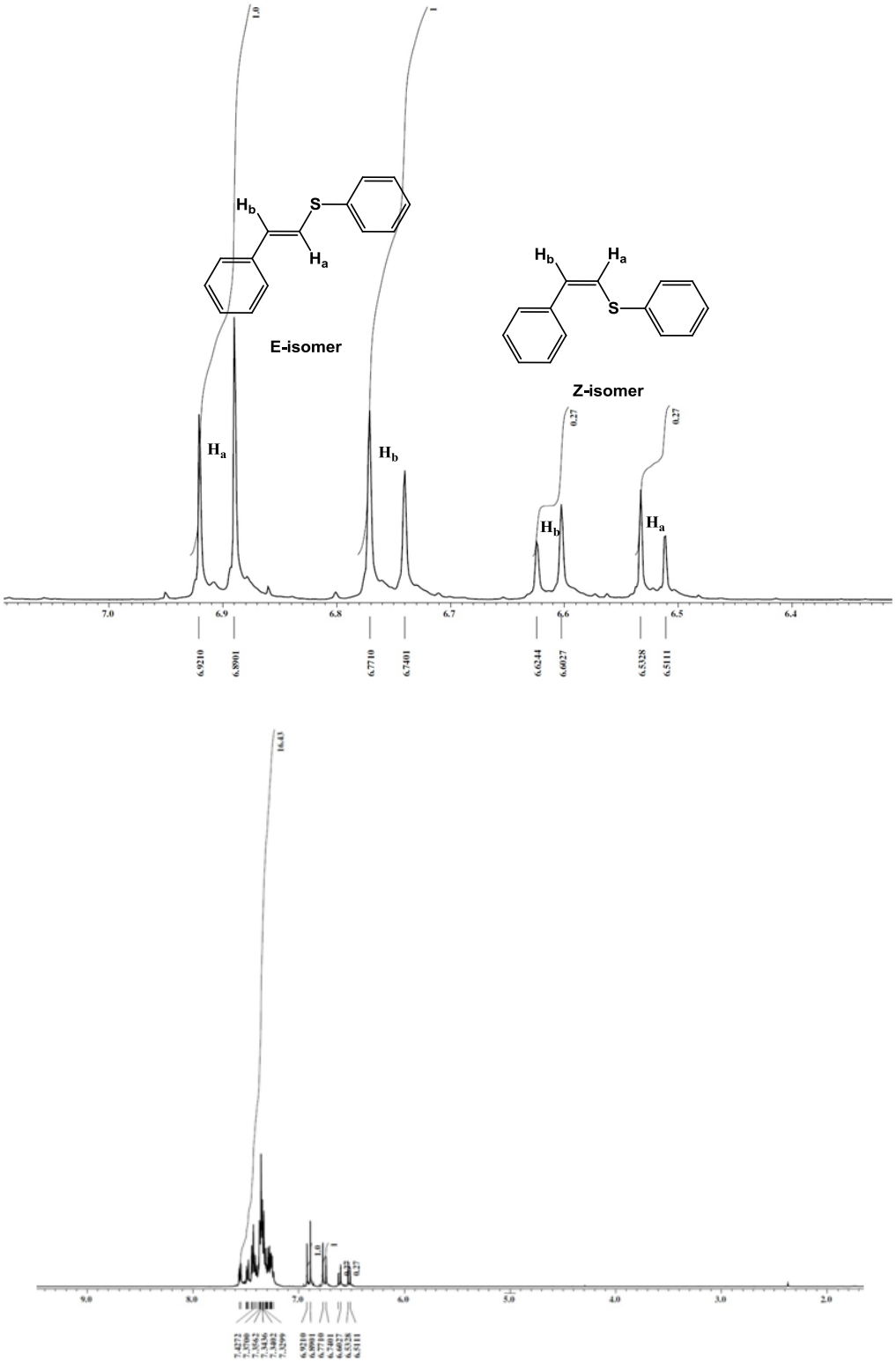

Figure S55. ^{1}H NMR spectrum of Phenyl(styryl)sulfane in $CDCl_3$ at the room temperature. Entry 4_N_2 atm. Isolated as light yellow oil in 81% yield, E/Z ratio: 34:66.

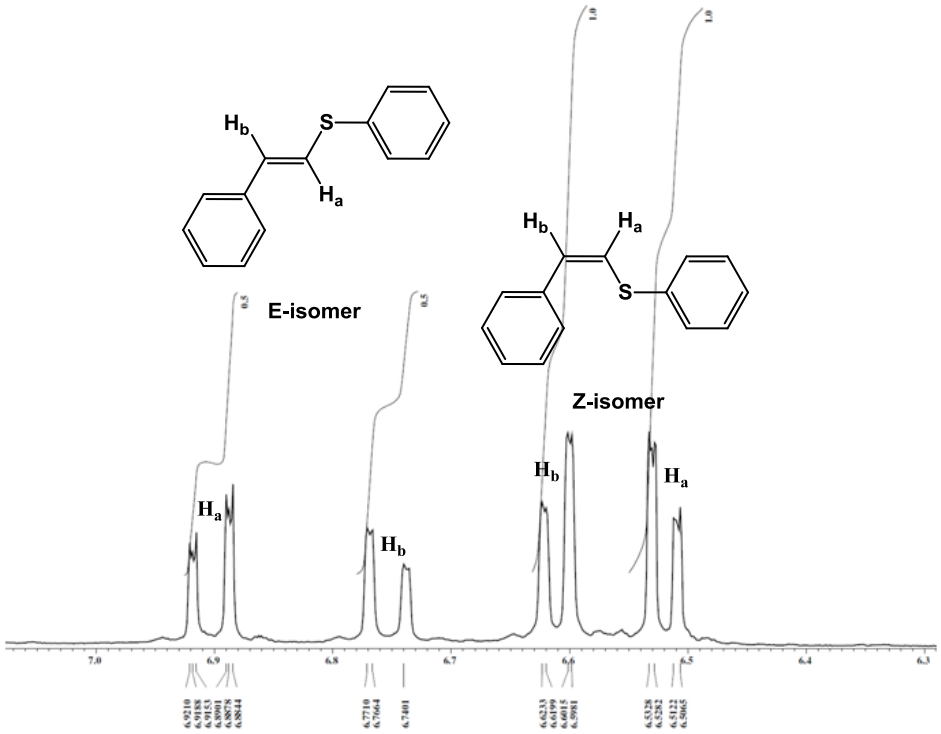

Figure S56. ^{1}H NMR spectrum of Phenyl(styryl)sulfane in $CDCl_3$ at the room temperature. Entry 3_CO_2 atm. Isolated as light yellow oil in 78% yield, E/Z ratio: 30:70.

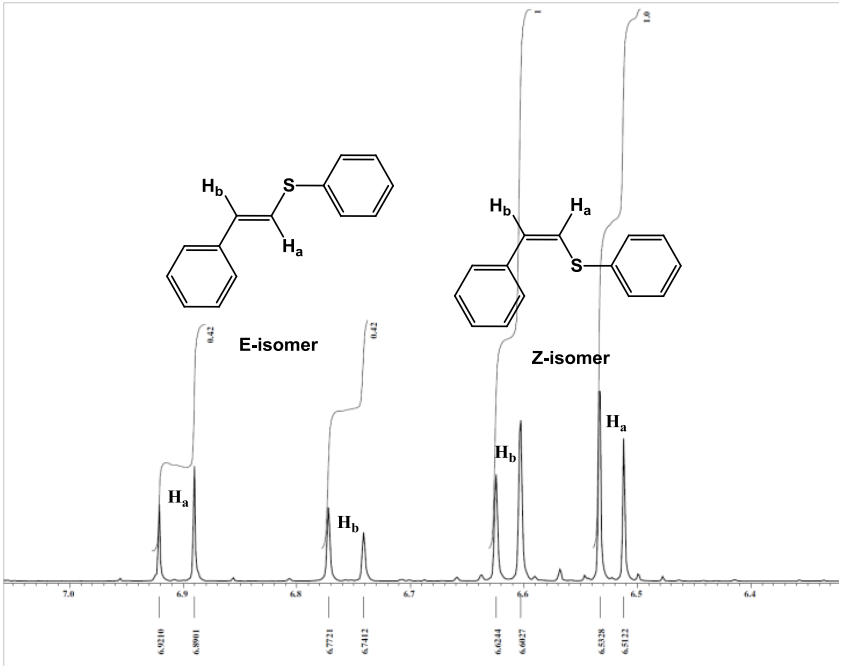

Figure S57. ^{1}H NMR spectrum of Phenyl(styryl)sulfane in $CDCl_3$ at the room temperature. Entry 3_N_2 atm. Isolated as light yellow oil in 62% yield, E/Z ratio: 56:44.

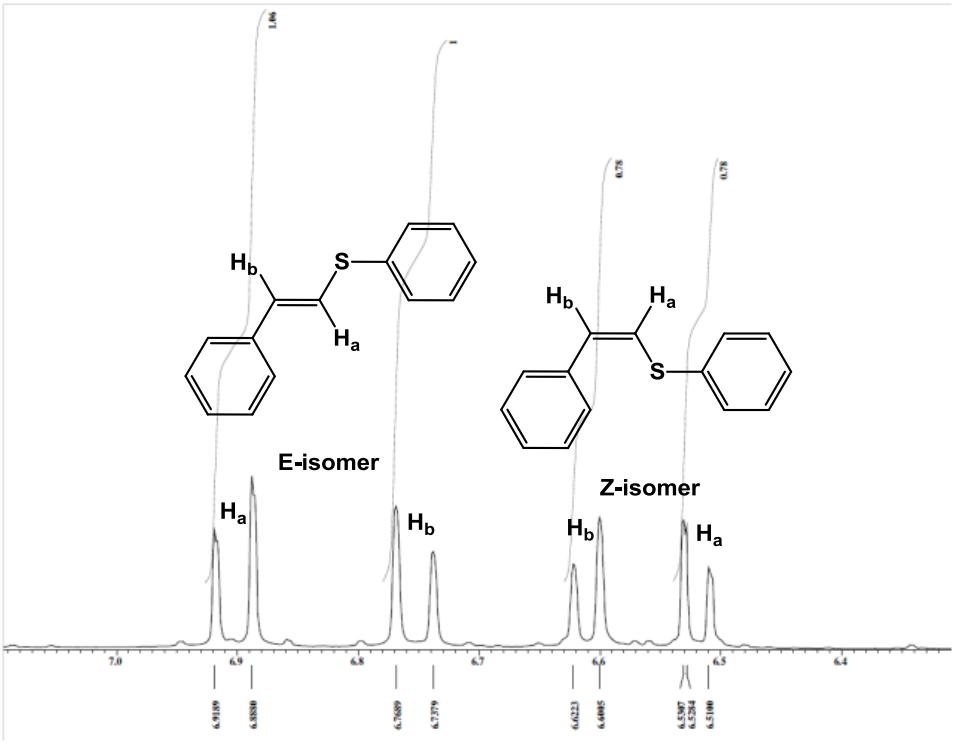

Figure S58. ^{1}H NMR spectrum of Phenyl(styryl)sulfane in $CDCl_3$ at the room temperature. Entry 2_CO_2 atm. Isolated as light yellow oil in 65% yield, E/Z ratio: 26:74.

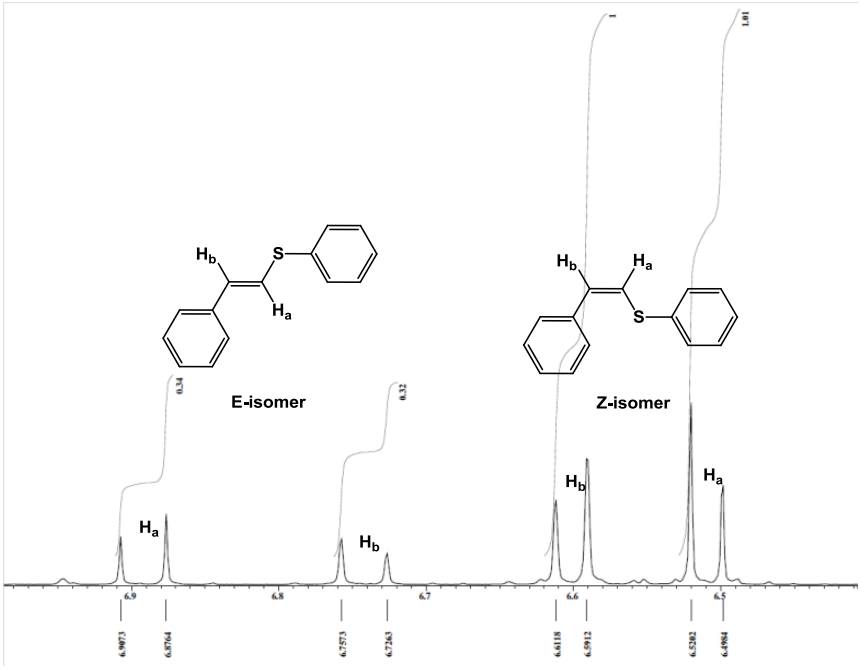

Figure S59. ^{1}H NMR spectrum of Phenyl(styryl)sulfane in $CDCl_3$ at the room temperature. Entry 2_N_2 atm. Isolated as light yellow oil in 48% yield, E/Z ratio: 10:90.

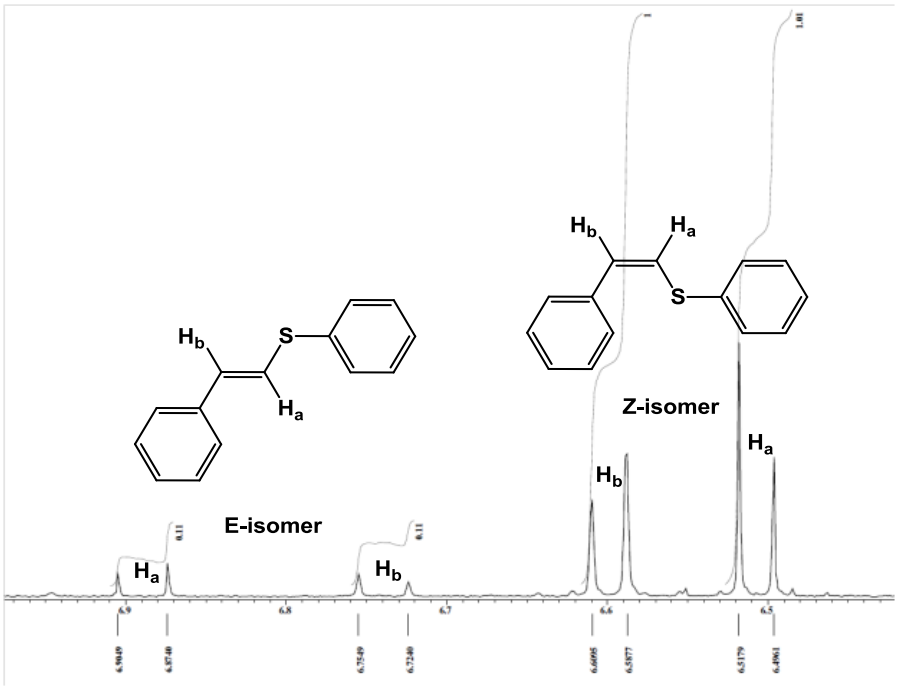

Figure S60. ^{1}H NMR spectrum of Phenyl(styryl)sulfane in $CDCl_3$ at the room temperature. Entry 1_CO_2 atm. Isolated as light yellow oil in 70% yield, E/Z ratio: 63:37.

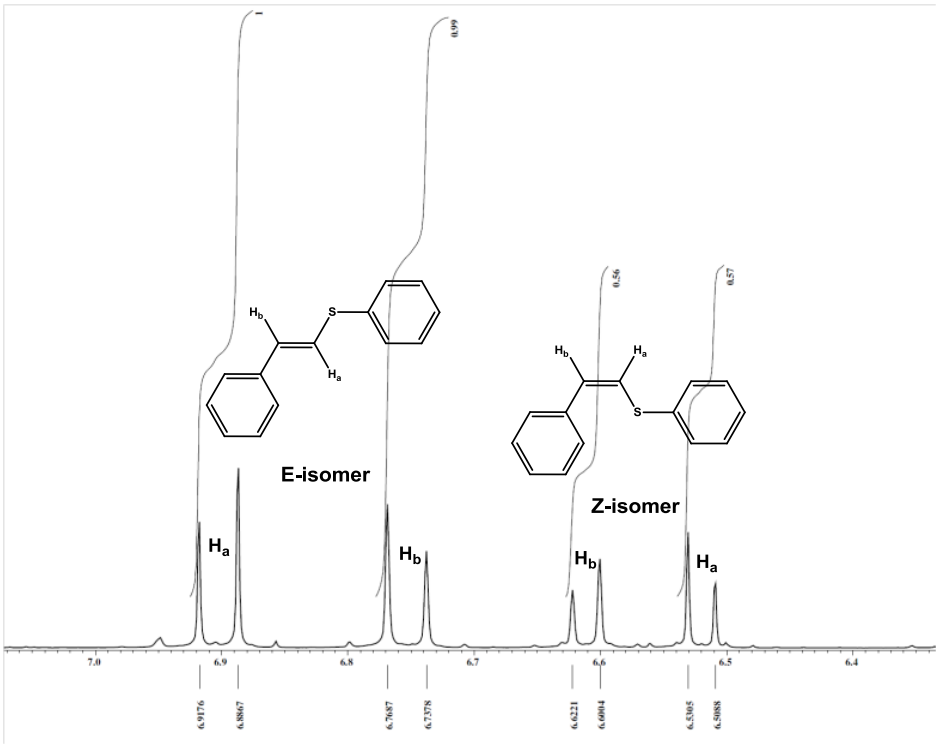

Figure S61. ^{1}H NMR spectrum of Phenyl(styryl)sulfane in $CDCl_3$ at the room temperature. Entry 1_N_2 atm. Isolated as light yellow oil in 56% yield, E/Z ratio: 50:50.

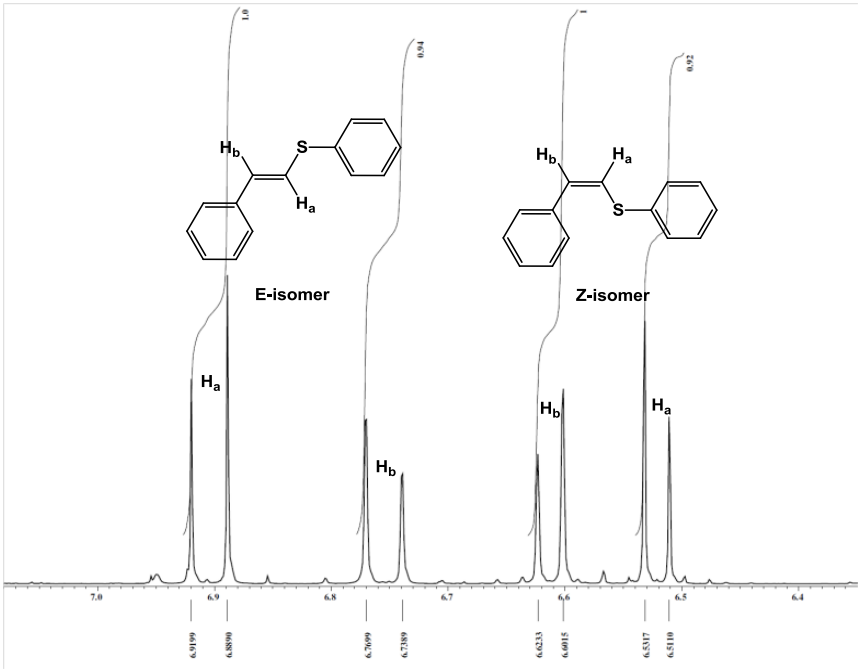

Useful Raman data of free alkynes

Figure S62. Raman spectrum of neat phenylacetylene

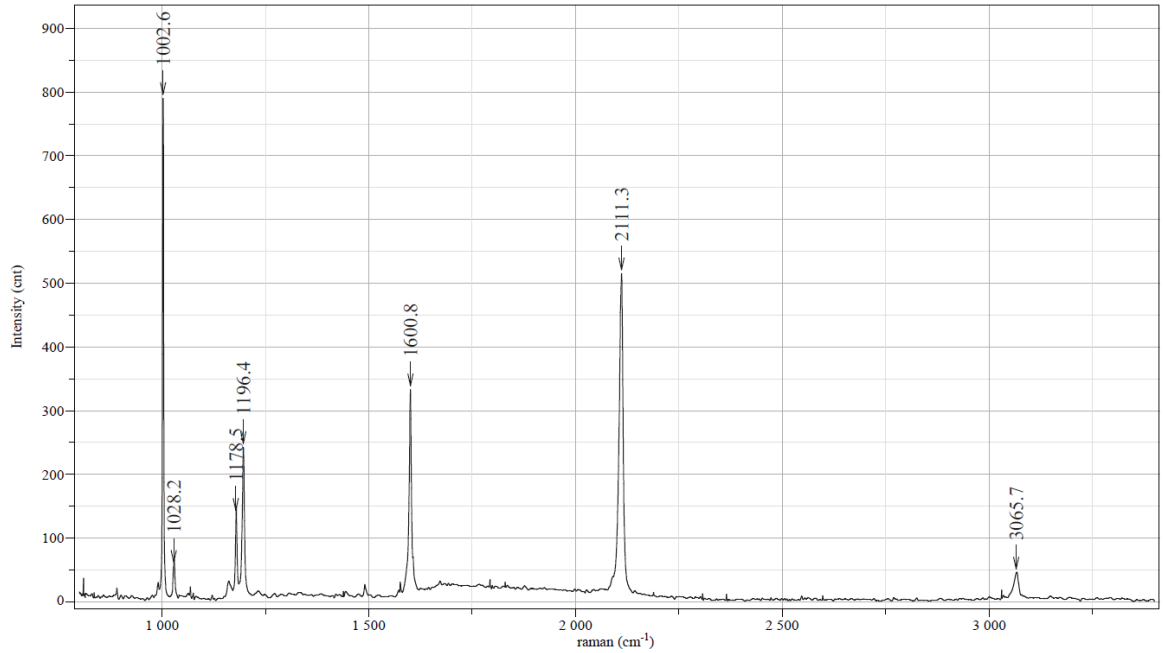

Exposition	5	Slit	100
Accumulation	10 x 4	Operator	
Laser	632.817	Sample	
Spectro	Multi	Remark	
Hole	200	Power	

HORIBA JOBIN YVON

Figure S63. Raman spectrum of neat 1,8-nonadiyne

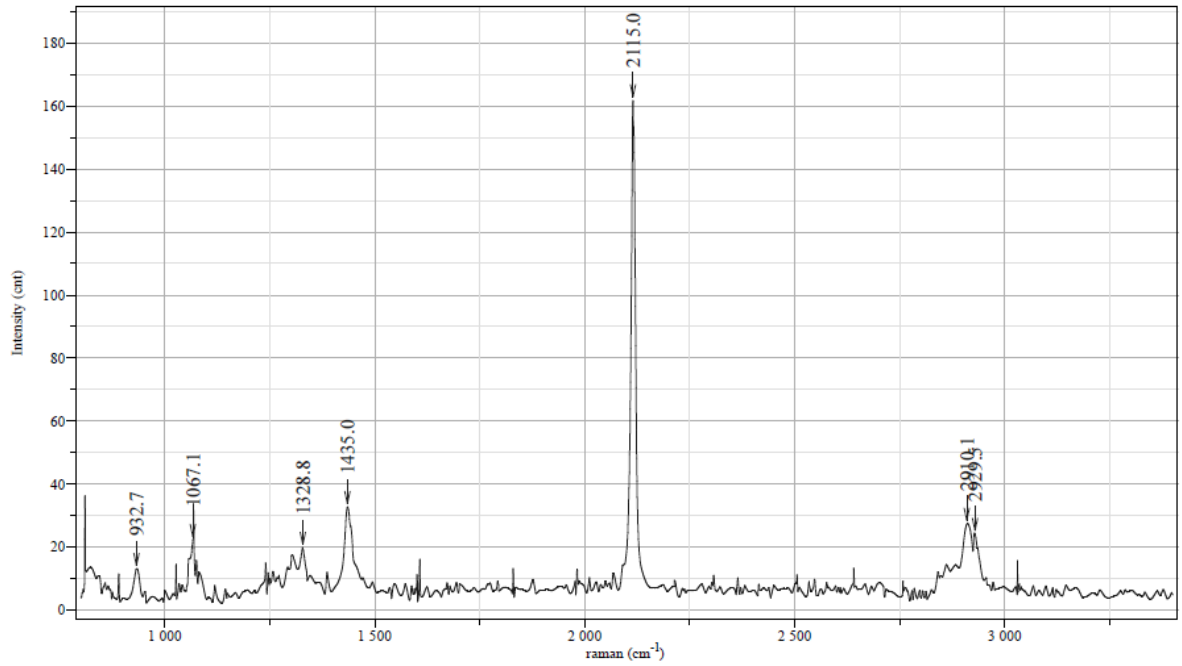

Exposition	5	Slit	100
Accumulation	10 x 4	Operator	
Laser	632.817	Sample	
Spectro	Multi	Remark	
Hole	200	Power	

HORIBA JOBIN YVON

Figure S64. Raman spectrum of neat 1,7-octadiyne

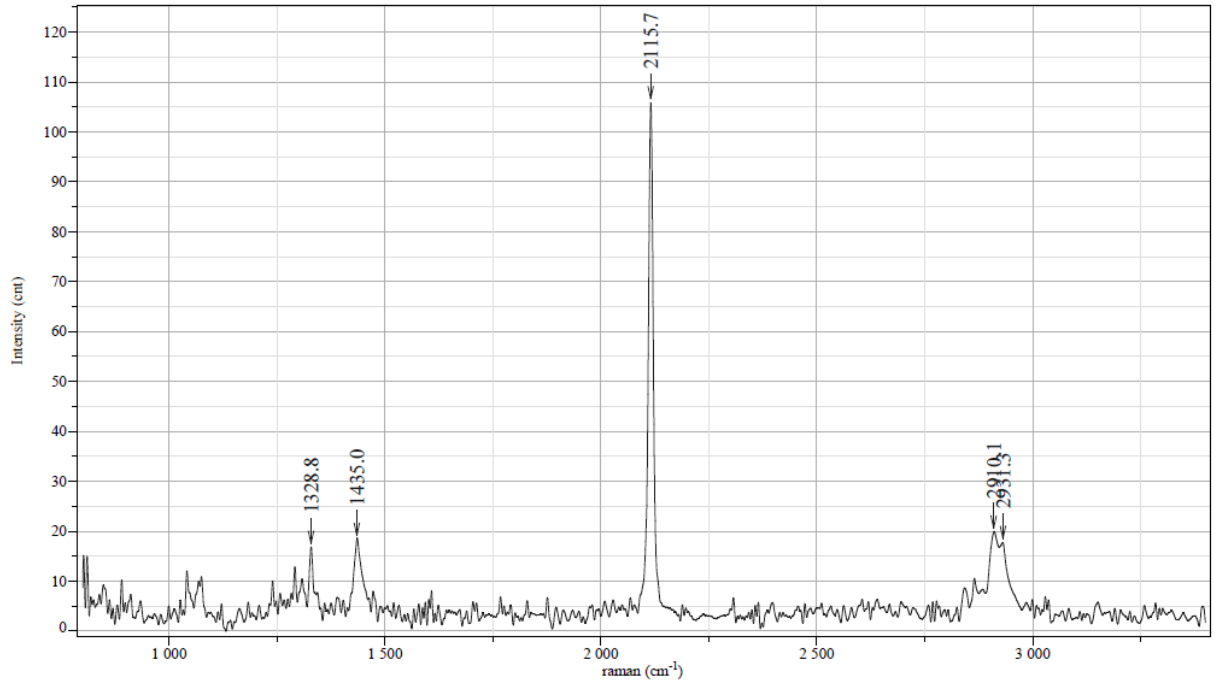

Exposition	5	Slit	100
Accumulation	10 x 4	Operator	
Laser	632.817	Sample	
Spectro	Multi	Remark	
Hole	200	Power	

HORIBA JOBIN YVON

Figure S65. Raman spectrum of neat 3,9-dodecadiyne

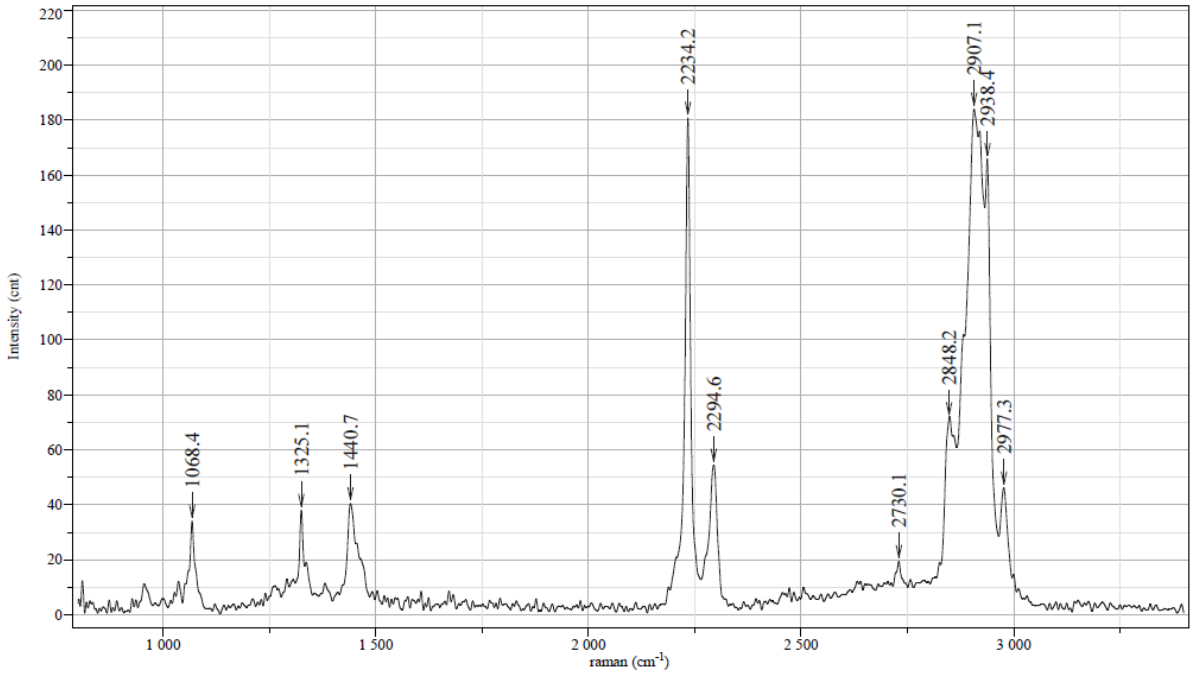

Exposition	5	Slit	100
Accumulation	20 x 4	Operator	Anurag
Laser	632.817	Sample	
Spectro	Multi	Remark	
Hole	200	Power	

HORIBA JOBIN YVON